
**Photodynamic Therapy with 5-Aminolaevulinic Acid -
Techniques for Enhancement**

Alison Curnow

**A thesis submitted in fulfilment of the degree of
Doctor of Philosophy (Ph.D.)**

1999

**National Medical Laser Centre
Institute of Surgical Studies
Royal Free and University College Medical School
University College London**

ProQuest Number: 10797753

All rights reserved

INFORMATION TO ALL USERS

The quality of this reproduction is dependent upon the quality of the copy submitted.

In the unlikely event that the author did not send a complete manuscript and there are missing pages, these will be noted. Also, if material had to be removed, a note will indicate the deletion.



ProQuest 10797753

Published by ProQuest LLC (2018). Copyright of the Dissertation is held by the Author.

All rights reserved.

This work is protected against unauthorized copying under Title 17, United States Code
Microform Edition © ProQuest LLC.

ProQuest LLC.
789 East Eisenhower Parkway
P.O. Box 1346
Ann Arbor, MI 48106 – 1346

For My Parents

Abstract

Photodynamic therapy (PDT) is a non-thermal technique which can be used to create localised tissue damage. It requires the activation of a pre-administered photosensitiser (in the presence of molecular oxygen) with light of a specific wavelength to form a cytotoxic species.

5-Aminolaevulinic acid (ALA) is an attractive photosensitising agent for PDT as its photoreactive derivative protoporphyrin IX (PPIX), is metabolised within one to two days, eliminating prolonged skin photosensitivity (the major side effect of other clinically used photosensitisers). However, at the maximum dose patients tolerate by mouth (60 mg/kg) only superficial effects are seen. A need exists for the outcome of this treatment modality to be enhanced without increasing the administered dose of ALA.

ALA PDT manipulates the haem biosynthesis pathway to create an accumulation of PPIX. By chelating iron (using a hydroxypyridinone iron chelator), this thesis shows that it is possible to amplify this PPIX accumulation and thus significantly enhance the effect of ALA PDT. This is demonstrated in normal and malignant rat colon, normal rat skin and normal rabbit uterus, using several routes of administration.

Various light dose fractionation regimes were also investigated in this thesis. A single 150 second interruption to the illumination, when placed appropriately, was found to

significantly enhance ALA PDT in normal and malignant rat colon. The reasons for this are unclear but marked differences in tissue oxygenation were observed during continuous and fractionated treatments. Additionally, relocalisation of PPIX during the dark interval was detected and the inhibition of reperfusion injury was found to prevent the tissue damage normally produced in this model.

This thesis has investigated two different methods of ALA PDT enhancement and found that the addition of a hydroxypyridinone iron chelator and the technique of light dose fractionation can both be used successfully *in vivo*, to significantly enhance ALA induced PDT.

Table of Contents

Title Page.....	1
Abstract	3
Table of Contents	5
List of Figures	7
List of Abbreviations	12
Acknowledgements.....	14

Section I - Introduction

1.1 General Introduction	17
1.2 Background	21
1.3 Thesis Scheme	35

Section II - Experimentation

2.0.0 Laser Comparison	37
------------------------------	----

Part I - Enhancement of ALA PDT using Iron Chelators

2.1.1 Introduction.....	46
2.1.2 Iron Chelator Pharmacokinetics in Normal Colon.....	51
2.1.3 PPIX Analysis	67
2.1.4 Iron Chelator PDT in Normal Colon.....	74
2.1.5 Iron Chelator Pharmacokinetics and PDT in a Colonic Tumour Model	82
2.1.6 Topical Iron Chelator Administration in a Normal Skin Model.....	89
2.1.7 Topical Iron Chelator Instillation in Normal Uterus	102
2.1.8 Discussion	117

Part II - Enhancement of ALA PDT using Light Dose Fractionation

2.2.1 Introduction	122
2.2.2 Light Dose Fractionation in Normal Colon.....	127
2.2.3 Light Dose Fractionation in a Colonic Tumour Model.....	140
2.2.4 Combining the Technique of Light Dose Fractionation with the Administration of an Iron Chelating Agent.....	146
2.2.5 Monitoring Oxygen During Light Dose Fractionation	153
2.2.6 PPIX Relocalisation During Light Dose Fractionation.....	168
2.2.7 The Effect of Reperfusion Injury During Light Dose Fractionation.....	177
2.2.8 Discussion	189

Section III - Discussion

3.1 General Discussion	194
3.2 Conclusions.....	202

References	205
Appendix I - Conference Presentations	217
Appendix II - Publications	220

List of Figures

Figure 1 - Schematic diagram of the haem biosynthesis pathway	23
Figure 2 - Schematic diagram summarising the reactions involved in the mechanism of ALA induced PDT	29
Figure 3 - Mean area of necrosis as a function of laser and wavelength using 50 mg/kg ALA i.v.	41
Figure 4 - Mean area of necrosis as a function of laser and wavelength using 200 mg/kg ALA i.v.	42
Figure 5 - The structures of CP20 (a) and CP94 (b)	49
Figure 6 - Fluorescence image (a) and matched histology section (b) of colon using ALA alone. Fluorescence image (c) and matched histology section (d) of colon using ALA plus CP94	55
Figure 7 - Fluorescence of colonic mucosa and muscle as a function of time with ALA (50 mg/kg i.v.) only (a), CP20 or CP94 (b), ALA plus simultaneous CP94 administration (c), ALA with CP94 administered 30 minutes prior to the ALA dose (d), ALA plus simultaneous CP20 administration (e), ALA with CP20 administered 30 minutes prior to the ALA dose (f).....	57
Figure 8 - Fluorescence of colonic mucosa and muscle as a function of time with ALA (25 mg/kg i.v.) only (a) and ALA plus CP94 (b)	61
Figure 9 - Peak fluorescence of the colonic mucosa and muscle, with or without CP94, as a function of ALA dose	62

Figure 10 - Ratio of peak fluorescence of the colonic mucosa (ALA + CP94 / ALA only) ^{as} a function of ALA dose ↑	63
Figure 11 - Emission spectra from colon treated with ALA only (a), ALA plus CP94 (b) and ALA plus CP20 (c)	70
Figure 12 - Table of chemically extracted levels of PPIX from colon treated with ALA, CP20 and CP94	72
Figure 13 - Mean area of necrosis as a function of the PDT treatment regime with CP94 being administered at various times relative to ALA	77
Figure 14 - Mean area of necrosis as a function of the PDT treatment regime with the compounds being administered as a mixed or separate solution	77
Figure 15 - Mean area of necrosis as a function of the PDT treatment regime using 25 mg/kg ALA i.v.	78
Figure 16 - Mean area of necrosis as a function of the PDT treatment regime using 200 mg/kg ALA i.v.	79
Figure 17 - Fluorescence of normal colonic mucosa, normal colonic muscle and colonic tumour as a function of the treatment regime (ALA with or without CP94)	86
Figure 18 - Mean volume of necrosis as a function of the PDT treatment regime in a colonic tumour model (ALA with or without CP94)	87
Figure 19 - Fluorescence image (a) and matched histology section (b) of skin using ALA alone. Fluorescence image (c) and matched histology section (d) of skin using ALA plus CP94	93

Figure 20 - Fluorescence of the epidermis as a function of time when administering ALA alone or ALA plus CP94, topically, treated flank (a) and untreated flank (b)	96
Figure 21 - Emission spectra from skin treated with ALA only (a) and ALA plus CP94 (b).....	97
Figure 22 - Treatment effect as a function of the time following topical administration of ALA with and without CP94	98
Figure 23 - Fluorescence image (a) and matched histology section (b) of uterus using ALA alone. Fluorescence image (c) and matched histology section (d) of uterus using ALA plus CP94	106
Figure 24 - Fluorescence of the endometrium and myometrium as a function of time when administering ALA alone (a) and ALA plus CP94 (b).....	109
Figure 25 - Emission spectra from uterus treated with ALA only (a) and ALA plus CP94 (b).....	110
Figure 26 - Histology sections of uterus taken following no treatment (a), ALA only (b) and ALA plus CP94 (c).....	111
Figure 27 - Mean area of necrosis as a function of the initial energy fraction.....	131
Figure 28 - Mean area of necrosis as a function of the number of energy fractions.....	131
Figure 29 - Mean area of necrosis as a function of the size of the energy fractions.....	132
Figure 30 - Mean area of necrosis as a function of the total energy delivered using 200 mg/kg ALA i.v.	134

Figure 31 - Mean area of necrosis as a function of the total energy delivered using 50 mg/kg ALA i.v.	134
Figure 32 - Mean area of necrosis as a function of the total energy delivered using 25 mg/kg ALA i.v.	135
Figure 33 - Fluorescence of the normal colonic mucosa, normal colonic muscle and colonic tumour as a function of the treatment regime (with or without 200 mg/kg ALA i.v.)	143
Figure 34 - Mean volume of necrosis as a function of the PDT treatment regime in a colonic tumour model (continuous or fractionated illumination)	144
Figure 35 - Mean area of necrosis as a function of the treatment regime using 200 mg/kg ALA i.v. and 25 J of 635 nm light.....	149
Figure 36 - Mean area of necrosis as a function of the treatment regime using 200 mg/kg ALA i.v. and 100 J of 628 nm light.....	149
Figure 37 - Tissue oxygen pressure as a function of time measured in the colon of groups of animals receiving neither ALA or light (a), ALA only (b) and light only monitored at 1 mm (c) and 3 mm (d)	158
Figure 38 - Tissue oxygen pressure as a function of time measured in the colon of groups of animals receiving ALA and continuous illumination monitored at 1mm (a) and 3 mm (b) or ALA and fractionated irradiation monitored at 1 mm (c) and 3 mm (d).....	161
Figure 39 - Fluorescence spectra recorded during continuous PDT	172
Figure 40 - Fluorescence spectra recorded during fractionated PDT using a single interval	172

Figure 41 - Fluorescence spectra recorded during fractionated PDT using multiple intervals	174
Figure 42 - Schematic diagram of the proposed mechanism for the ischaemia induced production of reactive oxygen species	178
Figure 43 - Schematic diagram summarising some of the reactions possible following reperfusion injury.....	179
Figure 44 - Table showing the mean area of necrosis as a function of the treatment regime, with SOD + CAT or Allopurinol being administered prior to illumination	183
Figure 45 - Table showing the mean area of necrosis as a function of the treatment regime, with SOD + CAT or Allopurinol being administered immediately after illumination.....	184

List of Abbreviations

ADP	Adenosine Diphosphate
ALA	5-Aminolaevulinic Acid
AlS ₄ Pc	Aluminium Tetrasulphonated Phthalocyanine
AMP	Adenosine Monophosphate
ATP	Adenosine Triphosphate
a.u.	Arbitrary Units
BPD-MA	Benzoporphyrin Derivative Mono-Acid
CAT	Catalase
CCD	Charge Coupled Device
CP20	1,2-dimethyl-3-hydroxypyridin-4-one
CP94	1,2-diethyl-3-hydroxypyridin-4-one
DHE	Dihaematoporphyrin Ether/Ester
DMSO	Dimethyl Sulphoxide
DNA	Deoxyribonucleic Acid
EDTA	Ethylene Diamine Tetra-acetic Acid
Fe ²⁺	Ferrous Iron
Fe ³⁺	Ferric Iron
H & E	Haematoxylin and Eosin
H ₂ O ₂	Hydrogen Peroxide
HpD	Haematoporphyrin Derivative
HPLC	High Performance Liquid Chromatography
Lu-TeX	Lutetium Texaphyrin
mTHPc	meta-Tetrahydroxyphenylchlorin
mRNA	Messenger Ribonucleic Acid
NPe6	Mono-Aspartyl Chlorin e6
¹ O ₂	Singlet Oxygen
O ₂ ^{•-}	Superoxide
•OH	Hydroxyl Radical

PBS	Phosphate Buffered Saline
Pc	Phthalocyanine
PDT	Photodynamic Therapy
PEG	Polyethylene Glycol
pO_2	Tissue Oxygen Pressure
PPIX	Protoporphyrin IX
SnET ₂	Tin Etiopurpurin
SOD	Superoxide Dismutase

Acknowledgements

This thesis was conducted at the National Medical Laser Centre, Institute of Surgical Studies, University College London and I would like to thank all the members of the department who have assisted me with its completion, particularly M.J. Postle-Hacon and Dr A.J. MacRobert. I am especially grateful to my supervisor Professor S.G. Bown for his shrewd advice and enthusiasm throughout.

I would also like to acknowledge the specific contributions of Dr R.J. Connell (section 2.1.7 - collaboration), Dr J.P. Connelly (section 2.1.7 - emission spectra), Dr J.C. Haller (and the Tunbridge Facility, University of Leeds) (section 2.2.5 - collaboration) and Dr B.W. McIlroy (section 2.1.3 - emission spectra and section 2.2.6 - fluorescence spectra).

Finally, I wish to thank all my friends and family for their unquestioning love and support and N. Lawrence and A. Curnow for their help in the final preparation of this thesis.

“One never notices what has been done;
one can only see what remains to be done.”

Marie Curie
(1867 - 1934)

SECTION I

INTRODUCTION

1.1 General Introduction

Photodynamic Therapy (PDT) is a non-thermal technique which can be used to produce localised tissue necrosis. It requires the systemic or topical administration of a photosensitiser which is activated *in situ* by light of a specific wavelength to form a cytotoxic species in the presence of molecular oxygen (Henderson and Dougherty, 1992). Lasers are generally employed to produce the light used and are coupled via an optical fibre to illuminate the treatment site which can be accessed directly, by endoscopy or surgery.

PDT is currently being investigated for a number of malignant, pre-malignant and other medical applications. These include the treatment of tumours and pre-malignant conditions in a whole range of organs, with particular interest being shown in pulmonary, gastrointestinal (particularly oesophageal cancer and Barrett's oesophagus), skin and brain tumours, as well as, superficial bladder cancer (Stewart *et al*, 1998). Non-malignant applications are just as varied and include the treatment of arterial restenosis after angioplasty, age-related macular degeneration and rheumatoid arthritis, in addition to endometrial ablation and a variety of dermatological conditions.

Many clinical trials are in progress around the world with a number of different photosensitisers but currently only PDT with the photosensitiser Photofrin, has health agency approval to be used as a clinical treatment. This includes superficial bladder

cancer (Canada), early stage lung cancer (Germany, Holland, Japan and USA), advanced lung cancer (France and Holland), advanced oesophageal cancer (Canada, France, Holland, Japan and USA), gastric cancer (Japan) and cervical cancer and dysplasia (Japan). Many other approvals are currently pending (Carruth, 1998; Dougherty *et al*, 1998).

Photofrin (otherwise known as dihaematoporphyrin ether/ester (DHE)) is the most established and tested photosensitiser. It is a mixture of haematoporphyrins, but is purer than its predecessor haematoporphyrin derivative (HpD). It is activated *in situ* with red light (at a wavelength of 630 nm) to cause localised tissue damage in the presence of molecular oxygen. Unfortunately, it causes prolonged cutaneous photosensitivity, which results in patients given this treatment having to avoid bright light for a period of up to three months (to avoid the sunlight activating the photosensitiser in their skin and creating unwanted PDT damage) (Levy, 1994). Photofrin, although being a clinically useful photosensitiser is, therefore, far from ideal and alternative photosensitisers are being investigated as a result.

There are a number of second generation photosensitisers currently being studied, one of the most promising is meta-tetrahydroxyphenylchlorin (mTHPc), otherwise known as Foscan. This photosensitiser shows greater activity than Photofrin, requiring little energy to be activated with 652 nm light which penetrates deep into tissue. Although less than that observed with Photofrin, cutaneous photosensitivity still remains a problem (duration of about one month). Other photosensitisers of note, include benzoporphyrin derivative mono-acid (BPD-MA, activated at 690 nm, photosensitivity up to one week), mono-aspartyl chlorin e6 (NPe6, activated at 664

nm, photosensitivity of only a day or two), tin etiopurpurin (SnET₂, activated at 660 nm with slightly better photosensitivity than Photofrin), lutetium texaphyrin (Lu-TeX, activated at 732 nm with little cutaneous photosensitivity) and aluminium or zinc phthalocyanine (Pc, activated at 670 nm with photosensitivity of a couple of weeks) (Bonnett, 1995; Stewart *et al*, 1998).

The photosensitiser investigated in this thesis, however, is 5-aminolaevulinic acid (ALA) induced protoporphyrin IX (PPIX). This photosensitiser is different from all those mentioned above, as it is a naturally occurring endogenous photosensitiser, normally present in controlled amounts in the majority of human cells. When ALA is administered exogenously, the haem biosynthesis pathway, which is responsible for the production of haem, is overloaded. This results in a temporary build up of PPIX (the precursor of haem) as the last step of this pathway, the chelation of iron to PPIX to form haem, is relatively slow. The resulting accumulation of PPIX can then be utilised to cause a photodynamic effect when it is activated using 635 nm light. Any PPIX remaining in untreated tissues of the body is metabolised normally, thus resulting in a short period of cutaneous photosensitivity (1 - 2 days) (Kennedy and Pottier, 1992).

Clinically, it has been found that ALA induced photosensitisation using the maximum tolerated oral ALA dose (60 mg/kg), only produces limited necrosis (Barr *et al*, 1996; Gossner *et al*, 1998; Regula *et al*, 1995) being more suitable for applications where a superficial effect followed by healing without scarring is required. These findings have resulted in a number of techniques being investigated, to see if it is possible to increase the PDT effect of this treatment without increasing the administered dose of

ALA. Two such techniques, namely, the administration of an iron chelating agent (Chang *et al*, 1997) or the fractionation of the light dose (Messmann *et al*, 1995), are investigated in the experimental section of this thesis.

1.2 Background

Although the concept of PDT has been around for a long time, ALA was not used clinically as a photosensitising agent until 1990 (Kennedy *et al*) and *in vitro* and *in vivo* experiments commenced in 1987 (Malik and Lugaci and Peng *et al*, respectively). ALA PDT has now become one of the most active fields in PDT research.

The concept of using ALA as a photosensitising agent has really developed from the knowledge that natural protoporphyrin IX is an excellent photosensitiser, inducing light sensitivity in the skin of porphyric patients. The porphyrias are a family of inherited diseases, each associated with a partial defect of one of the haem biosynthesis enzymes (beyond ALA synthase) which can result in porphyrin accumulation, skin photosensitivity and neurological dysfunction. The major point of regulation of the haem biosynthesis pathway is the negative feedback inhibition of haem on the enzyme ALA synthase. This enzyme is responsible for catalysing the committed step of the pathway, the formation of ALA from succinyl-CoA and glycine. If one of the enzymes between this step and the formation of haem is deficient, this inhibition is removed and an accumulation of porphyrins can occur (Batlle, 1993).

Since haem-containing enzymes are essential for energy metabolism, all nucleated cells have the capacity to form PPIX and therefore haem. It is, therefore, possible

through the exogenous administration of ALA, to bypass the normal rate limiting step of the pathway and create a temporary accumulation of PPIX; as the final step of the pathway, the chelation of iron to PPIX to form haem, is relatively slow. This enables the natural photosensitiser PPIX, to be used for PDT treatment (Kennedy and Pottier, 1992). ALA is, therefore, really a pro-drug which is metabolised by the body into its active form, PPIX. In many types of tumours, the haem biosynthesis pathway is known to be disrupted, which can result in porphyrin accumulation in these malignancies without exogenous ALA administration. This can enable, in certain circumstances, greater sensitivity to occur in these tumours (than the surrounding normal tissues) when ALA is administered (Peng^b *et al*, 1997).

The haem biochemistry pathway is shown in Figure 1. The majority of this pathway was determined in the 1950's by Shemin (USA) and Neuberger (UK), with ALA and ALA synthase being described for the first time (Jordan, 1991). It was discovered, that ALA synthase catalyses the committed step of the pathway, the condensation of glycine and succinyl-CoA to produce ALA. This enzyme is located in the mitochondria reflecting the fact that succinyl-CoA is one of the substrates and the major source of succinyl-CoA for haem biosynthesis is the Krebs cycle. It should also be noted that this is the only activated substrate required by the pathway, the rest of the steps being energetically 'downhill'. The enzyme is highly specific for glycine with no other amino acid being acceptable.

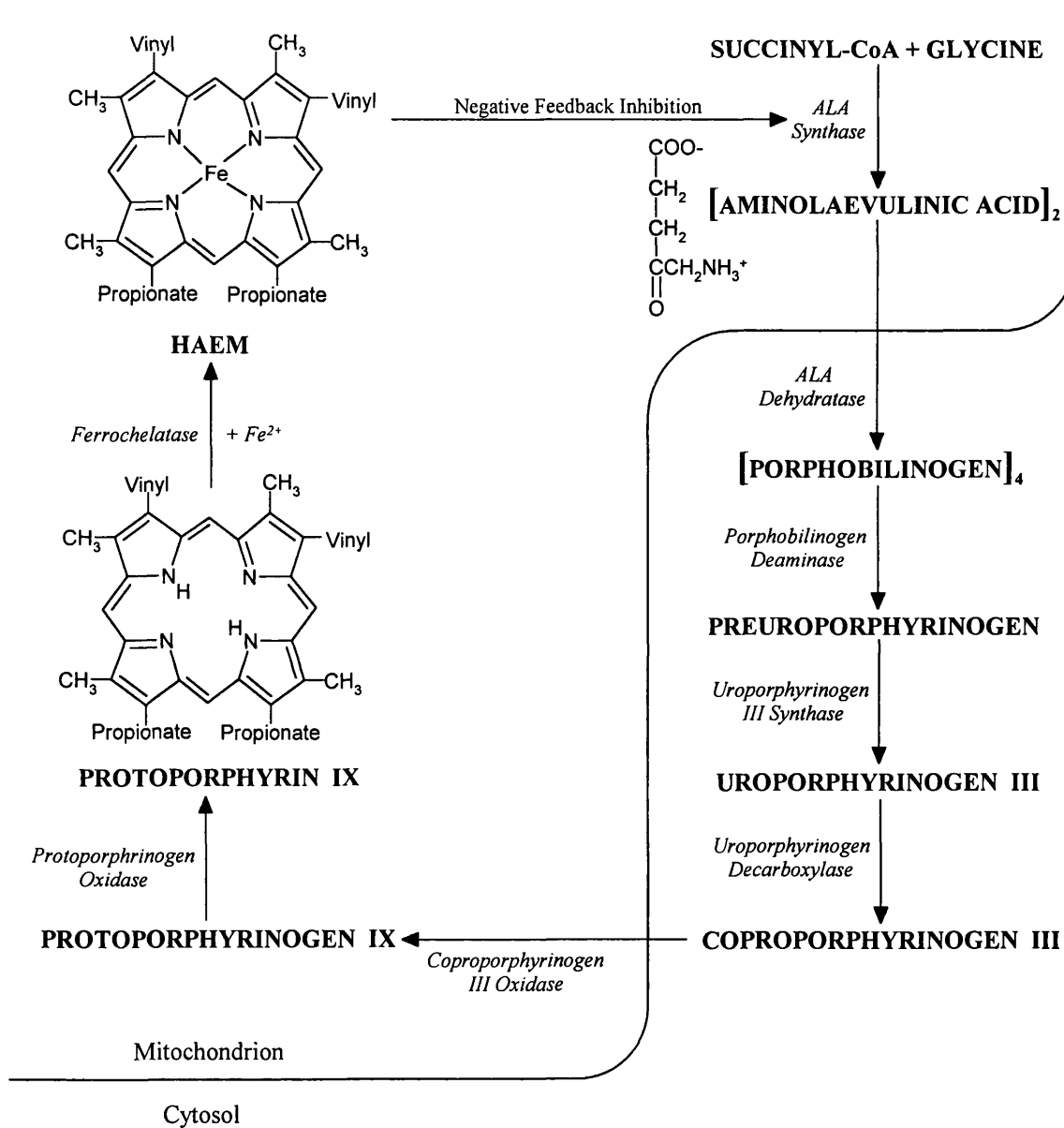


Figure 1 Schematic diagram of the haem biosynthesis pathway.

Haem is known to prevent its own formation through the inhibition of the production of ALA synthase on both the transcriptional and translational levels. This enzyme also has a short half-life so it rapidly depletes if the formation of new enzyme is prevented. Haem is also thought to directly inhibit ALA synthase and the movement of this enzyme from the cytosol into the mitochondrion. It is also known that the formation of ALA synthase is induced by cellular haem depletion (Batlle, 1993).

The next step in the pathway is the dimerization of two ALA molecules to form porphobilinogen, catalysed by ALA dehydratase which is located in the cytosol. This enzyme requires zinc for its action and is inhibited by lead, resulting in patients with lead poisoning having large amounts of ALA in their blood. Four molecules of porphobilinogen are then condensed by porphobilinogen deaminase to form the linear tetrapyrrole, preuroporphyrinogen which is then rearranged and cyclized by uroporphyrinogen III synthase to produce uroporphyrinogen III. Without the latter enzyme, it is possible for preuroporphyrinogen to cyclize without rearrangement to form uroporphyrinogen I. The acetate side chains of uroporphyrinogen III are decarboxylated by uroporphyrinogen decarboxylase to form coproporphyrinogen III. This is the last step that occurs in the cytoplasm. Coproporphyrinogen III oxidase (in the mitochondrion) then catalyses the oxidative decarboxylation of two of the propionate side chains of coproporphyrinogen III to create the vinyl groups of protoporphyrinogen IX. This is then oxidised by protoporphyrinogen oxidase to produce the final precursor of haem, PPIX (Jordan, 1991).

The last step of the haem biosynthesis pathway is the insertion of ferrous iron into the porphyrin ring of PPIX and is catalysed by ferrochelatase. Ferrochelatase has broad substrate specificity and will insert iron into a number of porphyrins. Ferrous iron can also be replaced by other metal ions such as zinc or cobalt but not ferric iron. Metal ions such as mercury and lead are known to be potent inhibitors of ferrochelatase (Jordan, 1991). As a substrate of the final step of haem synthesis, iron availability has an important regulatory action on this pathway. It also affects the free haem pool and induces the main regulatory enzyme of the pathway, ALA synthase (Batlle, 1993).

Haem production is so closely regulated as it is a prosthetic group of essential proteins such as haemoglobin, catalase, peroxidase and cytochrome c. Haem that has served its purpose is broken down and excreted from the body. The first step in this process is the conversion of haem to biliverdin which is catalysed by haem oxidase and requires oxygen. Biliverdin reductase then reduces biliverdin to form bilirubin, which is transported to the liver and glucuronidated (to make it more soluble) producing bilirubin diglucuronide which is secreted into bile. The iron component of haem is recycled during this process (Stryer, 1988).

So, during ALA induced PDT we are manipulating this complex and intricate biochemical system to create a temporary accumulation of PPIX. ALA is administered as it bypasses the major control point of the pathway (the negative feedback inhibition of haem on ALA synthase), overloads the pathway with substrate, thus, forcing all subsequent enzymes to operate at maximal rate. PPIX accumulates as

it is being produced faster than it can be converted into haem. This approach is used rather than just administering PPIX itself, as PPIX is poorly soluble in water at physiological pH. The administration of other precursors of PPIX has also been considered but problems of solubility and cost has been prohibitive (Kennedy and Pottier, 1992). ALA is water soluble and is usually administered systemically as an oral preparation or applied topically, although, intravenous administration and intravesical instillations have also been investigated. Aqueous solutions of ALA are chemically unstable when buffered to physiological pH. ALA hydrochloride powder dissolved in sodium hydroxide ~~buffer~~ to produce a solution of pH 2.35 is known to be stable, however (Elfsson *et al*, 1998). It is not normally necessary to extensively buffer oral or topical ALA preparations but care must be taken when preparing buffered ALA solutions for intravenous administration.

Sensitivity to ALA induced PDT depends, at least in part, on the rate of PPIX production within a cell. The metabolic activity of the cell may fluctuate at different times of the cell cycle, as may enzyme activity. It is known that actively proliferating cells produce more PPIX following ALA administration than quiescent cells and this may be related to iron availability (Wyld *et al*, 1998). When malignant and non-malignant cells of similar lineage are exposed to exogenous ALA, the malignant cells almost always accumulate more PPIX, probably as a result of altered enzyme expression and activity. The degree of cell differentiation may also play a role with malignant cells often being less differentiated than the normal ones from which they arose (Li *et al*, 1999). It is a characteristic of ALA induced PPIX photosensitisation that PPIX tends to accumulate in the mucosa of hollow organs, rather than in the

underlying muscle (Loh *et al*, 1993). This makes this PDT modality particularly suited to the treatment of dysplasias and malignancies of the linings of hollow organs such as the gastrointestinal tract, without damaging the muscle layers extensively and thus reducing the risk of scarring and strictures. There is also a lower risk of perforation as collagen is preserved.

When ALA is administered orally, it is absorbed from the gastrointestinal tract into the bloodstream. ALA is thus distributed to the tissues where it is taken up by cells. It is thought that ALA may enter cells by a mechanism of active transport. Once inside the cell, the abnormally high levels of ALA make it possible for iron catalysed, aerobic formation of reactive oxygen species to occur even without light administration. Respiration can also be uncoupled causing mitochondrial swelling and other toxic effects have been reported. The primary sites of damage of ALA induced PDT are likely to be those sites where PPIX is produced and because PPIX is generated in mitochondria, this is a major site of intracellular damage. It is likely though that the initial site of damage may only be the first step in a whole cascade of reactions, however, which can ultimately result in cell death (Peng^a *et al*, 1997).

Wherever sufficient quantities of PPIX, red light and oxygen are present, photodynamic reactions can occur. These are short lived and involve the transformation of the ground state photosensitiser into an excited triplet state. The process can then follow two courses. In type I reactions, this excited molecule reacts directly with biological substrates forming radicals and reactive oxygen species. Type

II reactions involve the transfer of energy to oxygen to form singlet oxygen, a highly reactive oxidative species (Henderson and Dougherty, 1992). Alternatively, the excited photosensitiser can emit fluorescence as it decays back to the ground state. This property is often utilised by investigators to locate and quantify photosensitisers in tissues and can also be used for photodynamic diagnosis (Baumgartner and Stepp, 1998). Both type I and II products are highly reactive with very short half-lives (10 - 50 μ s). Damage produced by these species is, therefore, localised to areas which are illuminated and contain sufficient amounts of photosensitiser and oxygen. This is the basis of selective PDT treatment. Both type I and II reactions are oxygen dependent and occur *in vivo* but singlet oxygen production is generally thought to be the major cause of PDT damage (Stewart *et al*, 1998). Figure 2 shows a schematic diagram summarising these reactions.

Being oxygen dependent, these reactions lead to oxygen depletion. This can happen for two reasons, either the consumption of oxygen by the photodynamic reactions is faster than the rate of oxygen replenishment, or the local vasculature collapses resulting in ischaemia. This latter mechanism is particularly important during Photofrin PDT as although oxygen depletion reduces the photodynamic process, such vascular damage could result in tissue damage to the whole region affected (Stewart *et al*, 1998). Direct cell damage can cause cell death by either inducing programmed cell death (apoptosis) or causing necrosis directly. Apoptosis is a protective mechanism possessed by cells to 'commit suicide' in response to some cellular injury. The mechanism by which cells die as a result of ALA PDT, depends on the treatment parameters employed (Noodt *et al*, 1996).

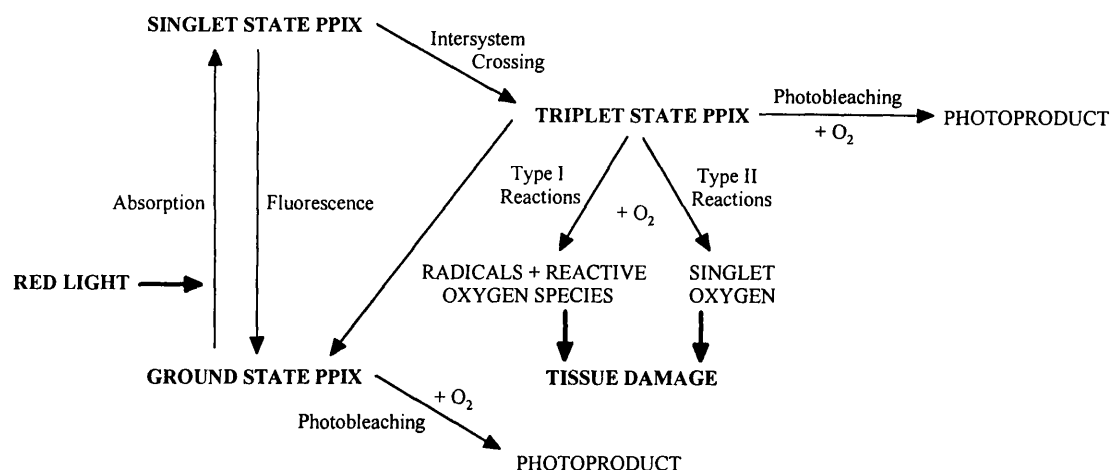


Figure 2 Schematic diagram summarising the reactions involved in the mechanism of ALA induced photodynamic therapy.

During illumination, PPIX can undergo photobleaching. This process of photosensitiser degradation (by products generated by the photochemical reaction) results in a reduction of PPIX available for PDT. It can occur in solution or *in vivo* and is oxygen dependent. When PPIX is photobleached a photoproduct (photoporphyrin) is produced. The generation of this photoproduct can be monitored as an increase in approximately 670 nm fluorescence on an emission spectrum. PPIX itself gives a characteristic emission spectrum with a maximum at approximately 636 nm. Light irradiation for ALA induced PPIX PDT is, therefore, usually delivered at 630 - 635 nm to match the PPIX absorption spectrum. This light is usually produced by a monochromatic laser, although some studies employ broad light sources. Many groups use tunable argon ion or copper vapour pumped dye lasers but as therapies become more established, specifically made, low maintenance, easily used

semiconductor lasers are being more commonly used clinically. Light of this wavelength (630 - 635 nm), however, does not penetrate deep into human tissue (only a few millimetres). Photosensitisers which can be activated using longer wavelengths, thus enabling greater tissue penetration are therefore being investigated (Peng^b *et al*, 1997). PPIX has a similar absorption spectrum to that of Photofrin and therefore has similar efficiency as a photosensitiser. PPIX is not as efficient as mTHPc, however, and therefore PDT using this photosensitiser requires substantially higher energy doses as a result (Stewart *et al*, 1998).

Over the past decade much research has been conducted investigating ALA PDT. *In vitro* studies have tended to concentrate on ALA cellular uptake, PPIX formation and localisation within cells, and mechanisms of cell death following illumination. *In vivo* investigations have focused on ALA/PPIX pharmacokinetics, PPIX distributions within different normal and malignant tissues, treatment parameter optimisation, techniques to enhance this modality as well as more mechanistic studies. This work has contributed to a better understanding of this technique, which has enabled clinical trials to commence for a number of applications, although, there are still questions yet to be answered (Peng^a *et al*, 1997).

Unlike many other photosensitisers, light irradiation can take place only a few hours after ALA administration (depending on route of administration, tissue to be treated etc.). This is a major improvement over Photofrin which needs to be administered two days prior to light delivery (Stewart *et al*, 1998). Side effects with ALA treatment are

also improved, skin photosensitivity being reduced to only a day or two. Pain is often experienced, however, during light irradiation, but may be controlled with appropriate analgesia/local anaesthesia (Kennedy *et al*, 1996). Other side effects include transient elevation of liver function tests (with high doses of oral ALA administration) and the possibility of some neurotoxicity (Marcus *et al*, 1996). These latter effects are also exhibited by some porphyric patients. It is these transient effects on liver function which are responsible for the maximum tolerated oral dose of ALA currently being only 60 mg/kg. These effects could be associated with entero-hepatic recirculation and the large capacity of the liver to synthesize porphyrins. One benefit of ALA PDT, however, is the ability of normal tissues to heal necrosed areas. This results in excellent healing, without scar formation and thus good cosmesis following PDT treatment using this photosensitiser (Fan *et al*, 1996).

Although, ALA induced PDT is being investigated for numerous clinical applications, it has become evident that this modality is best suited to superficial conditions such as dysplasia (Dougherty *et al*, 1998). This is partially the result of limited light penetration into tissue at this wavelength and partially due to the tissue distribution of PPIX being higher in mucosa layers than in underlying tissues. Thus, adequate light and drug doses are not present in deeper tissues to cause a significant effect. These properties can, however, be advantageous in certain circumstances where only superficial necrosis, followed by good healing and minimal cutaneous photosensitivity is desirable (Kennedy *et al*, 1996).

ALA PDT is currently being investigated for a number of malignant, pre-malignant and non-malignant conditions with particular interest being shown in dermatological applications, Barrett's oesophagus and endometrial ablation (Kennedy *et al*, 1996; Marcus *et al*, 1996; Peng^b *et al*, 1997; Roberts and Cairnduff, 1995). ALA can be applied topically for dermatological conditions and penetrates abnormal stratum corneum better than normal keratinized skin. This enables increased selectivity to occur when treating some cutaneous lesions (Kennedy and Pottier, 1992). Only superficial, thin lesions can usually be treated successfully, with poorer results being obtained with thicker nodular lesions. It is possible with ALA PDT, however, to repeat treatments after only a few days, if necessary. Systemic administration is usually conducted orally as a treatment for tumours and pre-cancers of the aerodigestive tract but it is also possible to use local instillations to treat the lining of organs such as the bladder and uterus. Once again limited success has been obtained, but, problems remain with the extent of the effect. It is for this reason that several techniques to enhance the effect produced by ALA PDT are being investigated (Peng^b *et al*, 1997).

As well as optimising the treatment parameters of ALA PDT numerous techniques of enhancement are currently being investigated. These include ALA esters which have been developed over the last few years, as they are more lipophilic than standard ALA preparations and, therefore, are taken up by cells more readily. The methyl ester has been found to be particularly good for topical applications (Peng^b *et al*, 1997). Another method to increase ALA penetration when treating skin is to pretreat with a

solvent such as dimethylsulfoxide (DMSO), or to use a physical technique such as tape-stripping to further enhance ALA penetration (Peng^b *et al*, 1997).

Oral administration can be split into several smaller doses in an attempt to deliver a higher overall dose without excessive adverse effects and treatments may be repeated as frequently as necessary to treat the condition (Fan *et al*, 1996). Investigations are also being conducted to determine the benefit of combining ALA PDT with other modalities such as low dose Photofrin to improve the PDT effect whilst minimising side effects (Peng^b *et al*, 1997). A recent study combining ALA PDT with simultaneous hyperthermia has shown this technique to be of some benefit, enabling light doses to be reduced, although further investigation will be necessary to optimise this method (Orenstein *et al*, 1999).

Light dose fractionation is another technique which can be used to enhance ALA PDT and can produce up to five times more necrosis than continuous irradiation. It is simple in concept and requires the light dose to be interrupted for only a short period of time, presumably allowing the tissue to reperfuse during this dark interval (Messmann *et al*, 1995). It is also possible to improve the effect of ALA PDT through the use of low fluence rates. This probably reduces the oxygen depletion often experienced at higher fluence rates and thus enhances the treatment (Robinson *et al*, 1998). Preliminary experiments combining PDT with bioreductive drugs (which are metabolised under hypoxic conditions to produce cytotoxic species) indicate that these

compounds may also improve the effect of PDT by taking advantage of the oxygen depletion that occurs during a normal PDT treatment (Bremner *et al*, 1992).

ALA PDT can also be enhanced through further manipulation of the haem biosynthesis pathway. Paradoxically, it has been shown that inhibition of protoporphinogen oxidase actually results in the product of the inhibited reaction, PPIX, accumulating. This happens as the substrate of the inhibited reaction, protoporphrinogen, accumulates and can be converted into PPIX through another, nonenzymatic route (Halling *et al*, 1994). Alternatively, inhibitors of ferrochelatase or iron chelators can be used to inhibit the formation of haem, thus, increasing PPIX accumulation by reducing its conversion into haem (Peng^a *et al*, 1997).

Much, however, can be done to enhance ALA PDT through the simple optimisation of its treatment parameters and the development of real-time monitoring systems to monitor clinical ALA PDT as it is in progress. This should allow treatment parameters to be determined and thus optimised on a patient to patient basis.

1.3 Thesis Scheme

The aim of this thesis is to investigate potential methods of ALA PDT enhancement, to try to overcome the present limitations associated with this PDT modality, namely, the limited amount of damage it produces clinically. Two of the previously mentioned techniques of enhancement are studied in this thesis. These are the administration of an iron chelating agent and the fractionation of the light dose.

The first half of the experimental section is devoted to investigating a relatively new class of iron chelating agents called the hydroxypyridinones, to observe whether these compounds can improve the outcome of ALA PDT in a number of animal models. This work follows that of Chang *et al* (1997) who found that one of these compounds could double the PPIX fluorescence in the urothelium of the bladder when applied as a local instillation with ALA. The second part of the experimental section studies the technique of light dose fractionation to initially determine its effect and optimal treatment parameters in a single animal model and then examines its mechanism of action. This research continues that of Messmann *et al* (1995) who found that this technique could increase the damage produced by ALA PDT by up to a factor of five.

Both methods have, therefore, previously been indicated to be of use when combined with ALA PDT and as such warrant further detailed study to determine if significant enhancement of ALA PDT can be achieved through the optimisation of these techniques, so that they may become of clinical benefit in the future.

SECTION II

EXPERIMENTATION

2.0.0 Laser Comparison

2.0.0.1 Introduction

The first experimental section of this thesis is really an aside to the main text. It concerns the comparison of the effect produced by the two lasers employed throughout the thesis. In an ideal world only one type of laser would have been used for all of these experiments, but unfortunately due to a major irreparable breakdown of the pulsed copper vapour laser used to start these experiments, it was necessary to continue using a laser diode system. The difference in type of laser isn't really a problem in itself, but the difference in excitation wavelength that resulted is.

The copper vapour laser employed during this thesis was tuned to 635 nm throughout, to match the peak in the absorption spectrum of PPIX. The wavelength of the laser diode was fixed by its manufacturer, and in this case although initially thought to be 630 nm as labelled, was actually set at 628 nm to match the absorption spectrum of Photofrin, the photosensitiser it was originally designed to be used with.

A series of control experiments, using the two major sets of parameters used in the experiments of this thesis, have therefore been conducted to investigate any differences produced by the different lasers, using slightly different excitation wavelengths.

2.0.0.2 Materials and Methods

Chemicals

ALA powder (ALA.HCl, 99% purity, DUSA Pharmaceuticals, Inc., New York, USA) was dissolved in physiological strength phosphate-buffered saline (PBS, pH 2.8) and administered intravenously (with a concentration of 50 or 200 mg/ml and a maximum volume of 0.2 ml).

Animal model

Normal, female, Wistar rats (120 - 200 g) supplied by the Imperial Cancer Research Fund (London, UK) were used throughout. The animals were anaesthetised for all parts of the procedure using inhaled halothane (ICI Pharmaceuticals, Cheshire, UK) and analgesia was administered subcutaneously following surgery (Buprenorphine hydrochloride, Reckitt & Colman Products Ltd, Hull, UK).

PDT studies

In the first series of experiments, all animals were given 50 mg/kg ALA intravenously, 75 minutes prior to surgery. The colon was accessed for PDT via a laparotomy. The light source was either a pulsed (12 kHz) copper vapour pumped dye laser (Oxford Lasers, Oxford, UK) tuned to 635 nm (+/- 1-2 nm) or a laser diode (Diomed Ltd, Cambridge, UK) set at 628 nm (+/- 1-2 nm). A total energy of 100 J was delivered via a 200 μ m plane cleaved optical fibre (output power, 100 mW) passed through the anti-mesenteric colon wall (approximately 1 cm distal to the caecum) so that it just touched the mucosa of the opposite side (area of contact = 0.03 mm²). The rest of the

abdominal viscera were shielded from forward light scatter by a piece of opaque paper positioned so that it did not touch the colon, or affect its light distribution.

This is a model that we have used many times successfully in the past (Barr *et al*, 1990; Messmann *et al*, 1995). The light fluence where the fibre touches the tissue is very high (320 W/cm^2) but no thermal effect was observed in the light only control group. As the light fluence falls off rapidly with increasing distance along the colon wall from the fibre tip, measuring the diameter of the zone of necrosis in the wall of the colon is a convenient way of comparing the efficacy of PDT necrosis with different treatment parameters.

All animals were recovered following surgery and killed after three days, as mucosal damage is maximal at this time (Barr *et al*, 1987). The treated area of colon was excised, cut longitudinally and flattened out so that the lesion produced by the treatment could be determined macroscopically by measuring the minimum (a) and maximum (b) perpendicular diameters of the lesion with a micrometer. These values were then used to calculate the area of necrosis using the formula $\pi ab/4$, as the lesions produced were approximately elliptical. All appropriate drug only and light only control groups were also conducted.

Representative specimens were fixed in formalin, sectioned and stained with haematoxylin and eosin, so that conventional light microscopy could confirm the macroscopic findings. This endpoint enabled a direct comparison of the treatment groups so that the most effective regime (the one which produced the most necrosis) could be determined.

The same experiment was repeated using an ALA dose of 200 mg/kg ALA i.v. and a total energy dose of 25 J delivered by either light source, two hours after ALA administration.

The experimental data of Messmann *et al* (1995) is also included on each of the figures, so that further comparisons can be made whilst using each set of experimental parameters and the copper vapour laser tuned to 630 nm.

The number of animals in each treatment group varied slightly and is, therefore, marked on each figure. Statistical analysis between the means of the different treatment groups was conducted using unpaired student t-tests. Error bars on all the figures were determined by the standard error of the mean.

2.0.0.3 Results

At post mortem, the lesions seen in the colon were approximately elliptical, the longer diameter being found along the colon and the shorter being found across the colon. Lesion diameters ranged from 3 - 15 mm, with an average ratio of 1.5:1 between the maximum and minimum diameters (maximum ratio 3:1). The elliptical shape of the lesions was thought to be due to the geometry of applying light to a cylindrical organ, and then measuring the effect when the organ had been opened and laid flat.

Histological analysis of fixed sections showed areas of necrosis in all the treated groups. This was full thickness in places. It is likely that this occurred (even though the level of PPIX is much lower in the colonic muscle than the colonic mucosa) because of the high incident fluence rate used in this model, as well as the thinness of the rat colon. A combination of these factors may have allowed a sufficient level of light to penetrate into the muscle to cause necrosis. Even though full thickness necrosis was observed in some sections and large lesions (relative to the size of the rat colon) were produced in some cases, no animal showed evidence of colonic perforation or stenosis at post mortem (even though occasional lesions were circumferential) and no other abdominal organs appeared affected by the treatment.

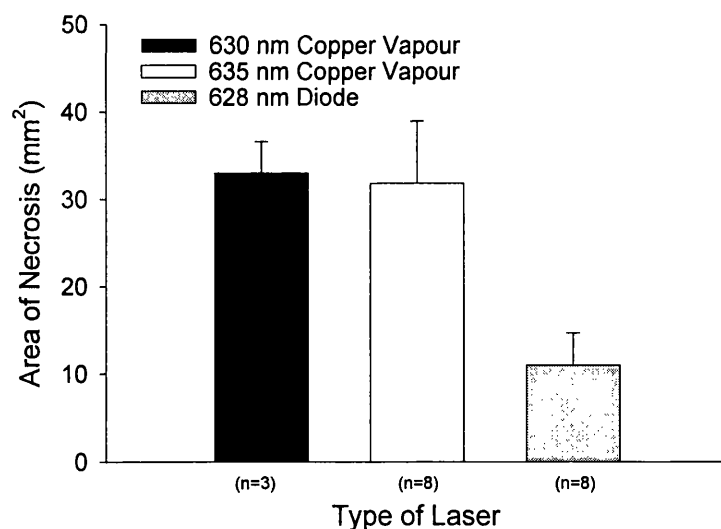


Figure 3 Mean area of necrosis (mm²) as a function of laser and wavelength. 50 mg/kg ALA i.v. was administered 75 minutes prior to 100 J of light (100 mW). Error bars as determined by the standard error of the mean. 630 nm copper vapour data from Messmann *et al* (1995).

The mean area of necrosis (mm^2) produced by each wavelength, using 50 mg/kg ALA i.v., is plotted in Figure 3. It shows that there is little difference between the area of necrosis produced, if the copper vapour laser is used to deliver the energy dose at either 635 nm or 630 nm. If the laser diode (set at 628 nm) was used, however, a significantly smaller area of necrosis was produced (635 nm = 32 mm^2 and 628 nm = 11 mm^2) ($p < 0.02$).

The mean area of necrosis (mm^2) produced by each wavelength, using 200 mg/kg ALA i.v., is plotted in Figure 4. It shows that there is a small difference between the area of necrosis produced if the copper vapour laser (tuned to 635 nm) is used to deliver the energy dose instead of the laser diode set at 628 nm. This difference, however, is not significant (635 nm = 22 mm^2 and 628 nm = 13 mm^2) ($p < 0.16$).

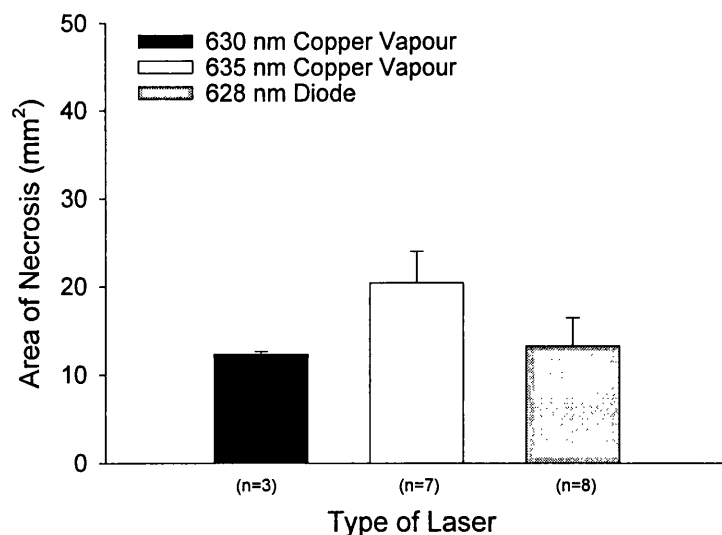


Figure 4 Mean area of necrosis (mm^2) as a function of laser and wavelength. 200 mg/kg ALA i.v. was administered 2 hours prior to 25 J of light (100 mW). Error bars as determined by the standard error of the mean. 630 nm copper vapour data from Messmann *et al* (1995).

2.0.0.4 Discussion

The results of this section indicate that the area of necrosis produced by ALA PDT in this model, using these parameters, is affected by the wavelength of the excitation light. There was greater evidence of this using the lower ALA dose of 50 mg/kg i.v. than at the higher dose of 200 mg/kg i.v. This may be due to the PDT effect being more reliant on the energy dose at the lower ALA dose, with 100 J being necessary not to be limiting, whereas, at 200 mg/kg ALA i.v. only 25 J is required to be above a threshold energy dose (Messmann *et al*, 1995).

The slight difference in wavelength, can in certain circumstances, make a significant difference to the outcome of the treatment. It is known that 635 nm is a better excitation wavelength of ALA induced PPIX *in vivo* than 630 nm (Szeimies *et al*, 1995) and as the wavelength is shifted either further towards the blue or into the red, less energy will be absorbed by the drug.

Comparisons have already been made between a copper vapour laser and diode laser at a wavelength suitable for mTHPc excitation (652 nm) (De Jode *et al*, 1996). At this wavelength, however, using this photosensitiser, no difference between the lasers (as determined by the outcome of the treatment) was observed. It is therefore unlikely that the use of a different type of laser has made a difference in the current study and it can probably be concluded, that it is the small shift in wavelength that is accountable for the differences observed.

Results obtained from experiments conducted with the 635 nm copper vapour laser and 628 nm diode laser are, therefore, not directly comparable and as a result, results using the two different lasers will be kept separate, with the laser employed being indicated in each figure legend throughout this thesis.

PART I

Enhancement of ALA PDT using Iron Chelators

2.1.1 Introduction

PDT using ALA is limited clinically by the ALA dose which can be tolerated orally. It is thought that the transient elevation of liver enzymes found after oral administration of ALA, is related to the high levels of ALA reaching the liver after absorption from the upper gastrointestinal tract. This is most likely due to the ALA itself, although it is difficult to be sure it is not due to the PPIX produced from the ALA. If it is due to the ALA, one way to overcome this problem may be the administration of an iron chelating agent in combination with the ALA, as reported here. This enhances the effect of the treatment, producing more necrosis, without increasing the administered dose of ALA.

This method further manipulates the haem biosynthetic pathway, as not only is the normal regulation of the pathway being avoided by the exogenous administration of ALA resulting in all subsequent enzymes being forced to operate at maximal rate, but the iron chelator also inhibits the final step of the pathway (and the secondary rate limiting point) by removing Fe^{2+} from the system. This results in an even greater accumulation of PPIX, which can then be utilised for PDT. In addition to this, the resultant low intracellular iron concentration also inhibits translation of ALA synthase mRNA, which would normally (without exogenous ALA administration) be a major point of regulation for this pathway (Cox *et al*, 1991).

Iron has the ability to exist in several oxidation states and the tendency to form stable co-ordination complexes, which makes it a vital component of the oxygen-transporting molecule haemoglobin, as well as cytochromes, and many other important enzymes. The average 70 kg man contains about 4 g of iron, 65 % of which is contained in haemoglobin (Rang & Dale, 1991). The body is very efficient at recycling iron and only small amounts are lost each day in the urine, faeces, sweat and cells sloughed from the skin (also in menstrual blood in women) (Vander *et al*, 1990).

In order to maintain the iron balance of the body, the iron lost must be replaced by ingestion of iron-containing foods, such as meat, beans, nuts and cereals. Iron in meat is usually in the form of haem and 20-40% of haem iron is available for absorption (Rang & Dale, 1991). Non-haem iron in food (and in vitamin supplements) is mainly in the ferric state (Fe^{3+}), which is poorly soluble in the neutral pH of the intestine. In the stomach, however, the iron dissolves and binds to a mucoprotein which functions as a carrier, transporting the iron to the intestine in the more soluble ferrous form (Fe^{2+}). The degree of iron absorption by intestinal mucosal cells is the main point of regulation of iron balance and is influenced by the body's iron stores. If the body's stores of iron are high, the iron is stored within the mucosal cells as ferritin, if stores are low, the iron is passed on to the plasma where it is transported bound to transferrin (Vander *et al*, 1990).

Iron in the body is stored in two forms, soluble ferritin (found in all cells, particularly liver, spleen and bone marrow) and insoluble haemosiderin, which is a degraded form of ferritin. As the body has no way of actively excreting iron, the iron balance is critically dependent on the active absorption mechanism in the intestine. A significant

upset of iron imbalance can result in either iron deficiency, leading to inadequate haemoglobin production (microcytic hypochromic anaemia) or iron excess which has serious toxic effects (Vander *et al*, 1990). Sometimes, iron overload can be caused by giving repeated blood transfusions to treat haemolytic anaemias such as thalassaemia and is usually treated by life-long, frequent, long, infusions (9 - 12 hours duration, 5 - 7 nights per week) of the iron chelating agent, desferrioxamine (Brittenham, 1992).

Desferrioxamine and other iron chelators such as ethylenediamine tetraacetic acid (EDTA) have been investigated as potential enhancers of ALA PDT. They can do this by chelating iron, thus reducing the conversion of PPIX to haem, resulting in an even greater accumulation of PPIX and thus a greater photodynamic effect (Chang *et al*, 1997). EDTA has lower activity than desferrioxamine, probably as a result of its membrane impermeability and low specificity for Fe^{3+} (Richardson *et al*, 1994) but it has been found to virtually double porphyrin production and triple photodynamic inactivation of K562 leukemic cells in culture (Hanania and Malik, 1992) and enhance the treatment of viral infections with ALA PDT (Smetana *et al*, 1997). Desferrioxamine, on the other hand, is both specific for iron and can penetrate into the cellular cytosol (Berg *et al*, 1996) resulting in an increased enhancement of ALA PDT (Ortel *et al*, 1993). Berg *et al* (1996) studied the effect of both desferrioxamine and EDTA in two different cell lines and found desferrioxamine to be the most effective. They also found that the relative gain in PPIX accumulation increased with decreasing concentration of ALA and that these modulations of ALA PDT did not result in the accumulation of any other porphyrin intermediate other than PPIX alone.

The hydroxypyridinones are a relatively new series of iron chelating agents. They can be administered orally and enter the intracellular iron pools rapidly, being both neutrally charged and of low molecular weight (Hoyes and Porter, 1993). Originally developed to supersede desferrioxamine for the treatment of thalassaemia and other disorders of iron overload, the hydroxypyridinones are now being investigated to enhance ALA-induced PDT. They are well suited to this application, having lower molecular weights and greater lipophilicity than desferrioxamine and the added benefit of oral administration (Brittenham, 1992).

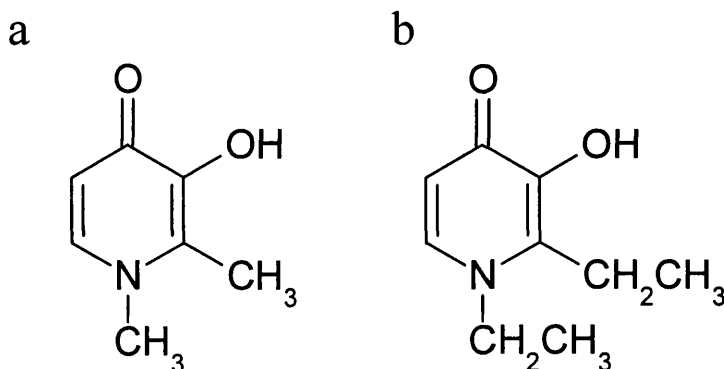


Figure 5 The structures of a) 1,2-dimethyl-3-hydroxypyridin-4-one (CP20) and b) 1,2-diethyl-3-hydroxypyridin-4-one (CP94).

Two hydroxypyridinones are studied in this thesis; the 1,2-dimethyl derivative (CP20) and the 1,2-diethyl derivative (CP94) and their structures can be seen in Figure 5. Both of these compounds have been administered orally to patients with iron-overload without significant toxicity and produced rapid and effective iron mobilisation (Brittenham, 1992). They are both absorbed rapidly and completely from the

gastrointestinal tract, entering cells by simple diffusion (Hoyes & Porter, 1993) and can be glucuronidated in humans and then excreted in urine, which is not possible in rats, so they are more rapidly cleared in patients (Porter *et al*, 1993). CP94 is a more effective iron chelator than CP20 as it has greater lipophilicity, it can therefore access the intracellular iron pools and inhibit metalloenzymes (such as lipoxygenase and ribonucleotide reductase) more rapidly than CP20 (Abeysinghe *et al*, 1996 and Cooper *et al*, 1996). It has greater affinity for iron than desferrioxamine being bidentate (rather than hexadentate), binding to iron in the ratio of 3:1, compared to 1:1 with desferrioxamine (Hershko *et al*, 1991).

Being a relatively new series of compounds, relatively little research has been conducted investigating the effects of the hydroxypyridinones on ALA induced PDT. It has, however, been previously found that CP94 enhanced porphyrin fluorescence and photosensitivity in all cell lines studied (Bech *et al*, 1997), as well as doubling the PPIX fluorescence in the urothelium of the normal rat bladder (when given in combination with 10% ALA solution instilled in the bladder), whilst maintaining the degree of selectivity between the urothelium and the underlying muscle (Chang *et al*, 1997).

This experimental section continues this research, to determine the effectiveness of hydroxypyridinone iron chelators as potential enhancers of ALA PDT, by investigating two compounds of this class (CP20 and CP94) in several animal models.

2.1.2 Iron Chelator Pharmacokinetics in Normal Colon

2.1.2.1 Introduction

The pharmacokinetics of both hydroxypyridinones, 1,2-dimethyl-3-hydroxypyridin-4-one (CP20) and 1,2-diethyl-3-hydroxypyridin-4-one (CP94) in combination with ALA, were studied initially in the normal rat colon. This is a model in which there is considerable experience with a number of photosensitisers (Barr *et al*, 1990; Messmann *et al*, 1995) and produces reproducible, clearly demarcated, areas of necrosis (in photodynamic studies), which are maximal at three days (Barr *et al*, 1987). This experimental model therefore allows different treatment parameters to be evaluated accurately *in vivo*, in a relatively short period of time.

The pharmacokinetic study utilised the inherent fluorescent properties of PPIX to identify, localise, and quantify this naturally occurring photosensitiser, within the different layers of the colon, using fluorescence microscopy. This was conducted on frozen sections prepared from tissue specimens obtained from animals receiving various combinations of the compounds (intravenously), at different points in time. This was necessary to determine the optimal treatment parameters, prior to commencing photodynamic studies.

2.1.2.2 Materials and Methods

Chemicals

ALA powder (ALA.HCl, 99% purity, DUSA Pharmaceuticals, Inc., New York, USA) was dissolved in physiological strength, phosphate-buffered saline (PBS, pH 2.8) and administered intravenously (with a concentration of 25, 50 or 200 mg/ml and a maximum volume of 0.2 ml). The iron chelators, CP20 and CP94 were synthesized and kindly donated in powder form by the Department of Pharmacy, Kings College London (90% and 95% purity respectively). These were also prepared in PBS and administered intravenously (with a concentration of 100 mg/ml and a maximum volume of 0.2 ml). Separate syringes were always used for the iron chelator and ALA solutions, even when administered at the same time, and all injections were made under general anaesthetic in different veins to avoid any potential interactions between the compounds. No adverse effects were observed when administering any of the compounds.

Animal model

Normal, female, Wistar rats (120 - 200 g) supplied by the Imperial Cancer Research Fund (London, UK) were used throughout. The animals were anaesthetised for all parts of the procedure using inhaled halothane (ICI Pharmaceuticals, Cheshire, UK).

Fluorescence studies

ALA (25, 50 or 200 mg/kg i.v.) and CP20 (100 mg/kg i.v.) or CP94 (100 mg/kg i.v.) were administered separately or in various combinations under general anaesthetic.

The animals were then recovered and killed serially at various times after injection (30 - 210 minutes). Sections of colon were removed and snap frozen in liquid nitrogen. Ten micrometer thick cryosections were prepared, together with adjacent sections for Haematoxylin and Eosin (H & E) staining.

Phase contrast microscopy with a slow-scan cooled charge coupled device (CCD) camera (Wright Instruments Ltd., Enfield, London, UK) was used to image and quantify fluorescence on the frozen sections. The fluorescence was excited using an 8 mW helium-neon laser (632.8 nm) and detected between 665 and 710 nm using bandpass and longpass filters, as described previously (Bedwell *et al*, 1992). A false colour-coded image of the fluorescence signal in counts per pixel was produced and the fluorescence intensity in each tissue layer was quantified digitally, by averaging over specified areas. All fluorescence measurements were corrected for background autofluorescence and structures were identified by correlation with the adjacent H & E stained section. Two measurements were made and averaged per section and two animals were treated with each set of parameters. Intensity calibrations were performed using a 0.1 mm thick ruby disc which emits near 690 nm under 633 nm excitation. A previous study using the same system (Loh *et al*, 1993) on normal rat colon using intravenous ALA has demonstrated that the CCD fluorometric measurements of porphyrin fluorescence correlate well with chemical extraction measurements.

Statistical analysis between the means of the ALA only and ALA + CP94 groups, at the time of peak fluorescence, was conducted using unpaired student t-tests. Error bars on all the figures were determined by the standard error of the mean.

2.1.2.3 Results

A representative set of photographs can be seen in Figure 6. One pair (Figures 6a & b) shows a typical false colour coded CCD image of the colon with its matched H & E stained histology photograph, 75 minutes after administration of 50 mg/kg ALA i.v. alone. The other pair (Figures 6c & d) shows the same images, 75 minutes after administration of 50 mg/kg ALA i.v. + 100 mg/kg CP94 i.v. It can be seen that the fluorescence is higher in the colonic mucosa than the underlying muscle and that the fluorescence observed is much greater with the administration of CP94 in combination with ALA, than ALA administration alone.

Figure 7 shows how the fluorescence in the colonic mucosa and muscle varied with time after each regime of drug administration with 50 mg/kg ALA i.v. The fluorescence profile in this model after administration of 50 mg/kg ALA i.v. alone, (Figure 7a) shows that the level of fluorescence is considerably higher in the mucosa than the underlying muscle and peaks at 75 minutes, (the time chosen for photodynamic studies). Figure 7b shows the level of fluorescence produced if the iron chelating agents are administered without ALA. There is a slight increase in fluorescence (particularly at 75 minutes) resulting from the effect of the iron chelators on the normal endogenous haem biosynthetic pathway. It should be noted that the background autofluorescence of the endogenous porphyrins from the colon of untreated control animals, has been subtracted from all fluorescence measurements.

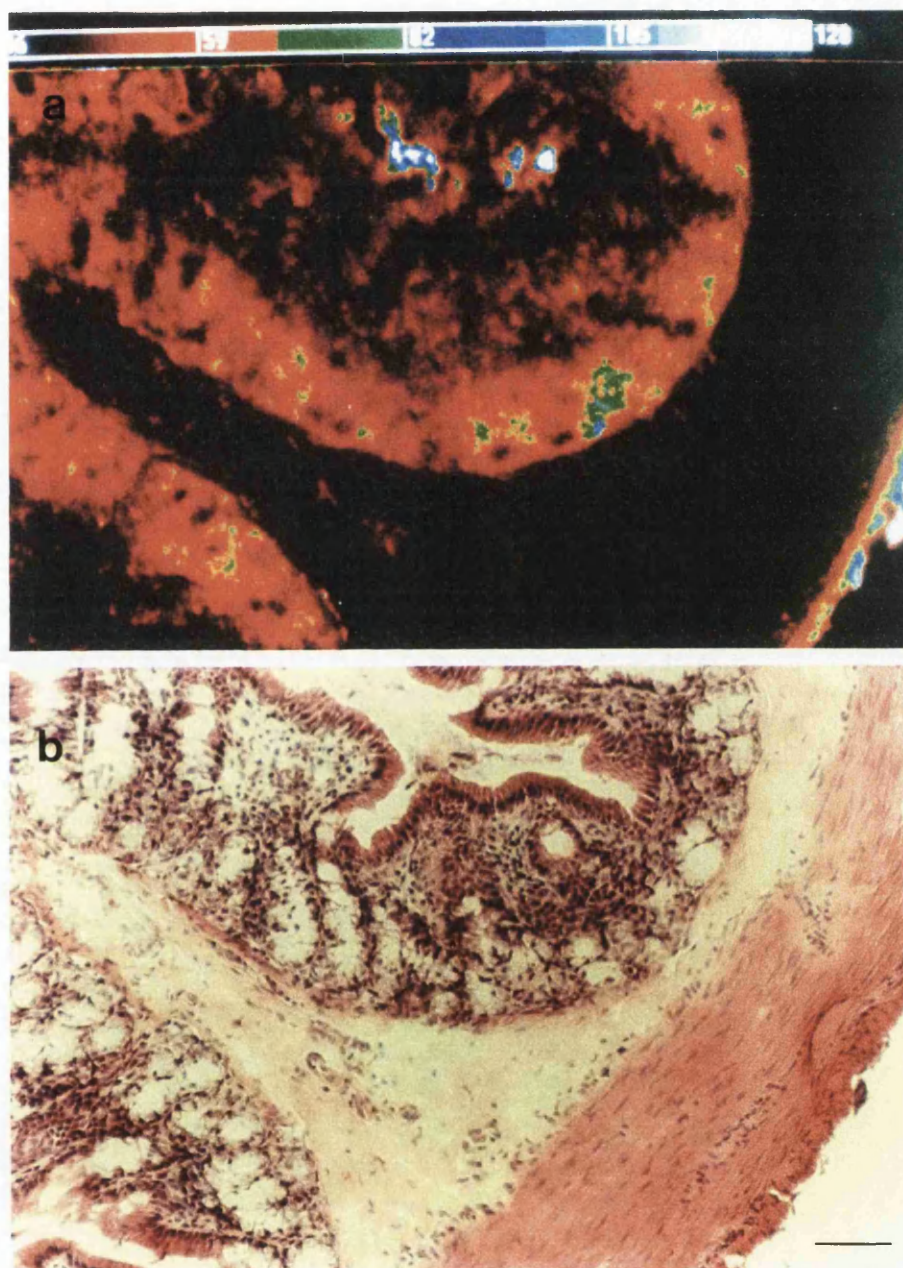


Figure 6 a) False colour coded fluorescence image and b) matched H & E stained histology photograph, of the colon, 75 minutes after administration of 50 mg/kg ALA i.v. Scale bar represents 70 μm.

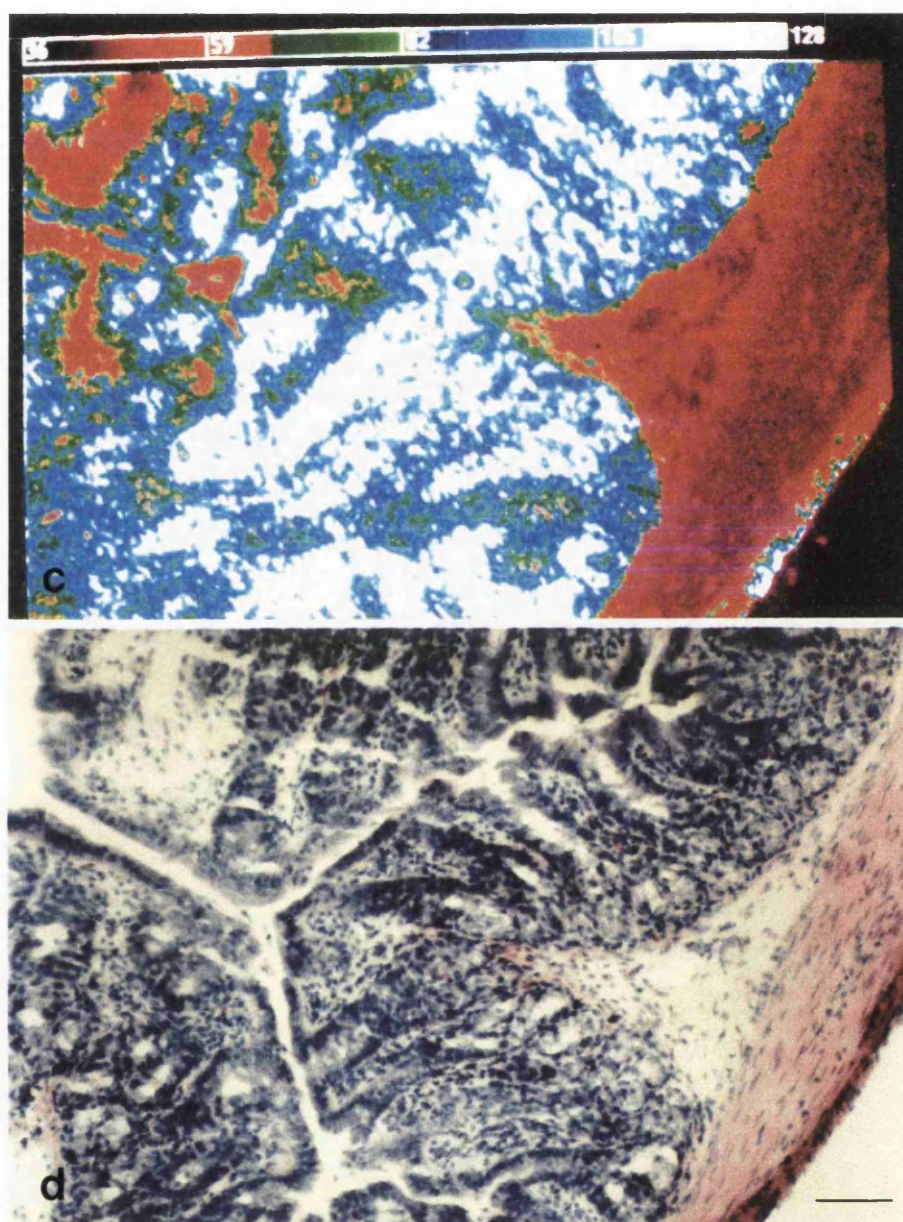


Figure 6 c) False colour coded fluorescence image and d) matched H & E stained histology photograph, of the colon, 75 minutes after the simultaneous administration of 50 mg/kg ALA i.v. and 100 mg/kg CP94 i.v. Scale bar represents 70 μm .

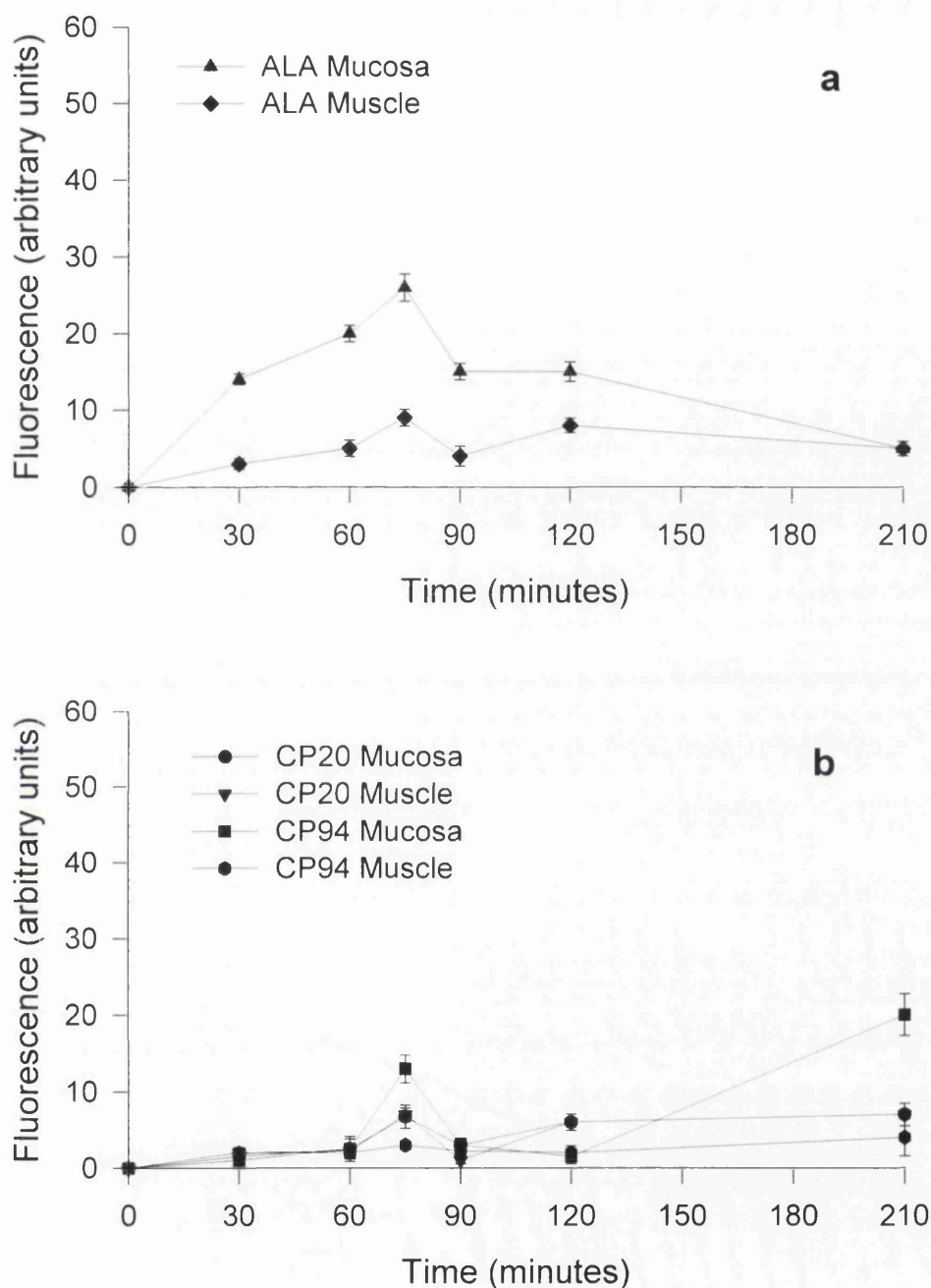


Figure 7 Fluorescence (arbitrary units) of the colonic mucosa and muscle as a function of time (minutes) with the following treatment regimes:- a) 50 mg/kg ALA i.v. and b) 100 mg/kg CP20 or CP94 i.v. Each point represents the mean values from two separate animals. Error bars as determined by the standard error of the mean.

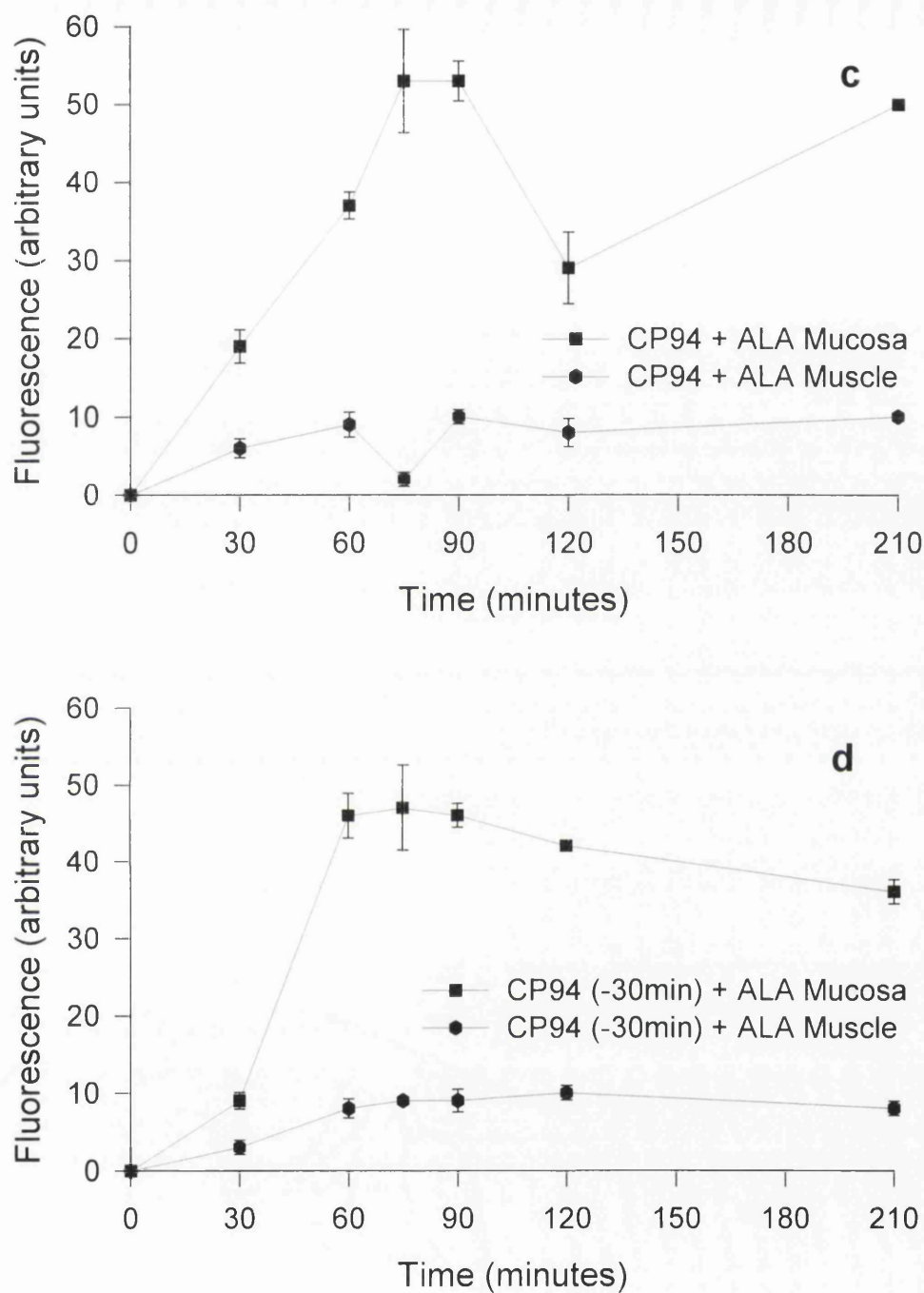


Figure 7 Fluorescence (arbitrary units) of the colonic mucosa and muscle as a function of time (minutes) with the following treatment regimes:- c) simultaneous administration of 50 mg/kg ALA i.v. and 100 mg/kg CP94 i.v. and d) administration of 100 mg/kg CP94 i.v. thirty minutes prior to 50 mg/kg ALA i.v. Each point represents the mean values from two separate animals. Error bars as determined by the standard error of the mean.

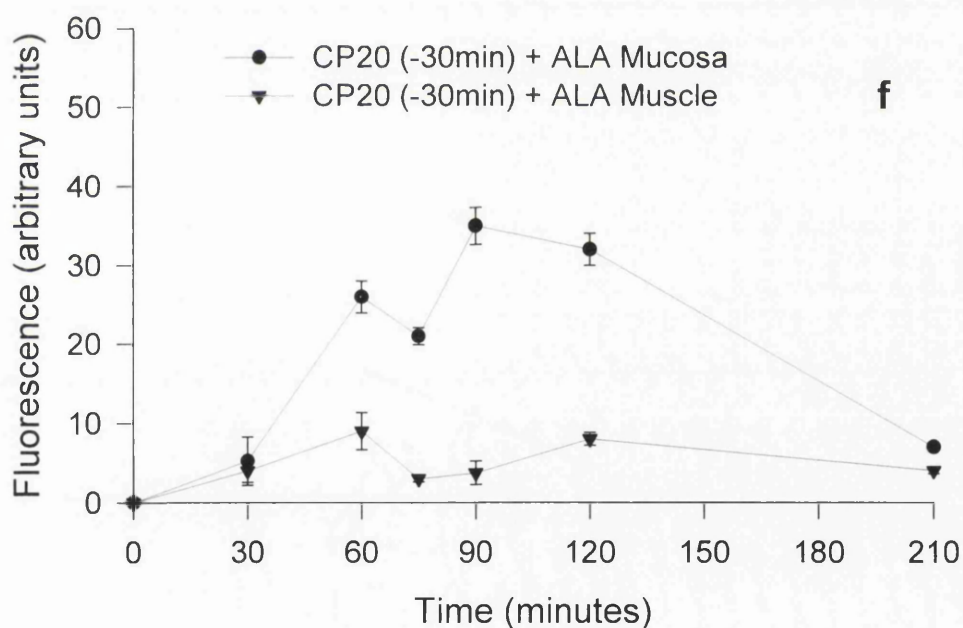
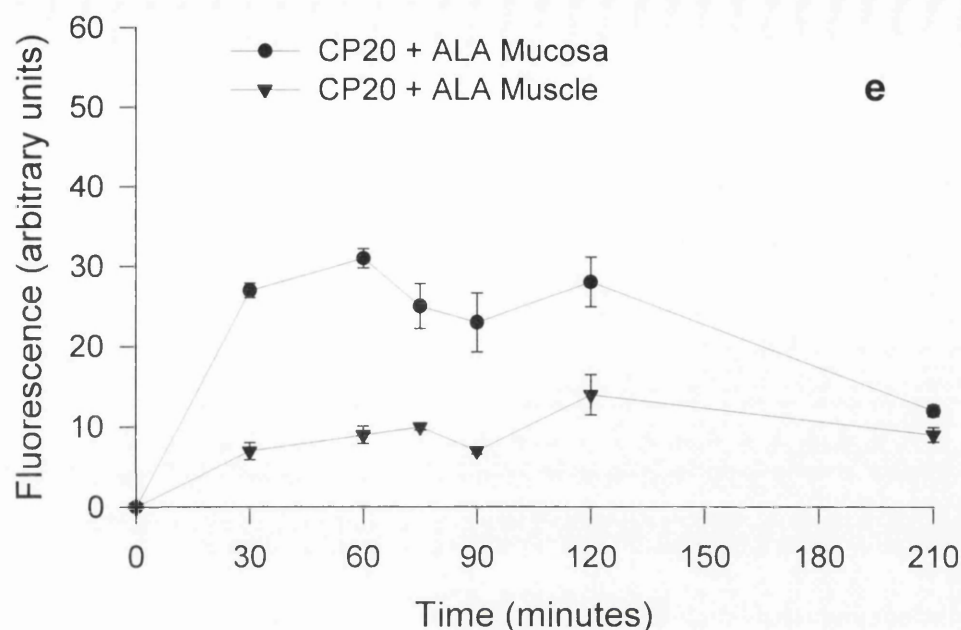


Figure 7 Fluorescence (arbitrary units) of the colonic mucosa and muscle as a function of time (minutes) with the following treatment regimes:- e) simultaneous administration of 50 mg/kg ALA i.v. and 100 mg/kg CP20 i.v. and f) administration of 100 mg/kg CP20 i.v. thirty minutes prior to 50 mg/kg ALA i.v. Each point represents the mean values from two separate animals. Error bars as determined by the standard error of the mean.

The simultaneous administration of CP94 with ALA (Figure 7c) doubles the peak fluorescence produced in the colonic mucosa (ALA only = 26 arbitrary units (a.u.), ALA + CP94 = 53 a.u.) ($p < 0.02$). The fluorescence in the muscle does not increase significantly and remains low, resulting in a large difference between the mucosal and muscle layers. By administering CP94 thirty minutes prior to ALA (Figure 7d) the enhancement of mucosal fluorescence is slightly reduced, but it appears that the profile might change, so there is potentially a larger therapeutic window in which PDT treatment could be conducted.

Figures 7e & f show the same treatment regimes but with CP20 instead of CP94. Although both treatments produce greater mucosal fluorescence than ALA alone, they do not produce the same degree of enhancement as CP94.

Figure 8 shows how the fluorescence in the colonic mucosa and muscle varied with time after each regime of drug administration with 25 mg/kg ALA i.v. The fluorescence profile in this model after administration of 25 mg/kg ALA i.v. alone (Figure 8a), shows that the level of fluorescence is only a little bit higher in the mucosa than the underlying muscle. The simultaneous administration of 100 mg/kg CP94 i.v. with 25 mg/kg ALA i.v. (Figure 8b), however, almost quadruples the peak fluorescence produced in the colonic mucosa (ALA only = 8 a.u., ALA + CP94 = 31 a.u.) ($p < 0.02$). The fluorescence in the muscle does not increase significantly and remains low, resulting in a substantial difference between the mucosal and muscle layers. The mucosal fluorescence starts to peak at 60 minutes (the time chosen for photodynamic studies). It should also be noted that the combination of 25 mg/kg ALA i.v. plus 100 mg/kg CP94 i.v. produces mucosal fluorescence (at the peak)

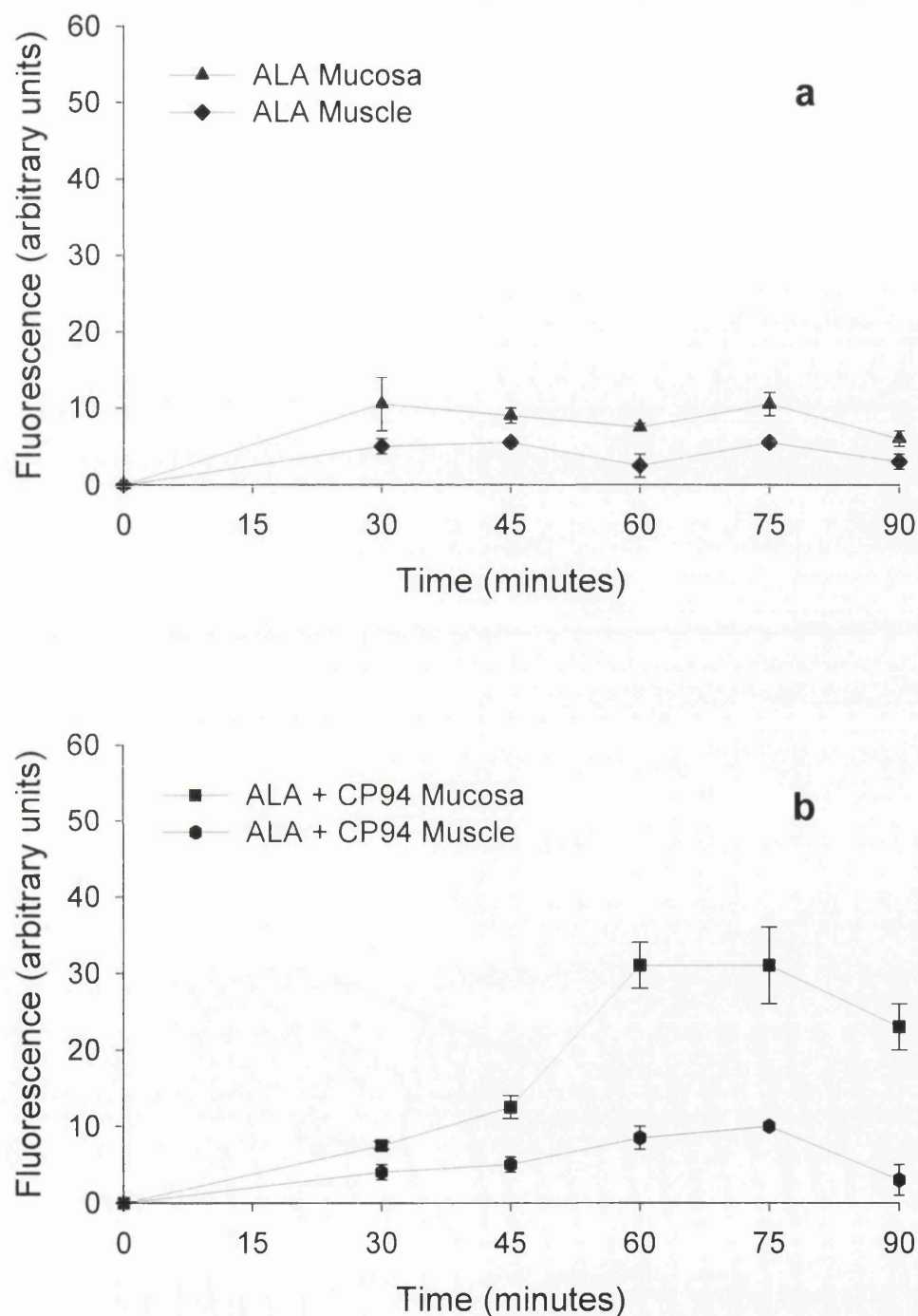


Figure 8 Fluorescence (arbitrary units) of the colonic mucosa and muscle as a function of time (minutes) with the following treatment regimes:- a) 25 mg/kg ALA i.v. and b) simultaneous administration of 25 mg/kg ALA i.v. and 100 mg/kg CP94 i.v. Each point represents the mean values from two separate animals. Error bars as determined by the standard error of the mean.

equivalent to that of 50 mg/kg ALA i.v. alone (25 mg/kg ALA + 100 mg/kg CP94 = 31 a.u., 50 mg/kg ALA = 26 a.u.) ($p < 0.20$).

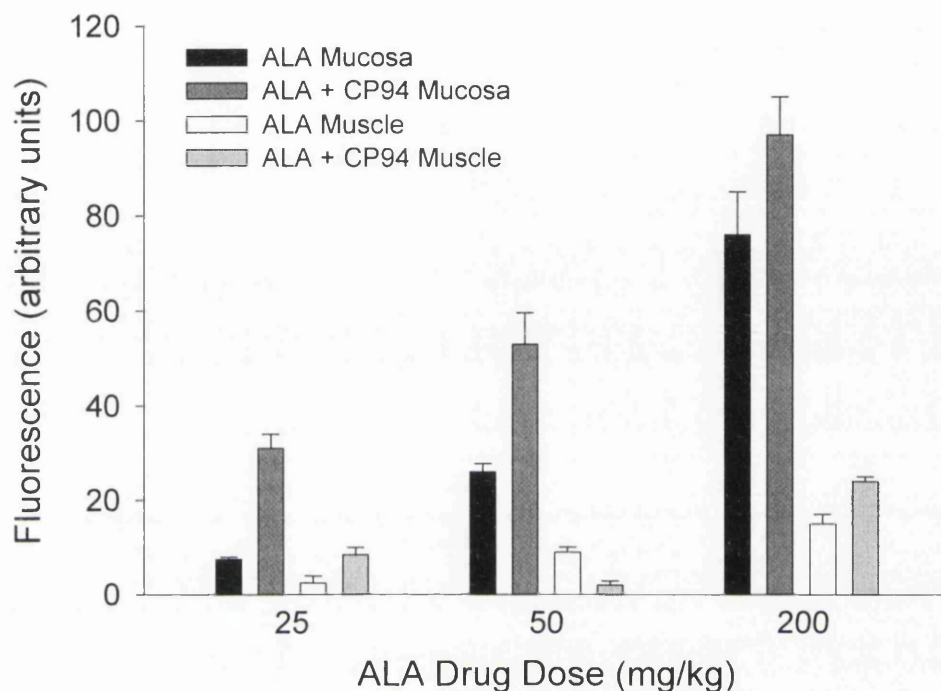


Figure 9 Peak fluorescence (arbitrary units) of the colonic mucosa and muscle, with or without CP94, as a function of ALA dose (mg/kg). Error bars as determined by the standard error of the mean.

Figure 9 summarises how the fluorescence in the colonic mucosa and muscle varied at the fluorescence peaks (60, 75 and 120 minutes), when treated with 25, 50 or 200 mg/kg ALA i.v., respectively, with or without the administration of 100 mg/kg CP94 i.v. This figure shows how the administration of CP94 affects the mucosal/muscular fluorescence at each of these three ALA doses and shows that the addition of CP94 only produces 28% more mucosal fluorescence than 200 mg/kg ALA alone (ALA only = 76 a.u., ALA + CP94 = 97 a.u.) ($p < 0.23$) but maintains the selectivity with the

underlying muscle layer. It can also be seen that as the ALA dose is increased, the peak mucosal fluorescence increases, but the degree of potentiation, the addition of 100 mg/kg CP94 i.v. generates, reduces.

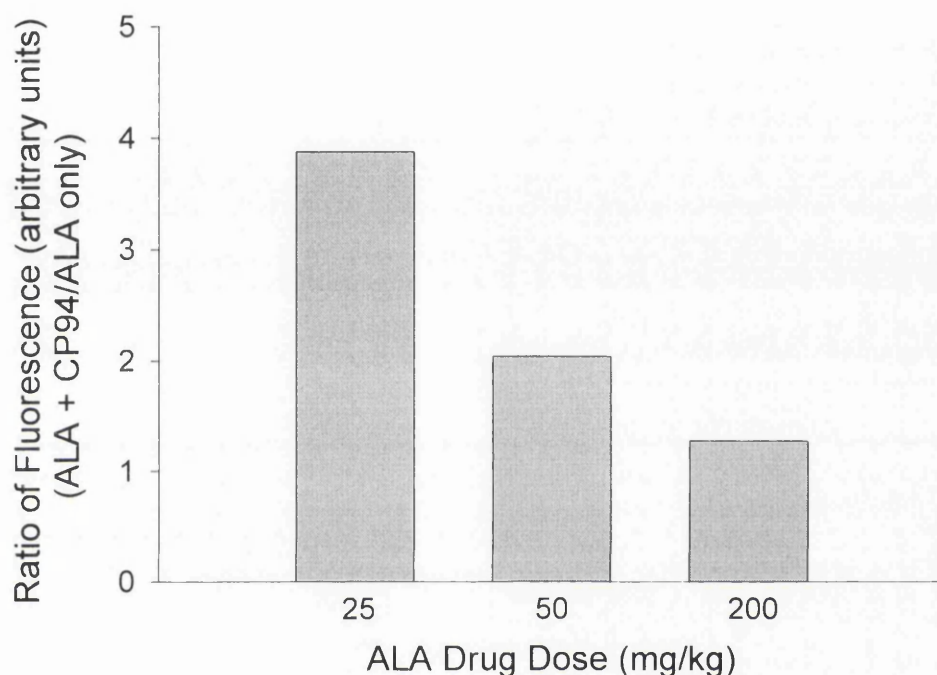


Figure 10 Ratio of peak fluorescence (arbitrary units) of the colonic mucosa (ALA + CP94 / ALA only) as a function of ALA dose (mg/kg).

This effect is emphasised in Figure 10, which plots the ratio of peak mucosal fluorescence between the ALA + CP94 and ALA only groups at each of the three ALA doses (ratios = 3.9, 2.0 and 1.3 (ALA + CP94 / ALA only) for ALA doses of 25, 50 and 200 mg/kg i.v. respectively).

2.1.2.4 Discussion

The results of this study, demonstrate that the hydroxypyridinone iron chelators studied are able to produce an enhanced build-up of mucosal fluorescence following ALA administration in this model. This is probably as a result of the iron chelators' ability to temporarily remove intracellular Fe^{2+} , thus limiting the final step of haem synthesis, the chelation of iron to PPIX (by the enzyme ferrochelatase), resulting in an enhanced build-up of PPIX.

The CCD fluorescence microscopy determined that the more lipophilic iron chelating agent CP94, was more effective at increasing the mucosal PPIX fluorescence producing up to four times that of ALA alone, when the two were given simultaneously and confirmed previous observations in the bladder (Chang *et al*, 1997). This was expected, as CP94 has greater lipophilicity than CP20 enabling it to access the intracellular iron pools more rapidly (Cooper *et al*, 1996).

The time of peak fluorescence (and therefore the optimum time of light dose administration) was the same as after ALA alone. The muscle fluorescence was not increased significantly by the administration of the iron chelators, so the selectivity between the different tissue layers was maintained.

It was found possible, with the simultaneous administration of CP94, to produce the same amount of mucosal fluorescence with 25 mg/kg ALA i.v. as would normally be produced by 50 mg/kg ALA i.v. alone. This is important as the aim of this study is to

make small (clinically tolerable) doses of ALA more effective than they are at present. The enhancement of mucosal fluorescence by CP94 increased as the ALA dose was reduced. This has been observed before with other iron chelators (Berg *et al*, 1996) and is probably the result of the saturation of the enzyme pathway with the higher doses of ALA alone.

Both CP94 and CP20 have previously been administered orally to humans, at a similar dosage, on a daily basis, for long periods of time, without significant toxicity (Brittenham, 1992). It is therefore unlikely, that the oral administration of these compounds, once (in combination with ALA), would pose a problem (from the point of view of the toxicity of the compounds themselves). It is possible, however, that the resultant enhanced build-up of PPIX and the other haem biosynthesis intermediates, may exacerbate the side-effects of ALA PDT itself, namely the skin photosensitivity, pain during treatment and/or liver enzyme fluctuations.

In this study, we have neither investigated the level of fluorescence at longer time points nor directly monitored the levels of the iron chelators themselves; but from the clinical work already conducted investigating CP20 and CP94 for haematological applications (Porter *et al*, 1993), both are rapidly cleared in patients. It is, therefore, likely that they will not be in the body for a period of time much longer than a day or two. It should also be noted, however, that these compounds will be more rapidly cleared in humans than in rats, as the main route of removal in humans is by liver glucuronidation, which is minimal in rats.

Another area for further investigation would be the oral administration of the iron chelator, as both CP94 and ALA are normally administered orally to patients. All the compounds were administered intravenously in this study, as this is a convenient, accurate, method of delivery in this species.

2.1.3 PPIX Analysis

2.1.3.1 Introduction

Although the results of the previous section established that the hydroxypyridinone iron chelators (particularly CP94) can increase mucosal fluorescence in the normal rat colon, there was no evidence presented to prove that this fluorescence was produced by either PPIX itself or any other fluorescent porphyrin. This is important as it is possible for the enzyme ferrochelatase to insert other metal ions, such as zinc (instead of iron) into PPIX, when iron is limited (Kennedy *et al*, 1996). It is also possible for other fluorescent intermediate porphyrins of the haem biosynthesis pathway, such as uroporphyrinogen or coproporphyrinogen, to build up. It was therefore important to establish which compound was producing the enhanced level of fluorescence, observed in the pharmacokinetic study, as only enhanced levels of the photoactive compound PPIX would enhance the outcome of ALA induced PDT.

The following section will, therefore, investigate the emission spectra from various frozen sections and analyse colon specimens by chemical extraction to determine whether the fluorescence was predominately produced by PPIX and how much was produced by each of the different treatment regimes.

2.1.3.2 Materials and Methods

The chemicals, animal model and method used to produce the frozen colon sections and specimens used in this section were the same as section 2.1.2.2.

Emission spectra

Fluorescence emission spectra were recorded from separate representative frozen sections to confirm that the fluorescence observed in the imaging was indeed produced by PPIX and no other fluorescent compound. This was done by connecting a spectrograph (Multispec 1/8m, Oriel Instruments, Connecticut, USA) with a slow-scan cooled CCD camera (600 x 400 pixels, Wright Instruments Ltd, Enfield, London, UK) via a fibre-optic bundle to an inverted microscope. Fluorescence was excited using a 1 mW helium-neon laser at 543 nm and emission spectra were recorded over the range 615 - 735 nm with 1 nm resolution. Scattered excitation light was suppressed using a RG590 filter and a grating blazed at 650 nm gave a relatively uniform detection efficiency over the range 615-735 nm so the spectra presented are uncorrected. Epi-fluorescence excitation was confined to a spot (100 μ m diameter) which was aligned (using phase contrast microscopy) to a region of interest. No photobleaching effects were observed (i.e. no diminution of the porphyrin spectra and/or photoproduct emission) with the short integration times (10 seconds) used to record the spectra in this study.

Chemical extraction

Chemical extraction was conducted on representative colon specimens snap frozen in the previously described experiment using a method adapted from Hua *et al* (1995) as outlined below. Two standard curves (one containing blank colon tissue extract and one without tissue) were set up and run daily, alongside specimens to be analysed using PPIX fluorescence standards (Porphyrin Products, Utah, USA). These curves were set up over the concentration range of zero to 0.2 μg of PPIX per ml of solution, using hydrochloric acid and methanol (1:1 v/v) as a solvent. The solutions were then analysed in a luminescence spectrometer (Perkin Elmer Ltd., Beaconsfield, Buckinghamshire, UK) exciting at 410 nm and collecting the emission over 560 -700 nm to determine the shape of the PPIX spectra before the emission intensity at 660 nm was measured. These intensities were used to draw the standard curves. The colon specimens to be analysed were homogenised prior to suspension in solvent and centrifugation (1000 rpm for 10 minutes). The supernatant produced was then analysed in the same way as the standard curves. The intensities produced were background corrected using the blank tissue control value to remove autofluorescence and then the amount of PPIX in $\mu\text{g/g}$ of colon tissue in each tissue specimen was calculated from the standard curves.

2.1.3.3 Results*Emission spectra*

Fluorescence spectra were recorded, using the microscope, from frozen sections of tissue taken from animals given each treatment regime and representative spectra

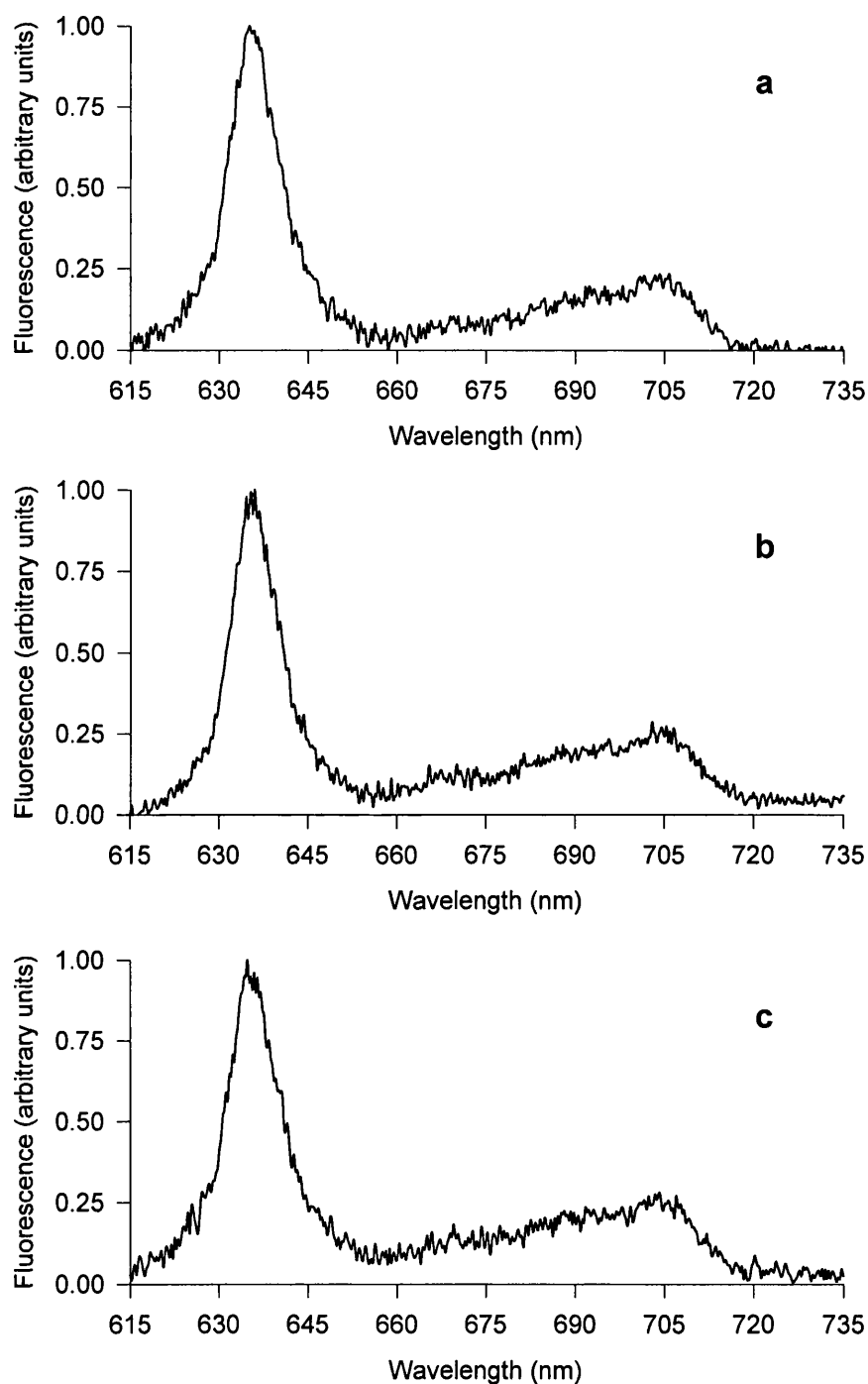


Figure 11 Emission spectra obtained from frozen colon sections from the following treatment groups:- a) 50 mg/kg ALA i.v., 75 minutes after administration, b) 50 mg/kg ALA i.v. and 100 mg/kg CP94 i.v., 75 minutes after simultaneous administration and c) 50 mg/kg ALA i.v. and 100 mg/kg CP20 i.v., 75 minutes after simultaneous administration.

from mucosal areas are shown in Figure 11. The spectra from blank control sections (no compounds injected) were subtracted. There were no significant differences between the ALA only (Figure 11a), and combinations of CP94 and ALA (Figure 11b) or CP20 and ALA (Figure 11c) spectra, or in fact any other spectra recorded during this study, which demonstrates that the iron chelating agents do not induce significant production of other fluorescent species. Maxima were at 636 ± 2 nm in each case and the spectral profiles recorded conform to the standard PPIX emission spectra described by Dietel *et al* (1997) and Sailer *et al* (1997). A previous HPLC analysis of colon samples after intravenous administration of ALA to Wistar rats (Loh *et al*, 1993) has shown that PPIX is the predominant porphyrin present ($> 95\%$). It can, therefore, be concluded that the fluorescence measured in the present study is produced predominantly by PPIX.

Chemical extraction

The amount of PPIX (μg of PPIX per g of colon tissue) determined in each of the treatment groups is shown in Figure 12. It can be seen that the amount of PPIX produced in the CP20 only and CP94 only control groups was hardly above background. The peak PPIX value was $0.8 \mu\text{g/g}$, which was almost doubled to $1.5 \mu\text{g/g}$ in the groups receiving simultaneous administration of ALA in combination with CP20 or CP94. Administration of the iron chelator, thirty minutes prior to the ALA dose, did not produce quite as much PPIX. The spectra produced, throughout this study, all conformed to that of PPIX, although it was slightly blue shifted, as the PPIX was ionised by the hydrochloric acid (used in this method to make the PPIX more soluble so that it could dissolve into the organic phase (methanol) for extraction).

Drug / Sampling Times (minutes) (relative to ALA administration)	Compounds Administered	Amount of PPIX (μg of PPIX per g of colon tissue) (Blank corrected)
0 / 75 0 + 0 / 75 0 + -30 / 75	CP20 only ALA + CP20 ALA + CP20	0.2 1.5 1.3
0 / 75 0 + 0 / 75 0 + -30 / 75	CP94 only ALA + CP94 ALA + CP94	0.0 1.5 1.2
0 / 75	ALA only	0.8

Figure 12 Chemically extracted levels of PPIX ($\mu\text{g/g}$) in normal colon tissue, 75 minutes after administration of 50 mg/kg ALA i.v. and various combinations of the iron chelators, CP20 or CP94 (100 mg/kg i.v.).

These results support the findings of the pharmacokinetic study, with approximately double the amount of PPIX being produced with the addition of an iron chelator. In the pharmacokinetic study, the level of fluorescence produced in the colonic mucosa by the combination of ALA and CP20 was not quite as much as that produced by ALA and CP94. In this chemical extraction analysis, however, these groups produced similar amounts of PPIX. It should be noted, however, that the chemical extraction technique analysed the amount of PPIX in all of the colon tissue and the result produced is, therefore, a summation of the amount of PPIX in all of the tissue layers together, not just the colonic mucosa and although the results of the two sets of experiments support one another they are, therefore, not directly comparable.

2.1.3.4 Discussion

Microspectrofluorimetry using 543 nm excitation confirmed that the fluorescence observed in each treatment group, could be attributed to PPIX and not water-soluble porphyrins or other fluorescent metalated porphyrins (also excited by 543 nm) which could be produced by the altered biochemistry induced by the iron chelators.

Chemical extraction also determined the presence and amount of PPIX in the colon specimens of each treatment group. These results support the earlier findings that the addition of an iron chelator can enhance the amount of PPIX produced by ALA in this model, by a factor of two. The quantity of PPIX produced in the tissue was small (μg amounts) but comparable to Loh *et al's* previous work (1993) which determined the amount of PPIX in colon tissue by CCD fluorescence microscopy, chemical extraction (a similar but slightly different method) and high performance liquid chromatography (HPLC) following ALA administration in the same species. They found 6 μg PPIX per g of colonic mucosa 2 hours after administration of 200 mg/kg ALA i.v. using HPLC. Therefore, considering the higher ALA dose, the separation of the different layers of the colon and the more sensitive technique (in their study), the current results appear to be reasonable.

2.1.4 Iron Chelator PDT in Normal Colon

2.1.4.1 Introduction

The previous sections have established that through the administration of a hydroxypyridinone iron chelator, it is possible to double the fluorescence produced in the colonic mucosa when using 50 mg/kg ALA i.v. and that CP94 produced slightly better results than CP20. This section will investigate whether this increase in PPIX fluorescence, with CP94 administration, can be utilised to produce an enhanced PDT effect. This will be conducted in the same animal model, using the most successful treatment parameters (as determined by the pharmacokinetic study) but with the administration of an energy dose.

2.1.4.2 Materials and Methods

Chemicals

ALA powder was dissolved in physiological strength PBS (pH 2.8) and administered intravenously (with a concentration of 25, 50 or 200 mg/ml and a maximum volume of 0.2 ml). The iron chelator, CP94, was also prepared in PBS and administered intravenously (with a concentration of 100 mg/ml and a maximum volume of 0.2 ml).

Animal model

Normal, female, Wistar rats (120 - 200 g) were used throughout. The animals were anaesthetised for all parts of the procedure using inhaled halothane (ICI Pharmaceuticals, Cheshire, UK) and analgesia was administered subcutaneously following surgery (Buprenorphine hydrochloride, Reckitt & Colman Products Ltd, Hull, UK).

PDT studies

In the first series of experiments, all animals were given 50 mg/kg ALA intravenously, 75 minutes prior to surgery. 100 mg/kg CP94 i.v. was given at times from 30 minutes before, to 60 minutes after the ALA dose. The colon was accessed for PDT via a laparotomy as described in section 2.0.0.2. The pulsed (12 kHz) copper vapour pumped dye laser (tuned to 635 nm) was used to deliver a total energy of 100 J (output power, 100 mW). The area of necrosis produced in the colon at three days was determined using image analysis software.

The same experiment was repeated using a mixed solution of 50 mg/kg ALA i.v. and 100 mg/kg CP94 i.v. This was to determine if the same results could be produced using this single, mixed preparation of the compounds, instead of separate solutions being injected independently.

In subsequent experiments, the same experimental method was used but the effect of the simultaneous administration of 100 mg/kg CP94 i.v. on 25 and 200 mg/kg i.v. ALA induced PDT, was investigated. In 25 mg/kg ALA i.v. experiments an energy dose of 100 J was delivered 60 minutes after ALA administration using the 628 nm

diode laser. In the 200 mg/kg experiments, the same energy dose and laser was used but the light was administered two hours after ALA administration.

There were eight animals in each of the treatment groups, throughout these experiments. Statistical analysis between the means of the different treatment groups was conducted using unpaired student t-tests. Error bars on all the figures were determined by the standard error of the mean.

2.1.4.3 Results

The area of necrosis (mm^2) produced by each treatment regime, using 50 mg/kg ALA i.v., is plotted in Figure 13. Only the effects of CP94 on ALA induced PDT were investigated, as it was found to be the more promising iron chelator in the fluorescence studies. The time of CP94 administration relative to ALA administration was varied and the success of the PDT treatment regime determined by the area of necrosis produced. The simultaneous administration of 50 mg/kg ALA i.v. and 100 mg/kg CP94 i.v. was found to be the most effective, producing almost three times (ratio = 2.9) the area of necrosis of ALA alone (ALA only = 32 mm^2 , ALA + CP94 = 93 mm^2) ($p < 0.0003$). CP94 only plus light controls, laser only controls, ALA only and CP94 only controls were also conducted, none of which produced any necrosis.

The effect of administering the iron chelator in a mixed solution with the ALA was also investigated and the results of this experiment can be seen in Figure 14. It appears that there is no difference ($p < 0.85$) between the separate and mixed

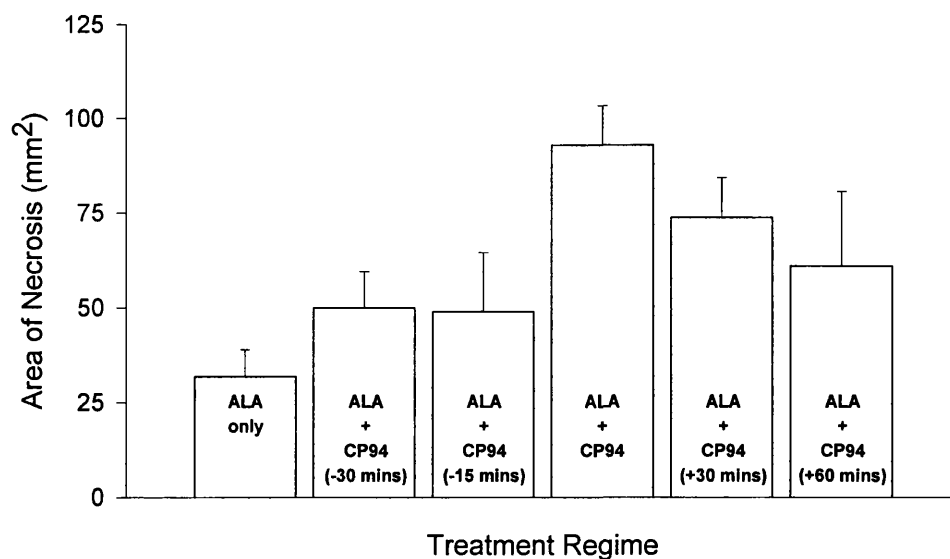


Figure 13 Mean area of necrosis (mm²) as a function of the PDT treatment regime. 100 mg/kg CP94 i.v. was administered at various times relative to 50 mg/kg ALA i.v. which was given 75 minutes prior to 100 J of 635 nm light (100 mW) using a copper vapour pumped dye laser. Each group represents the mean (with the standard error of the mean) from eight separate animals.

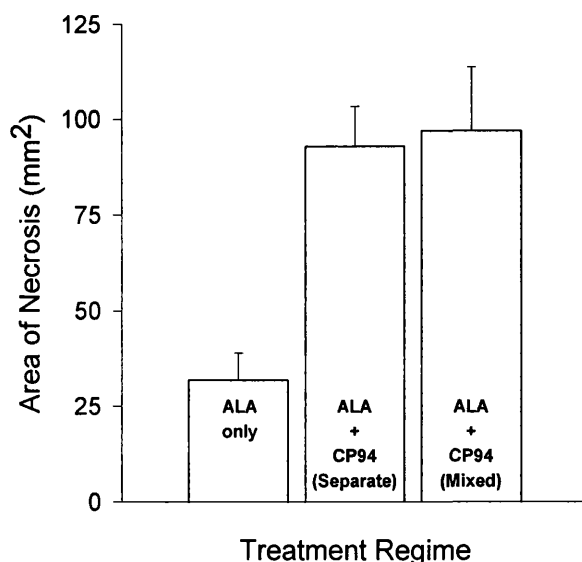


Figure 14 Mean area of necrosis (mm²) as a function of the PDT treatment regime. 100 mg/kg CP94 i.v. was administered either in a separate or a mixed solution with 50 mg/kg ALA i.v. 75 minutes prior to 100 J of 635 nm light (100 mW), using a copper vapour pumped dye laser. Each group represents the mean (with the standard error of the mean) from eight separate animals.

administration of ALA and CP94, when conducted in this manner (separate solutions = 93 mm², mixed solutions = 97 mm²). This indicates that there is no discernible reason why these compounds cannot be administered in a mixed solution in the future.

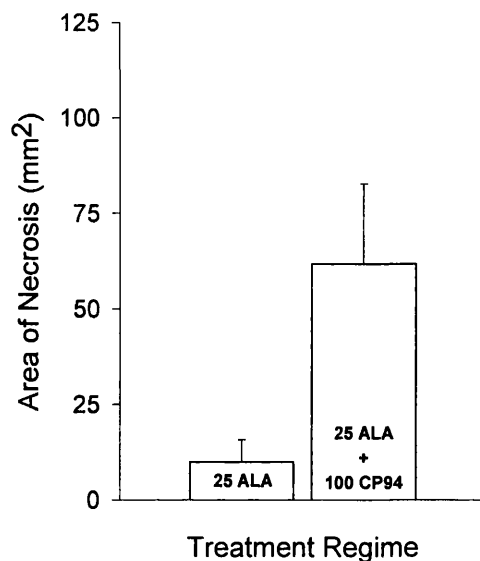


Figure 15 Mean area of necrosis (mm²) as a function of the PDT treatment regime. 25 mg/kg ALA i.v. was administered separately, or in combination with 100 mg/kg CP94 i.v. (separate solutions), 60 minutes prior to 100 J of 628 nm light (100 mW) using a diode laser. Each group represents the mean (with the standard error of the mean) from eight separate animals.

Figure 15 shows how the area of necrosis (mm²) produced by 25 ALA ^{mg/kg} i.v. is altered by the simultaneous (but separate) administration of 100 mg/kg CP94 i.v. It can be seen that there is a substantial, six fold (ratio = 6.2) increase in effect, when the iron chelator is administered (ALA only = 10 mm², ALA + CP94 = 62 mm²) ($p < 0.04$).

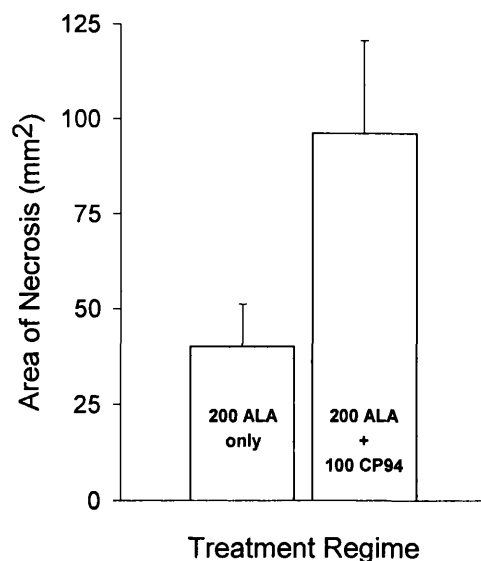


Figure 16 Mean area of necrosis (mm²) as a function of the PDT treatment regime. 200 mg/kg ALA i.v. was administered, separately or in combination with (separate solutions) 100 mg/kg CP94 i.v., 120 minutes prior to 100 J of 628 nm light (100 mW) using a diode laser.

Figure 16 shows how the area of necrosis (mm²) produced by 200 ALA i.v. is altered by the simultaneous (but separate) administration of 100 mg/kg CP94 i.v. It can be seen that the area of necrosis is at least doubled (ratio = 2.4) by the administration of the iron chelator (ALA only = 40 mm², ALA + CP94 = 96 mm²) ($p < 0.06$).

2.1.4.4 Discussion

The results of this section have shown, that it is possible to utilise the increased PPIX fluorescence demonstrated in the pharmacokinetic study, to substantially enhance the area of necrosis produced by PDT in this model.

Using 50 mg/kg ALA i.v., it was found to be particularly advantageous if the CP94 was administered at the same time as the ALA dose and subsequent studies (using the other doses of ALA) continued to use this, most beneficial, treatment protocol. The mixed solution of ALA and CP94 was also found not to produce significantly different results from the separate solutions of ALA and CP94 (administered at the same time). This will make the administration of these compounds, in future studies, more convenient.

Once again, it was found that as the ALA dose was reduced, the degree of potentiation obtained increased. Although the results with the two different light sources cannot be directly compared, the addition of 100 mg/kg CP94 i.v. produced 2.4, 2.9 and 6.2 fold amplification of the area of necrosis created with 200, 50 and 25 mg/kg ALA i.v. induced PDT, respectively. This follows the same pattern of enhancement as established in the pharmacokinetic study (1.3, 2.0 and 3.9 fold amplification, with 200, 50 and 25 mg/kg ALA i.v., respectively) and shows that the degree of enhancement created by CP94, is even greater in the PDT study, than in the pharmacokinetic study, with each of the three ALA doses studied in this model.

It is difficult to equate intravenous doses to oral ones, normal tissues with malignant ones and results in animal models to human studies, but the 25 mg/kg ALA i.v. dose used in this study, would probably give us some idea of the kind of effect expected in humans using the currently maximum tolerated oral dose of 60 mg/kg ALA. It is at least encouraging, that as the ALA dose is reduced the positive effect of CP94 increases, so we would expect CP94, if used appropriately, to produce a substantial

benefit in the clinical situation. To establish this conclusively, however, will require much further study.

2.1.5 Iron Chelator Pharmacokinetics and PDT in a Colonic Tumour Model

2.1.5.1 Introduction

The previous sections have established that the iron chelator CP94 can increase normal colonic mucosal fluorescence (following the simultaneous administration of ALA) and that this increase in PPIX can be used to substantially improve the outcome of PDT. The question still remains, however, if this is possible in a tumour model, and this section will investigate this.

Tumours often show altered biochemistry when compared with the normal tissues in which they arise. This includes modified enzyme expression and activity, which when occurring in the haem biosynthesis pathway, may result in a natural accumulation of PPIX (without the administration of ALA). It is, therefore, not a surprise that many malignancies, with the administration of ALA, will produce a slightly greater amount of PPIX than their corresponding normal tissue (Peng^a *et al*, 1997).

The outcome of the addition of an iron chelator, as used in this technique, to further manipulate the innate haem biochemistry of a tumour model was, therefore, unknown. A series of experiments were consequently conducted to establish the effect of CP94 on firstly, PPIX fluorescence and secondly, PDT efficacy, in a colonic tumour model. The tumour model selected for these experiments was a MC28 cell line, already

established in our department (Lawrance *et al*, 1990; Murphy *et al*, 1988; Skipper *et al*, 1988). The MC28 tumour is syngeneic for the Hooded Lister rat and is a transplantable fibrosarcoma (methylcholanthrene-induced) which naturally metastasizes.

2.1.5.2 Materials and Methods

Chemicals

ALA powder was dissolved in physiological strength PBS (pH 2.8) and administered intravenously (with a concentration of 50 mg/ml and a maximum volume of 0.2 ml). The iron chelator, CP94, was also prepared in PBS and administered intravenously (with a concentration of 100 mg/ml and a maximum volume of 0.2 ml).

Animal model

Female, Hooded Lister rats (120 - 200 g) (Harlan UK Ltd., Blackthorn, Oxfordshire, UK) were used throughout. The animals were anaesthetised for all parts of the procedure using inhaled halothane (ICI Pharmaceuticals, Cheshire, UK) and analgesia was administered subcutaneously following surgery (Buprenorphine hydrochloride, Reckitt & Colman Products Ltd, Hull, UK).

Tumour model generation

Tumours were produced by injection of $2-3 \times 10^6$ MC28 cells (total volume of 0.1 ml) into the site of an anastomosis in the colon. This anastomosis was created at laparotomy by making a cut halfway across the colon (at the normal site of PDT).

This small incision was then sutured shut before the cells were injected, the laparotomy repaired and the animals recovered. Ten days after tumour cell injection, the colonic tumour models had grown to a suitable size for experimentation (approximately 6 by 7 mm). They were solid (without necrotic centres), well defined, pale nodules, located on the exterior of the colon.

Fluorescence studies

Using the same basic method as the fluorescence studies in section 2.1.2.2, 50 mg/kg ALA i.v. and 100 mg/kg CP94 i.v. were administered separately or in combination under general anaesthetic, 10 days after tumour cell injection. The animals were then recovered and killed 75 minutes after ALA injection, so that frozen colonic tumour sections could be analysed by fluorescence microscopy (as described previously).

PDT studies

In separate animals, 10 days after tumour cell injection, PDT experiments were conducted using the same basic method as described in section 2.0.0.2. All animals received, 50 mg/kg ALA i.v. and 100 mg/kg CP94 i.v. separately or in combination under general anaesthetic, 75 minutes prior to surgery. A total energy of 100 J was delivered to the colonic tumour model via a 200 μ m plane cleaved optical fibre (output power, 100 mW) positioned so that it just touched the outside of the tumour, using the 628 nm diode laser as the light source. The rest of the abdominal viscera were shielded from forward light scatter by a piece of opaque paper positioned so that it did not touch the colon or affect its light distribution.

All animals were recovered following surgery and killed three days later. The diameters of the width (a), length (b) and depth (c) of necrosis produced in the tumour were measured using a micrometer and recorded. In all cases the zone of necrosis fell within the limits of the tumour. These measurements were then used to calculate the volume of necrosis produced by each treatment regime (in mm³) using the formula of an ellipsoid, $\pi abc/6$. Tumour specimens were fixed in formalin, sectioned and stained with haematoxylin and eosin, so that conventional light microscopy could confirm the macroscopic findings.

There were three animals in each of the treatment groups in the fluorescence studies, and four in each of the PDT groups. Statistical analysis between the means of the different treatment groups was conducted using unpaired student t-tests. Error bars on all the figures were determined by the standard error of the mean.

2.1.5.3 Results

Fluorescence studies

The results of the normal and tumour fluorescence studies can be seen in Figure 17. It can be seen that the fluorescence in the untreated colonic tumour (autofluorescence) is higher than that of the normal mucosa and muscle. These fluorescence results have only been corrected externally (to remove the inherent background of the experimental set-up) rather than with the background fluorescence of the tissue, so that we can see the autofluorescence of each of the tissues. The administration of ALA, increases the fluorescence in all three tissues. The fluorescence in the normal mucosa increases

more than that in the colonic tumour model, however. The administration of ALA and CP94 together, increases the fluorescence of the normal mucosa and colonic tumour even more, with the colonic mucosa being affected more than the tumour. This results in a similar degree of PPIX fluorescence being produced in the normal mucosa and colonic tumour model, using these experimental parameters ($p < 0.80$).

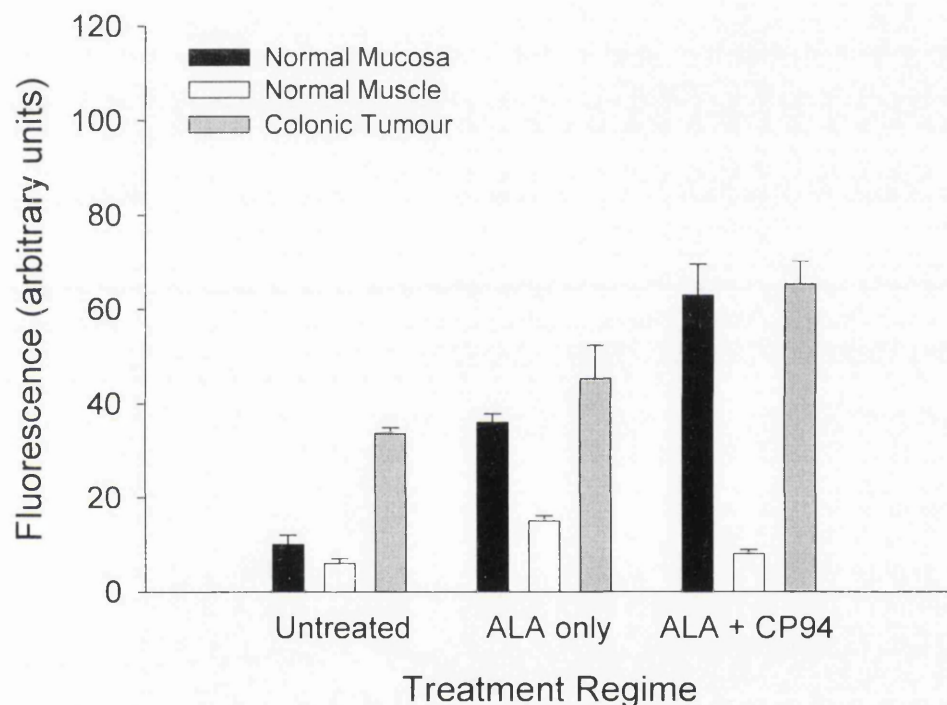


Figure 17 Fluorescence (arbitrary units) of the normal colonic mucosa, normal colonic muscle and colonic tumour model of either blank control tissue or tissue 75 minutes after administration of 50 mg/kg ALA i.v. alone or 50 mg/kg ALA + 100 mg/kg CP94 i.v. Each bar represents the mean values from three separate animals. Error bars as determined by the standard error of the mean.

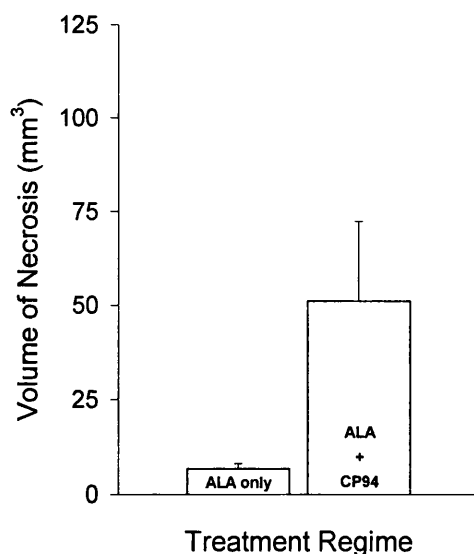


Figure 18 Mean volume of necrosis (mm³) as a function of the PDT treatment regime. 50 mg/kg ALA i.v. was administered alone or in combination with 100 mg/kg CP94 i.v. 75 minutes prior to 100 J of 628 nm light (100 mW) using a diode laser. Each group represents the mean (with the standard error of the mean) from four separate animals.

The results of the PDT studies can be seen in Figure 18. It shows the volume of necrosis (in mm³) produced in the colonic tumour model with the administration of ALA with or without CP94. The figure shows that a much greater volume of necrosis was produced when the iron chelator was given in combination with ALA than when ALA was given alone (ALA only = 7 mm³, ALA + CP94 = 51 mm³) ($p < 0.09$).

2.1.5.4 Discussion

The fluorescence studies show that the amount of PPIX fluorescence produced in the MC28 colonic tumour model, with the simultaneous administration of ALA and CP94, was very similar to that observed in the normal colonic mucosa. This indicated that comparable results should be obtained when using this technique in this tumour model as with the normal mucosa already studied. Both normal and malignant tissues showed maximal PPIX fluorescence when CP94 was administered with the ALA and a greater proportion of this fluorescence, in the tumour, was as a result of autofluorescence.

It is, therefore, possible to use an hydroxypyridinone iron chelator to increase the PPIX fluorescence produced in this tumour model. The degree of selectivity observed between the tumour and surrounding normal tissue may be reduced, however.

The PDT studies investigated whether this increase in PPIX fluorescence could be utilised to produce a bigger PDT effect and this was found to be the case. ALA administration with the iron chelator, CP94, produced over seven times (ratio = 7.6) the volume of necrosis as that produced by ALA alone, which is an immense improvement. It remains to be seen, however, if these results can be replicated in clinical studies.

2.1.6 Topical Iron Chelator Administration in a Normal Skin Model

2.1.6.1 Introduction

The previous sections have investigated and established the beneficial effect of the iron chelator, CP94, in the normal and malignant rat colon, which is a convenient experimental model. It is most likely, however, that the first clinical application of this technique (and one of the largest current uses of ALA PDT) would be the treatment of malignant and pre-malignant skin lesions using a topical preparation. The iron chelator, desferrioxamine, has already been investigated in this field with some success (Fijan *et al*, 1995). This section will therefore investigate whether CP94 can be used topically to improve the treatment of skin conditions when using ALA induced PDT.

Good cosmetic results make ALA induced PDT particularly suitable for many dermatological applications (Kennedy and Pottier, 1992). Kennedy *et al* first reported the use of topical ALA for PDT in 1990 and extensive clinical trials have been conducted since on many malignant and non-malignant skin conditions. On the whole good results are obtained with superficial non-melanoma lesions (basal and squamous cell carcinomas) but nodular lesions fare less well (Peng^b *et al*, 1997). Higher ALA concentrations and longer application times, however, do tend to increase the PPIX content and thus improve the outcome for these nodular lesions. We are, therefore,

investigating the use of an iron chelating agent to increase the effectiveness of this treatment modality without having to increase either, the ALA dose or application time.

2.1.6.2 Materials and Methods

Chemicals

ALA and the iron chelator, CP94, were prepared in a polyethylene glycol (PEG) base for topical application. A basic PEG cream (containing neither compound) was used as a blank control. Preparations containing 200 mg/ml ALA, 100 mg/ml CP94 and 200 mg/ml ALA plus 100 mg/ml CP94 were also used. No adverse effects were observed when administering any of the compounds.

Animal model

Normal, female, Wistar rats (120 - 200 g) were used throughout. The animals were anaesthetised for all parts of the procedure using inhaled halothane.

Fluorescence studies

An area of skin on the animal's flank was prepared prior to application. This was done by removing the animal's hair using electric clippers followed by hand shaving using a scalpel blade. A foil stencil was applied so that only a 1 cm² area of skin was exposed. 0.1 ml of the appropriate cream (ALA, CP94, combined or PEG control) was then spread over the 1 cm² spot and covered with a dressing, two animals being treated with each set of parameters. Completely blank, untreated, control animals

were also studied. The animals were recovered and killed serially at various times after topical application (1 - 8 hours). The treated area of skin along with a similar untreated (but shaven) area of skin from the opposite flank were removed and snap frozen in liquid nitrogen, so that frozen sections could be analysed by fluorescence microscopy (as described previously in section 2.1.2.2). There were two animals in each of the treatment groups in the fluorescence study. Statistical analysis between the means of the ALA only and ALA plus CP94 groups, at the time of maximum fluorescence, was conducted using an unpaired student t-test and error bars were determined by the standard error of the mean.

Fluorescence emission spectra were also recorded from separate representative frozen specimens to confirm that the fluorescence observed in the imaging was indeed produced by PPIX and no other fluorescent porphyrin. This was carried out by placing the skin specimen on a glass slide under the plate well reader of a luminescence spectrometer (Perkin Elmer Ltd., Beaconsfield, Buckinghamshire, UK). This was set to read over the range of 600 - 750 nm, exciting with 410 nm light and using 10 nm slits with a 530 nm cut off filter in place to remove scattered excitation light. Normal autofluorescence was detected in skin from untreated control animals and subtracted from the treated spectra. Calibration using a rhodium disc was conducted both before and after taking spectra.

PDT studies

All compounds were administered to prepared skin (in the same way as the fluorescence studies) 5 hours prior to irradiation. The light source was a Medi-Sun arclamp (Medical Light Technologies, Glasgow, Scotland) irradiating at 630 nm (+/-

20 nm). A total energy dose of 100 J was administered to 1 cm² areas of skin (with the surrounding skin shielded) at a fluence rate of 150 mW/cm². The shielding was then removed and the animals recovered. Each treatment site was assessed regularly over 14 days using the following scale (adapted from Robinson *et al*, 1998 & 1999):-

0	No effect
1	Minimal redness
2	Redness
3	Dry desquamation
4	Thin scab formation
5	Thick scab formation

This enabled the effect of each treatment (ALA + light, CP94 + light, ALA plus CP94 + light, light only control, ALA only control, CP94 only control and blank control) to be compared, with four animals being treated with each set of parameters. Statistical analysis between the means of the ALA + light and ALA plus CP94 + light groups, at the time of maximum PDT damage, was conducted using a Wilcoxon signed-rank test.

2.1.6.3 Results

Tissue fluorescence quantification

A representative set of photographs can be seen in Figure 19. One pair (Figures 19a & b) shows a typical false colour coded CCD image of the skin with its matched H & E stained photograph, five hours after topical administration of 0.1 ml of 200 mg/ml ALA cream to a 1 cm² area of skin. The other pair (Figures 19c & d) shows the same images, five hours after administration of 0.1 ml of 200 mg/ml ALA + 100 mg/ml CP94 cream to another 1 cm² area of skin. The fluorescence observed in the

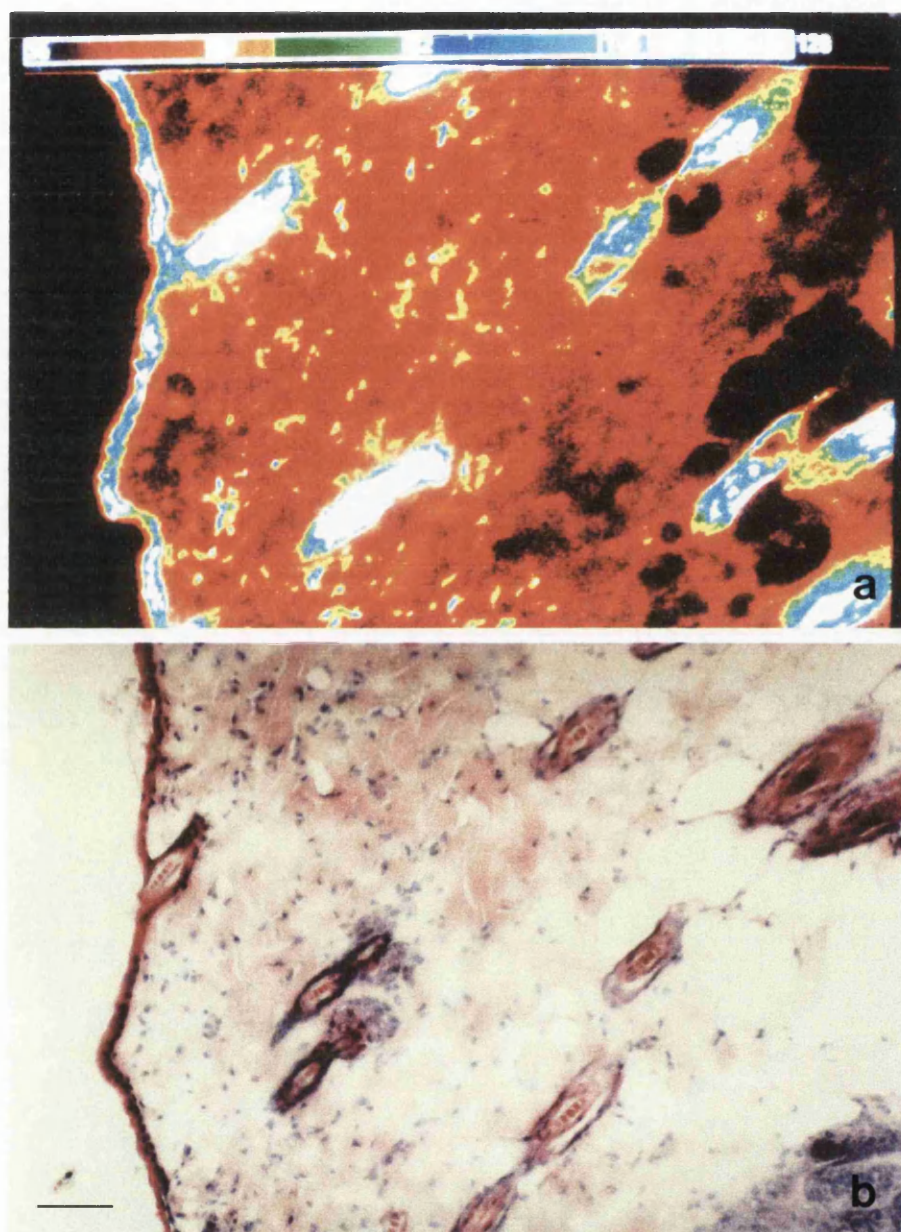


Figure 19 a) False colour coded fluorescence image and b) matched H & E stained histology photograph of the skin, five hours after topical administration of 20 mg ALA. Scale bar represents 70 µm.

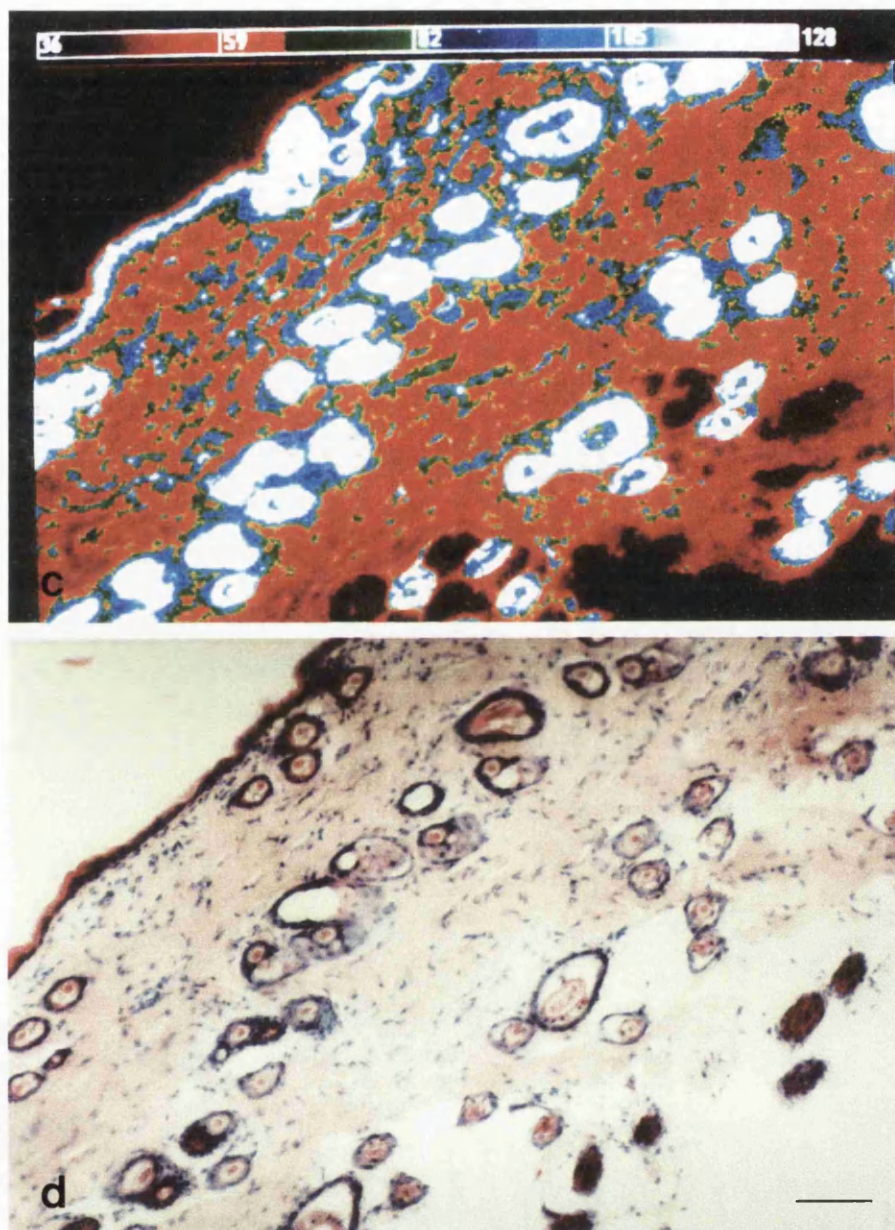


Figure 19 c) False colour coded fluorescence image and d) matched H & E stained histology photograph of the skin, five hours after topical administration of 20 mg ALA + 10 mg CP94. Scale bar represents 70 μ m.

epidermis is much greater with the administration of CP94 in combination with ALA, than ALA administration alone. The hair follicles can be seen to fluoresce greatly, as does the stratum corneum.

Figure 20a shows how the fluorescence in the epidermis of the skin varied with time after topical application of ALA alone and ALA plus CP94. Measurements were taken from the epidermis of each section avoiding the highly fluorescent hair follicles and stratum corneum. The combination of ALA plus CP94 produced a slightly higher level of fluorescence (29% increase) in the tissue than ALA alone ($p < 0.09$), peaking at 5 hours (the time chosen for photodynamic studies). Figure 20b shows the fluorescence profile from the matched untreated skin specimens taken from the opposite flank of the same animals. Fluorescence in these untreated areas hardly rose above background levels (which have been subtracted from all fluorescence measurements).

Fluorescence spectroscopy

Fluorescence spectra were recorded (using the spectrometer) from frozen specimens of tissue taken from animals given each treatment regime and representative spectra are shown in Figure 21. The spectra from blank control sections (no compounds administered) were subtracted from each spectrum to correct for endogenous autofluorescence. No significant differences were observed between the ALA only (Figure 21a) and the combination of CP94 and ALA (Figure 21b) spectra or any other spectra recorded during this study, which supports the previous findings in the colon, that the iron chelating agents do not induce significant production of fluorescent species other than PPIX. Maxima were at 636 ± 2 nm in each case.

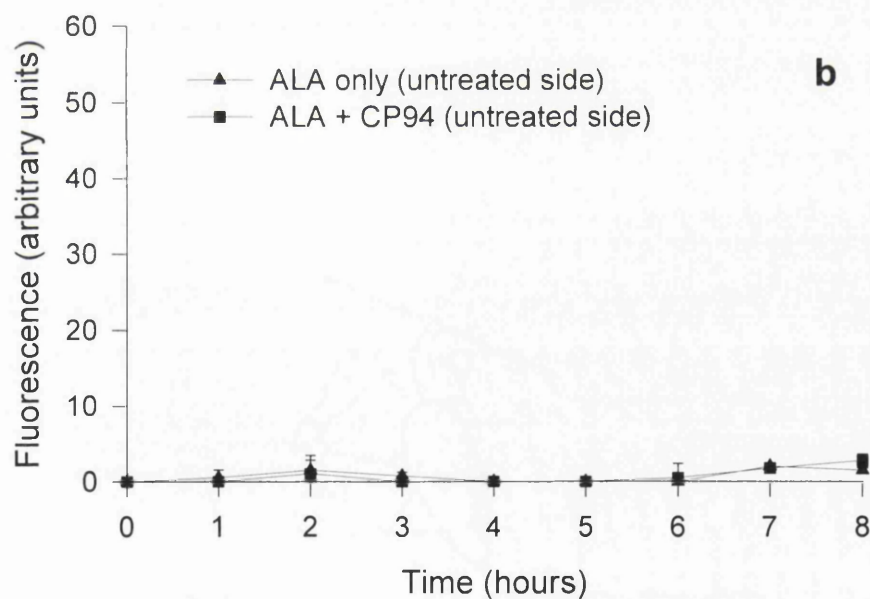
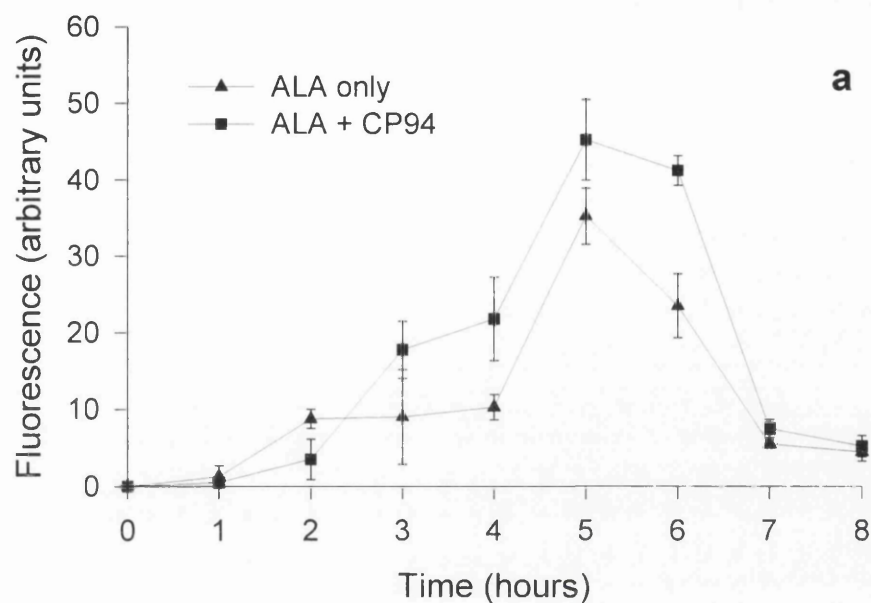


Figure 20 Fluorescence (arbitrary units) of the epidermis as a function of time (hours) when a) treated with 20 mg ALA only or 20 mg ALA plus 10 mg CP94, topically or b) untreated (when the opposite flank of the animal had been treated with 20 mg ALA only or 20 mg ALA plus 10 mg CP94, topically). Each point represents the mean (with the standard error of the mean) from two separate animals.

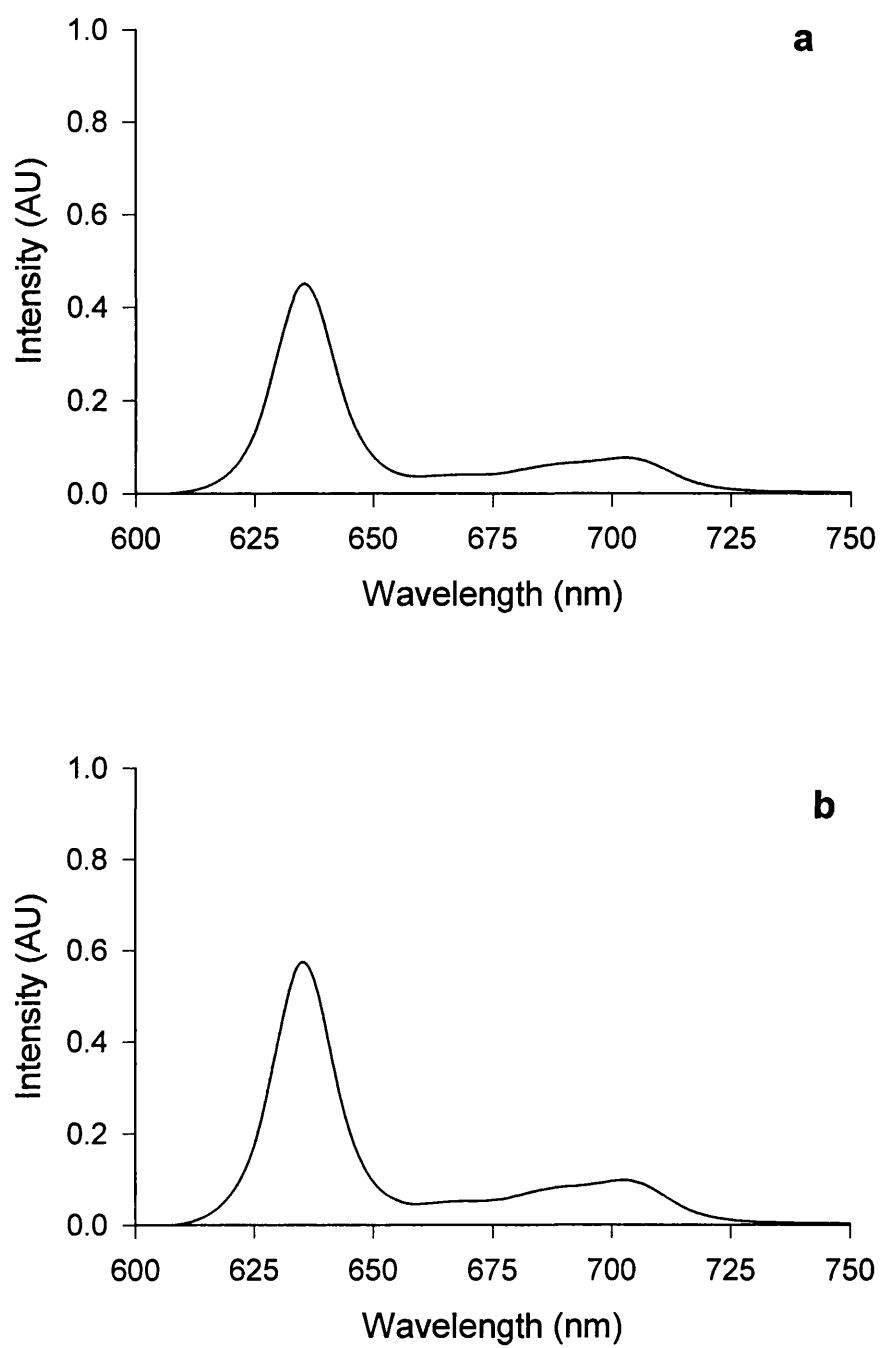


Figure 21 Emission spectra obtained from skin specimens treated topically with
a) 20 mg ALA only or b) 20 mg ALA plus 10 mg CP94, 5 hours after administration.

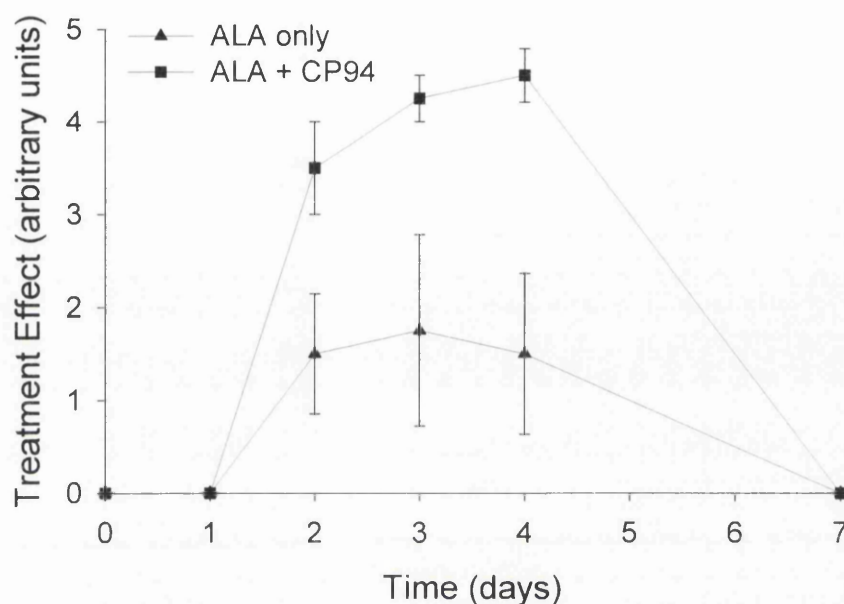
Photodynamic effects

Figure 22 Treatment effect (arbitrary units) as a function of time (days) following topical PDT treatment with 20 mg ALA only or 20 mg ALA plus 10 mg CP94 and 100 J/cm², 630 nm irradiation (150 mW). Each group represents the mean (with the standard error of the mean) from four separate animals.

The effect of CP94 on ALA induced PDT is shown in Figure 22. Each point represents the four animals treated in each group, the assessment scale score of each being averaged for each day. A much greater effect (an increase by up to a factor of three) was obtained when using the combination of ALA plus CP94 rather than ALA alone ($p < 0.07$). It should be noted, however, that the assessment score recorded was the highest that occurred within the treated area and in general “patchy” effects were produced, some parts of the 1 cm² spot being affected more than others. No effect was

seen until day 2. The maximum effect was observed at 4 days and resolved completely by day 7. At day 14, all treatment sites appeared normal and in all but one instance, substantial hair re-growth had occurred. CP94 only plus light, light only, ALA only, CP94 only, PEG only and blank controls were also conducted, none of which produced any effect.

2.1.6.4 Discussion

PDT using topical ALA has been shown over the last few years to be an effective treatment for conditions like actinic keratosis, Bowen's disease and superficial basal cell carcinomas, with the only main side effect being discomfort/pain during irradiation (Szeimies *et al*, 1996). The treatment of nodular basal and squamous cell carcinomas and other thicker cutaneous lesions with topical ALA PDT is as yet, however, unsatisfactory, with low complete response rates and high recurrence rates (Peng^b *et al*, 1997) as the depth of necrosis produced is insufficient. One way to overcome this problem may be the administration of an iron chelating agent in combination with ALA, as reported here. This enhances the effect of the treatment, producing more damage, without increasing the administered dose of ALA or prolonging the duration of treatment.

The quantitative CCD fluorescence microscopy determined that the CP94 when administered in combination with ALA was able to increase the PPIX fluorescence detected in the epidermis of the skin by 29% at the fluorescence peak and this enabled an increase in the photodynamic effect by up to a factor of 3 to be achieved (when

compared with the effect of ALA alone). These results support the findings of the previous sections which employed intravenous ALA plus CP94 in the rat colon.

No significant production of PPIX was detected in the untreated skin from the opposite flank. This was investigated as there are reports in the literature (Casas *et al* (in press), Stringer *et al*, 1996) which describe porphyrins in untreated areas of skin indicating that some systemic effect may be produced when ALA is applied topically. There was no evidence in this study to support these findings.

The PDT changes produced were not found to affect all parts of the treatment site to the same extent. The reasons for this are unclear. It could be explained by uneven drug distribution in the cream base employed or small scratches (produced during shaving) allowing uneven drug absorption; but this should have been observed in the fluorescence microscopy investigation and all preparations were thoroughly mixed prior to use and great care was taken during shaving. The patchy effect may have also been caused by uneven light irradiation, although the damage appeared to be completely random and the power was checked both before and after the treatment and did not vary significantly over this period. Alternatively, it may have been due to naturally occurring irregularities in skin thickness or follicle distribution (which are particularly fluorescent).

Although normal skin was investigated in this study, it is expected that the PDT effect induced by the treatment will be greater in clinical application to abnormal skin. This is because the uptake of ALA is impeded (to some extent) by the epidermis in normal skin and that many malignancies have abnormal overlying epidermis which allows

greater penetration to occur. This is why many experimental studies employ skin stripping prior to drug application (Goff *et al*, 1992).

Fluorescence spectral analysis using a spectrometer also confirmed the previous findings in the rat colon, that the fluorescence observed, could be attributed to PPIX and not other porphyrins which might have been produced by the altered biochemistry induced by these compounds.

No attempt was made in this study to determine the depth of the PDT effect and future studies must investigate this factor which is crucial to the success of this technique in dermatological applications. Nonetheless, this section has established (in normal rat skin) the feasibility of using the iron chelating agent, CP94, topically, to increase the PDT effect produced by ALA induced PPIX photosensitisation.

2.1.7 Topical Iron Chelator Instillation in Normal Uterus

2.1.7.1 Introduction

Another large, potential clinical application of ALA induced PDT is as a technique of endometrial ablation. Hysterectomy, is one of the most commonly performed major operations in the United Kingdom and is often conducted as the result of dysfunctional uterine bleeding (Pinion *et al*, 1994). Minimally invasive procedures are being investigated as an alternative to major surgery in these cases and usually involve thermal coagulation of the endometrial layer (Tadir *et al*, 1999). Unsatisfactory bleeding control, uterine perforation and the need for anaesthesia, however, has led to ALA PDT being investigated as an alternative technique of endometrial ablation.

Current clinical experience with ALA induced PDT as a method of endometrial ablation has had limited success (Gannon *et al*, Conference Presentation, 1998) partly due to inadequate light devices resulting in not all parts of the uterus receiving enough light to completely ablate the endometrium and partly due to insufficient levels of PPIX being present throughout the endometrial layer. Without total destruction of the endometrial layer, including the deep glands and stem cells from which the endometrium regenerates, prolonged endometrial ablation and therefore symptom relief, cannot be obtained (Fehr *et al*, 1996). It is known, however, from fluorescence studies in humans (Gannon *et al*, 1995) that PPIX accumulates preferentially in the

endometrium, rather than in the underlying myometrium, which reduces the risk of uterine perforation.

This section will, therefore, investigate the effect of the iron chelating agent CP94, when administered topically in combination with ALA, as an instillation in the normal rabbit uterus. The rabbit uterus is a convenient model for these experiments as it is split into two separate uterine horns, which can be used to compare and contrast treatment regimes within the same animal. In addition to this, ovulation in the rabbit is triggered by copulation, resulting in all the animals used in this study being in the same early, proliferative phase of their menstrual cycle.

2.1.7.2 Materials and Methods

Chemicals

ALA and the iron chelator CP94, were prepared in saline and buffered (immediately prior to instillation) to pH 4.5 - 5.0 with phosphate. Solutions containing 400 mg/ml ALA only or 400 mg/ml ALA in combination with 100 mg/ml CP94 were prepared. No adverse effects were observed when administering any of the compounds.

Animal model

Normal, female, New Zealand White rabbits (3 - 4 Kg) supplied by Charles River UK Ltd. (Margate, Kent) were used throughout. The animals were anaesthetised for all parts of the procedure using Hypnorm (Fentanyl and Fluanisone, Janssen Pharmaceutical Ltd., Oxford, UK) as pre-medication 15 minutes prior to induction

with Diazepam (Phoenix Pharmaceuticals Ltd, Gloucester, UK). Analgesia was administered subcutaneously following surgery (Buprenorphine hydrochloride, Reckitt & Colman Products Ltd., Hull, UK).

Fluorescence studies

The uterine horns were exposed via a laparotomy. 0.5 ml of the buffered drug solution (either 400 mg/ml ALA alone or 400 mg/ml ALA in combination with 100 mg/ml CP94) was instilled into each uterine horn using a small gauge needle. Loose silk ties were applied for identification purposes and the distal end of each horn tied to prevent leakage. The animals were then recovered and killed serially at various times after instillation (3 - 12 hours). Uterine specimens were removed and snap frozen in liquid nitrogen, so that frozen sections could be analysed by fluorescence microscopy (as described previously in section 2.1.2.2). Two animals were studied at each time point as well as complete blank controls. Statistical analysis between the means of the ALA only and ALA plus CP94 groups, at the time of maximal fluorescence, was conducted using an unpaired student t-test and error bars were determined by the standard error of the mean.

Fluorescence emission spectra were also recorded from separate representative frozen specimens to confirm that the fluorescence observed in the imaging was indeed produced by PPIX and no other fluorescent porphyrin, as described previously in section 2.1.3.2 but with the fibre-optic bundle being positioned directly above the opened specimen (endometrium uppermost) instead of through a microscope.

PDT studies

All compounds were administered to the uterine horns (in the same way as the fluorescence studies) 7 hours prior to irradiation. A second laparotomy was then performed under general anaesthetic so that a 4 cm diffuser fibre could be inserted into each horn in turn and a total light dose of 100 J/cm fibre (output power, 100 mW/cm fibre) could be delivered to each, using the 628 nm diode laser. The animals were then recovered and killed at three days for histological examination of the uterine horns. There were four animals treated with ALA in one horn and ALA + CP94 in the other horn. Two light only, drug only and complete blank controls were also conducted.

2.1.7.3 Results

Tissue fluorescence quantification

A representative set of photographs can be seen in Figure 23. One pair (Figures 23a & b) shows a typical false colour coded CCD image of the uterus with its matched H & E stained histology slide, seven hours after topical instillation of 0.5 ml of 400 mg/ml ALA into the uterine horn. The other pair (Figures 23c & d) shows the same images, seven hours after instillation of 0.5 ml of 400 mg/ml ALA + 100 mg/ml CP94 into the other uterine horn. The fluorescence observed in the endometrium is much greater with the administration of CP94 in combination with ALA, than ALA administration alone and is higher, in both cases, than the fluorescence observed in the underlying myometrium.

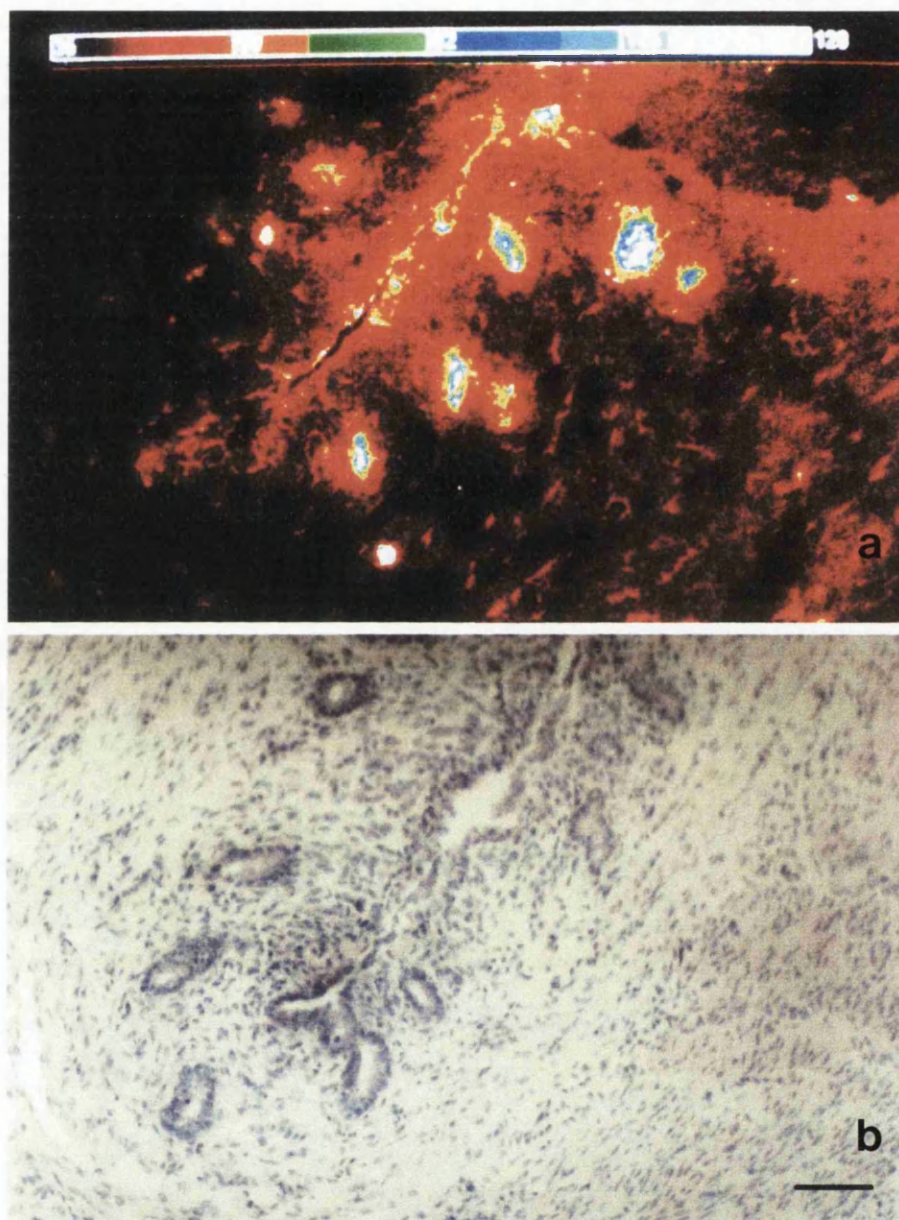


Figure 23 a) False colour coded fluorescence image and b) matched H & E stained histology photograph, of the uterus, seven hours after topical instillation of 200 mg ALA. Scale bar represents 70 μm .

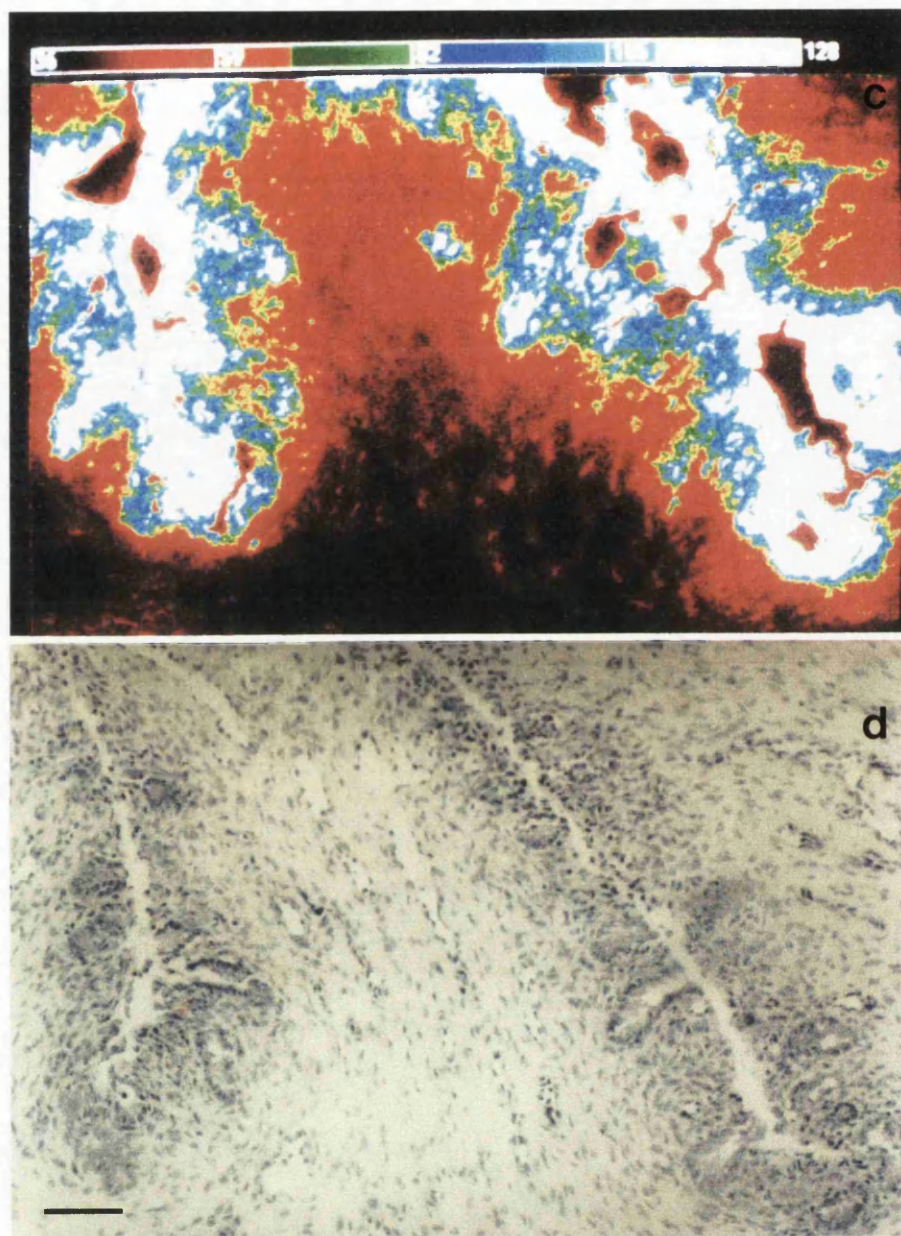


Figure 23 c) False colour coded fluorescence image and d) matched H & E stained histology photograph, of the uterus, seven hours after topical instillation of 200 mg ALA + 50 mg CP94. Scale bar represents 70 µm.

Figure 24a shows how the fluorescence in the endometrium and myometrium varied with time after topical instillation of ALA alone into the uterus. A slightly higher level of fluorescence was observed in the endometrium than in the underlying myometrium. The highest fluorescence was observed at 8 hours although there was no definite peak, both the curves being relatively flat. The combination of ALA plus CP94 (Figure 24b) produced a higher level of fluorescence (66% increase) in the endometrium than ALA alone (ALA only = 30 a.u., ALA + CP94 = 50 a.u.) ($p < 0.03$), peaking at seven hours (the time chosen for photodynamic studies). The difference between the level of fluorescence in the endometrium and underlying myometrium was also large (ratio = 7.1) at the time of the peak (endometrium = 50 a.u., myometrium = 7 a.u.) ($p < 0.0001$). Background levels taken from blank controls have been subtracted from all fluorescence measurements.

Fluorescence spectroscopy

Fluorescence spectra were recorded from frozen specimens of uterine tissue taken from animals given each treatment regime and representative spectra are shown in Figure 25. The spectra from blank control sections (no compounds administered) were subtracted from each spectrum to correct for endogenous autofluorescence. No significant differences were observed between the ALA only (Figure 25a) and the combination of CP94 and ALA (Figure 25b) spectra or any other spectra recorded during this study. This supports the previous findings in the colon and skin of normal rats, that the iron chelating agents do not induce significant production of fluorescent species other than PPIX. Maxima were at 635 ± 2 nm in each case.

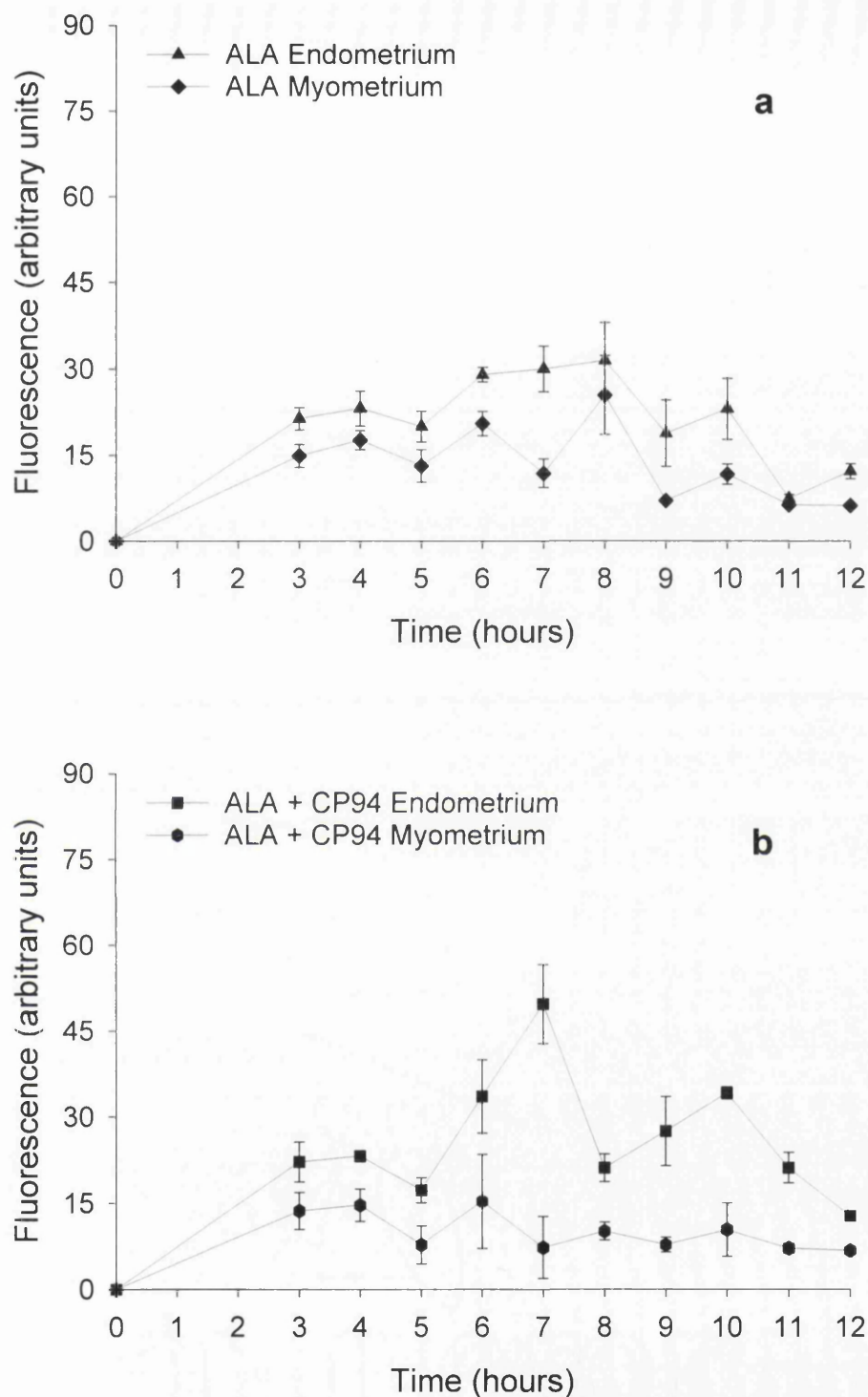


Figure 24 Fluorescence (arbitrary units) of the endometrium and myometrium as a function of time (hours) when the uterine horn had been treated with a topical instillation of a) 200 mg ALA only or b) 200 mg ALA plus 50 mg CP94. Each point represents the mean (with the standard error of the mean) from two separate animals.

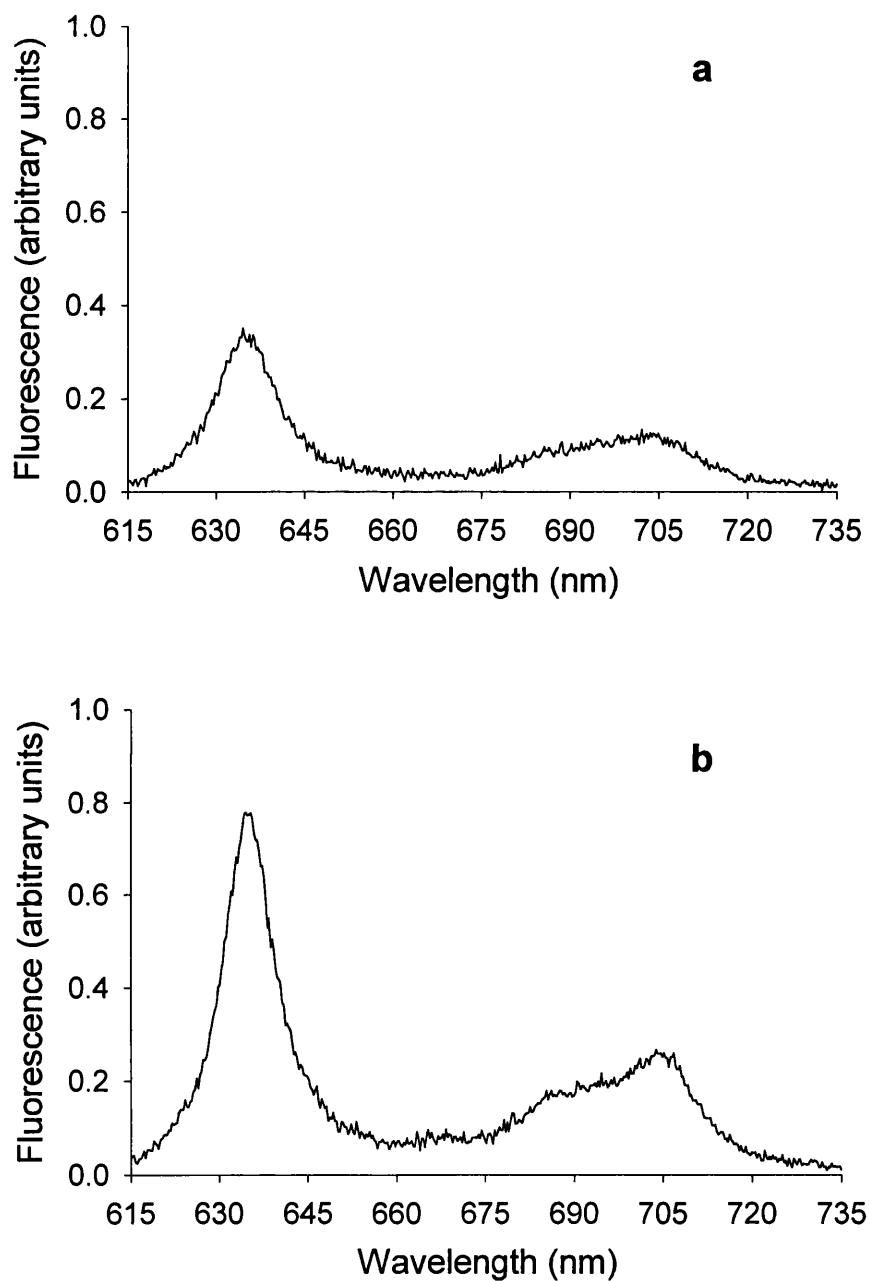


Figure 25 Emission spectra obtained from uterine specimens which had been treated with a topical instillation of either a) 200 mg ALA only or b) 200 mg ALA plus 50 mg CP94, 7 hours previously.

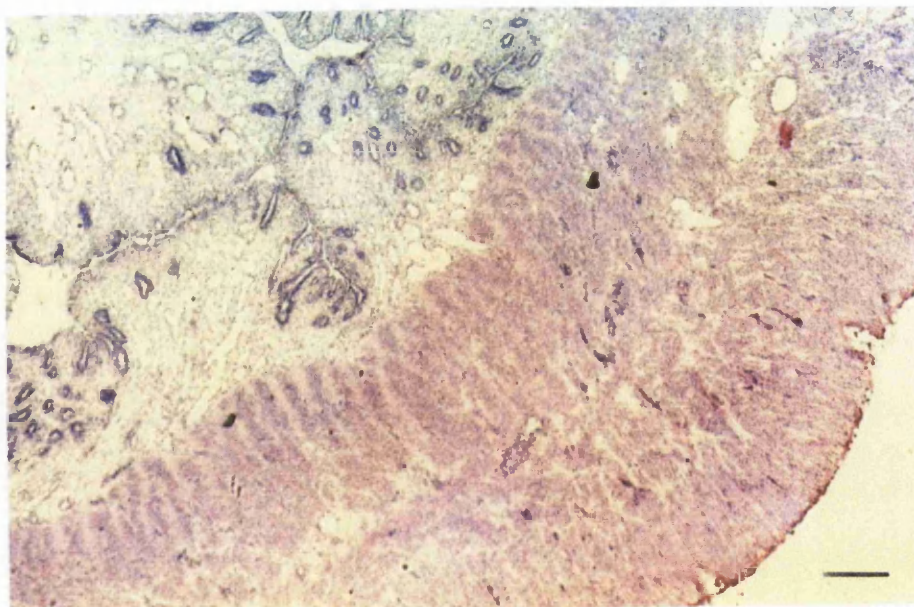


Figure 26a Photograph of a H & E histology slide showing the normal histology of the uterus (blank control). Scale bar represents 150 μm .

Photodynamic effects

The effect of CP94 on ALA induced PDT can be seen in the photographs of representative H & E histology slides presented from each of the treatment groups in Figure 26. Figure 26a shows the normal histological architecture of the normal rabbit uterus as obtained from the blank controls. Light only, ALA only and ALA + CP94 only controls were also conducted, none of which produced any histology significantly different to this. The natural folds of the normal endometrium can be seen (as this specimen was not opened prior to histology sections being made). There are numerous glands in the normal endometrium, some of them located deep in the folds and the entire endometrial surface is covered by a thin layer of columnar surface epithelium. Underlying the endometrium is the stroma, which consists of loosely

structured fibroblasts with extracellular matrix and capillaries of varying density. Beneath the stroma is the myometrium which has an inner layer of circular and an outer layer of longitudinal muscle.

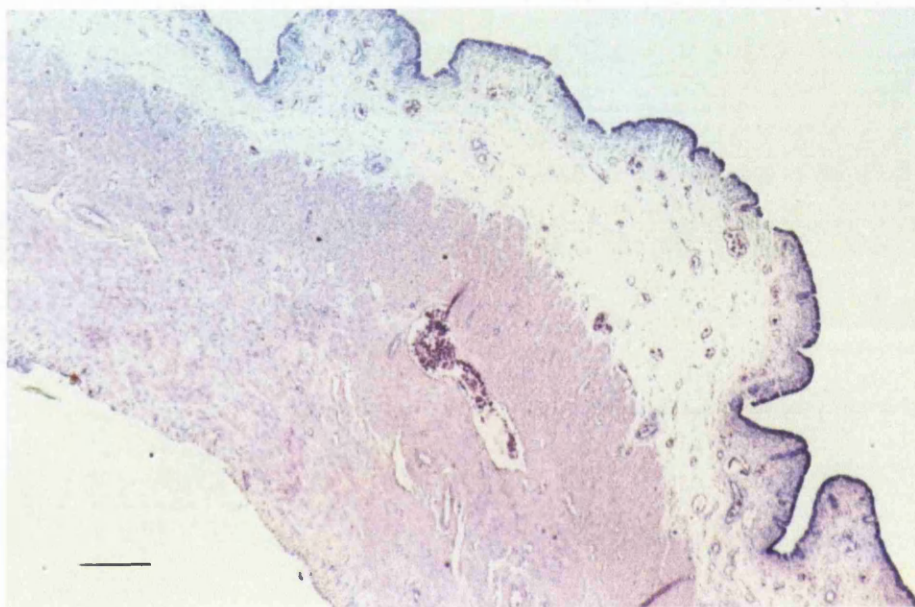


Figure 26b Photograph of a H & E histology slide showing the histological effect on the uterus three days after instillation of 200 mg ALA only, seven hours prior to 100 J/cm, 628 nm diode laser irradiation (100 mW/cm) using a 4 cm diffuser fibre. Scale bar represents 150 μ m.

The endometrial morphology was changed completely following ALA PDT and can be seen in Figure 26b. Although this specimen had been opened out prior to histology slides being cut (to check for signs of macroscopic damage) it was treated in exactly the same way, with the same cross-sectional aspect and magnification being presented. The endometrium from specimens in this ALA only treatment group had a flattened appearance, with few or no folds present. The epithelial layer was altered and few

glands were observed, although some deeper glands remained. There was no apparent effect of the treatment on the underlying myometrial layer but the endometrium showed signs of extensive damage following ALA PDT.

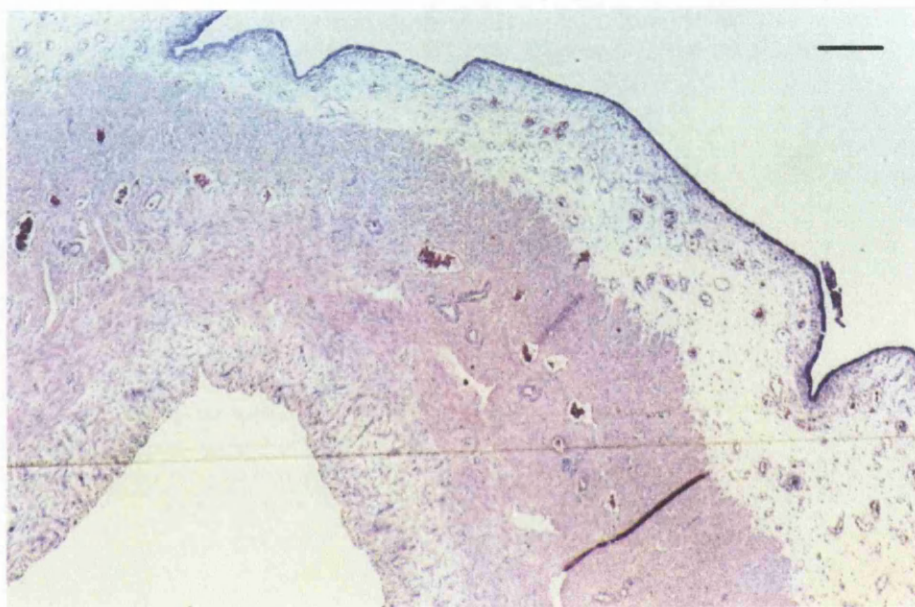


Figure 26c Photograph of a H & E histology slide showing the histological effect on the uterus three days after instillation of 200 mg ALA and 50 mg CP94, seven hours prior to 100 J/cm, 628 nm diode laser irradiation (100 mW/cm) using a 4 cm diffuser fibre. Scale bar represents 150 μ m.

Figure 26c shows a photograph of a representative H & E histology slide from the ALA + CP94 PDT group, prepared in the same manner as the ALA PDT group. This group showed signs of even greater endometrial damage with the endometrium being even flatter, than that of the ALA only group, with even less evidence of folds. Endometrial glands were absent even deep into the endometrial layer. A greater effect was therefore obtained, in this model, when the combination of ALA plus CP94 was

instilled topically into the uterus, rather than ALA alone, with the combination producing complete endometrial ablation.

2.1.7.4 Discussion

The fluorescence studies show that PPIX accumulates mainly in the endometrium of the uterus and not in the underlying myometrium. This is consistent with previous studies conducted in both rats (Yang *et al*, 1993) and humans (Fehr *et al*, 1996; Gannon *et al*, 1995). It is important that the myometrial layer is unaffected by the treatment (if this modality is going to be a successful clinical technique of endometrial ablation) so that it maintains its function, reducing the risk of uterine perforation. However, scarring in this situation is not of major concern.

In the ALA only group the level of fluorescence was only a little higher in the endometrium than in the myometrium. With the combination of ALA and CP94, however, a significant seven fold difference in level of fluorescence was obtained between the two tissues at the peak (7 hours). This indicates that the addition of CP94 to the instillation improved the selectivity of fluorescence between the endometrial and myometrial layers.

The highest level of endometrial fluorescence measured in the ALA only group was after 8 hours, with the addition of CP94, this was found to be slightly earlier, at 7 hours. Both these times are consistent with the range of times of peak fluorescence as determined in clinical studies (Fehr *et al*, 1996), 4 - 8 hours. Once again the spectral

analysis confirmed that the fluorescence was produced by PPIX and no other fluorescent porphyrin.

As well as improving selectivity, the addition of the iron chelator also significantly increased the level of fluorescence in the endometrium (at the peak) by 66%. The histological results of the PDT study indicate that this increase in endometrial PPIX enabled greater endometrial destruction to occur on irradiation. The histological examination of endometrial damage following ALA induced PDT of this study produced similar findings to those of Wyss *et al* (1996) who have studied this in detail (also in the rabbit) using light and scanning electron microscopy. The only discrepancy between the studies is that they found endometrial regeneration to be complete by 72 hours. This may be due to a lower light dose being employed in their study resulting in little endometrial damage and therefore rapid healing. Yang *et al* (1993) in the rat uterus, found that there was no evidence of endometrial regeneration 10 days after ALA PDT.

The ALA only PDT group, although showing signs of extensive endometrial damage, did have a few deeper, endometrial glands still present following PDT treatment. Once again, this is consistent with the findings of Yang *et al* (1993). If this reflects accurately what is happening clinically, this may explain the current limited clinical effect, as it is likely that the endometrial regeneration occurs from these residual glands. To enable prolonged symptom relief to occur, all of the endometrial glands must be destroyed throughout the whole thickness of the endometrial layer. This appeared to be the case in the ALA + CP94 PDT group which showed evidence of complete endometrial destruction. Further work must be conducted, however, to

determine whether this destruction is prolonged, before preliminary clinical trials can commence with this treatment modality.

2.1.8 Discussion

This experimental section has investigated the effectiveness of hydroxypyridinone iron chelators as potential enhancers of ALA PDT, in several animal models. The initial studies in the normal rat colon determined that the more lipophilic hydroxypyridinone, CP94, was more promising for this application than the other hydroxypyridinone studied, CP20 (which is more hydrophilic). Subsequent experiments, therefore, concentrated on CP94.

The fluorescence microscopy studies found that the addition of CP94 produced greater fluorescence, in all the models studied (rat colon, rat colonic tumour model, rat skin and rabbit uterus), than the administration of ALA alone. In the normal rat colon it was also observed that as the ALA dose increased, the degree of potentiation the addition of CP94 generated, reduced. Spectrofluorimetry confirmed that the fluorescence produced could be attributed to PPIX and no other fluorescent porphyrin.

PDT studies determined that it was possible to utilise the increased PPIX fluorescence demonstrated in each of the fluorescence microscopy studies (through the addition of CP94) to substantially enhance the PDT effect produced by ALA. Once again, it was found in the normal colon model that as the ALA dose was increased, the degree of potentiation obtained with the addition of CP94, reduced. The extent of enhancement produced by CP94 in the PDT study was even greater than that observed in the pharmacokinetic study.

It was found in the colon that CP94 increased peak mucosal fluorescence by up to four times, whereas with light irradiation the effect on PDT damage was a six fold increase (when using 25 mg/kg ALA i.v.). Results in the colonic tumour model were slightly better than, but still comparable with those from the normal colon studies. In normal rat skin, a small increase in PPIX fluorescence (29%) could be obtained with the addition of CP94 and produced a substantial improvement in PDT effect.

The combination of ALA and CP94 in the rabbit uterus improved both the selectivity between the endometrium and underlying myometrium and increased the PPIX fluorescence in the endometrium (by 66%). This enabled greater endometrial destruction to occur with irradiation, when CP94 was administered in combination with ALA.

It has, therefore, been shown that the simultaneous administration of CP94 with ALA can enhance ALA PDT and in certain circumstances this enhancement can be very substantial. It has also been demonstrated that the compound CP94 can be used to enhance ALA PDT as an intravenous solution, topical cream or instillation. This makes it potentially possible to apply this technique of enhancement to many clinical applications of ALA PDT and several of these have been investigated here, with positive results.

The clinical application of CP94 as a method of enhancement of ALA PDT should be relatively simple to implement. The technique only requires the CP94 to be combined with the ALA preparation at the time of formulation (prior to application) and then the PDT treatment can proceed as normal. Preliminary clinical trials will need to confirm

the best drug/light interval with the ALA/CP94 combination to achieve the best results.

Although CP94 will potentially increase the PDT effect produced when administered clinically (in combination with ALA) it is also likely that it will also increase the side effects of the treatment, namely cutaneous photosensitivity, when administered systemically, as the level of PPIX produced will be greater. Although this is a disadvantage, it is likely that the photosensitivity produced will be short lived and will still remain substantially shorter than that experienced with other photosensitisers and the higher levels of PPIX in the tissue to be treated, should improve the outcome of the treatment.

CP20 has been investigated more extensively in humans as a treatment of iron overload than CP94 and although these compounds are safe with few side effects experienced in the short-term, some adverse effects (agranulocytosis) have been recorded with long-term, high dose hydroxypyridinone administration (Al-Refaie *et al*, 1992). It is very unlikely that any such problems should be experienced with the one off administration of CP94 suggested here, as a technique of enhancement of ALA PDT.

Although, the effects of desferrioxamine (a clinically established iron chelator) on ALA PDT have not been investigated in this study, it has been previously found to be beneficial (Ortel *et al*, 1993). Desferrioxamine, however, is a relatively large compound (molecular weight, 657) with lower lipophilicity than CP94 (molecular weight, 206) which makes it a less efficient iron chelator in this situation

(Abseysinghe *et al*, 1996). Desferrioxamine also has the disadvantage of being administered to patients as an infusion, so the orally active hydroxypyridinones are a much more attractive group of iron chelators for this particular application.

This experimental section has, therefore, both established and confirmed, in a number of different animal models, that the iron chelator CP94, can substantially improve ALA induced PDT. Although further investigation is still required (particularly with oral administration), preliminary clinical trials utilising CP94 should be seriously considered, as an effective, safe and simple, technique of enhancement for this treatment modality.

PART II

Enhancement of ALA PDT using Light Dose Fractionation

2.2.1 Introduction

Another method which can be used to enhance the outcome of a PDT treatment is light dose fractionation and this experimental section will begin by investigating the effect of this technique on ALA induced PDT and will conclude with some preliminary experiments to start to determine its mechanism of action.

In clinical practice, PDT with ALA is most effective for treating superficial disease such as thin basal cell carcinomas of the skin, or dysplasia in the mucosa lining hollow organs of the body. The effect is limited partly by the maximum dose of ALA that can be tolerated by mouth (60 mg/kg) but also by the large light doses required, which inevitably means long treatment times compared with PDT using other photosensitisers like mTHPc (Bonnett, 1995). One way to alleviate this is to fractionate the light dose, which may make it possible to produce the same area of necrosis with a shorter total treatment time.

This simple technique has been described by several investigators. It has been successful when used with photosensitisers as different as HpD (Bourletias *et al*, 1994; Pe *et al*, 1994), AlS₄Pc (Anholt and Moan, 1991) and mTHPc (Muller *et al*, 1998; Mlkvy *et al*, 1996) in a variety of normal tissues and tumour models, but is particularly effective when used with ALA induced PPIX (Messmann *et al*, 1995; van der Veen *et al*, 1994; Hua *et al*, 1995).

Numerous experimental parameters have been used, however, which make comparisons difficult. Not only can the photosensitiser, its dose and the light dose vary, but the single or multiple intervals employed during irradiation can be as short as 10 seconds (Messmann *et al*, 1995) or as long as 24 hours (van Geel *et al*, 1996). It was with this in mind, that these experiments were undertaken, to investigate light dose fractionation in a single animal model with one photosensitiser (ALA induced PPIX), so that the important factors affecting its success could be identified.

Only interrupted, light dose fractionation, is studied here, the delivery of the light dose being interrupted for a period of seconds or minutes on one or more occasions. Anholt & Moan (1991) have described a fractionation regime where the light was switched on and off repeatedly for periods of 15 seconds and postulated that their success could be explained by localisation of the photosensitiser (AlS₄Pc) during the dark periods. Hua *et al* (1995) obtained similar results using ALA with on/off periods of 30 seconds.

The mechanisms involved in this situation are likely to be different from an alternative regime which could be termed periodic fractionation, where the dark intervals last hours or days, sometimes with readministration of the photosensitiser. Such a regime has been used by van Geel *et al* (1996) with mTHPc. They concluded that intervals of less than one hour would probably be preferable, with intervals longer than this being unsuccessful as a result of repair of sub-lethal damage during the dark period.

There are three main processes which are currently thought to be involved (albeit to varying degrees) in the enhancement of PDT by light dose fractionation:-

- i) Reoxygenation of the treatment site during the dark period
- ii) Reperfusion injury
- iii) Relocalisation of the photosensitiser during the dark period

Foster *et al* (1991) stated that the photochemical oxygen consumption during PDT is a critical factor, which although recognised, is frequently overlooked. This consumption resulting from photooxidation reactions is so substantial that it only takes a few seconds for some cells in the treatment area to become anoxic thus preventing further damage. This aspect is even more vital when treating tumours, as they are often less well oxygenated, at least in places. Fractionated regimes have been suggested to overcome this problem because as long as the microcirculation remains functional, it is possible to temporarily pause the photochemical processes by switching off the light. Reoxygenation can then take place during the dark period thus enhancing the final effect. Effective reoxygenation even of cells furthest away from the circulation can occur in times of the order of 45 seconds (Foster *et al*, 1991) but this obviously depends on the degree of hypoxia caused by the previous light fraction and the maintenance of a viable microcirculation.

Other studies have reported effects on the microcirculation which may contribute significantly to the mechanism of damage (Leveckis *et al*, 1995; Roberts *et al*, 1994). This includes arteriolar and venular constriction, reduced blood flow, numerous platelet thrombi and sometimes irreversible capillary shutdown. Leveckis *et al* (1995)

also found that these factors were affected by the rate of energy delivery (fluence rate) with arterioles constricting faster and slightly more with higher fluence rates. Arteriolar constriction reached its maximum by the end of the illumination time and recovered back to normal within two hours. In a previous and separate study (McIlroy *et al*, 1998), a rapid and significant decrease in oxygen levels (up to 10 fold within 4 minutes) has been observed during ALA induced PDT of the rat liver (using 50 mg/kg ALA i.v. and 60 J (100 mW) of 635 nm light). This fall in oxygen could be the result of oxygen consumption by the photodynamic reactions coinciding with microvascular constriction. Light dose fractionation could limit microvascular constriction, reducing the drop in oxygen levels in the treatment site, thus allowing more PDT damage to be produced.

Reperfusion injury could also occur as tissue is reperfused after a transient period of ischaemia. This happens as the enzyme, xanthine oxidase, becomes activated in a poorly oxygenated environment. Concomitantly, ATP is broken down, producing the purine substrates necessary for this enzyme to produce superoxide when oxygen is reintroduced (McCord, 1987). If at least partly reversible vasoconstriction is occurring during the first fraction of a PDT treatment as some studies indicate (resulting in an oxygen and thus energy compromised environment) then it is conceivable that free radical damage could occur in this manner.

Relocalisation of the photosensitiser during a short dark period could contribute to the enhanced effect of light fractionation, as suggested by Anholt and Moan (1991). This has also been observed during the longer dark period of 75 minutes, described by van der Veen *et al* using ALA (1994), where there was partial recovery of the

photobleaching of PPIX fluorescence observed after the first light fraction which was attributed to new PPIX production.

Currently, it is difficult to be sure which of the possible mechanisms introduced above is most relevant, or crucial, to the success of this technique when applied to ALA PDT, but some preliminary experiments, towards the end of this experimental section, have been included to commence investigating this point in greater depth.

This thesis extends the work of Messmann *et al* (1995), exploring ways of enhancing PDT with light fractionation in a single tissue, the rat colon, with the hope that this simple modification to ALA induced PDT could markedly reduce current treatment times, as well as increase clinical efficacy.

2.2.2 Light Dose Fractionation in Normal Colon

2.2.2.1 Introduction

Although, the principle of light dose fractionation is a simple concept, investigating it can be complex, with numerous treatment parameters to be studied individually. One set of standard ALA PDT parameters was, therefore, used for the initial studies, so that the critical factors effecting the outcome of the fractionation regime could be identified. Subsequent experiments then investigated the effect of altering the energy and drug doses on the success of particular fractionation regimes. All experiments were conducted on the colon of normal rats.

As an extension of the previous work conducted by Messmann *et al* (1995), the same treatment parameters and animal model were used as in their studies. They found that no lesion was produced in the normal rat colon when using an ALA dose of 25 mg/kg i.v. and no benefit was seen by increasing the ALA dose above 200 mg/kg i.v. The ALA dose used in this series of experiments has, therefore, been kept within these limits. They also found that when treating animals with 200 mg/kg ALA i.v. and an energy dose of 25 J (100 mW, copper vapour pumped dye laser tuned to 630 nm) by simply splitting the energy dose into two equal fractions using an interval (dark period) of 150 seconds (2½ minutes), the area of necrosis produced could be increased from 13 mm² (continuous light dose) to 94 mm² (fractionated light dose). This is a massive increase, simply achieved by turning off the laser for a short period of time.

Little benefit was seen by increasing the length of the dark interval and so a standard interval of 150 seconds has been used throughout all the experiments in this section.

Exactly the same experimental technique has been used in this study as Messmann *et al* (1995) employed, except the output of the copper vapour laser used for the initial studies was tuned to 635 nm rather than 630 nm, as this wavelength (635 nm) produces better results with ALA induced PPIX sensitisation than 630 nm (Szeimies *et al*, 1995). Subsequent studies used a 628 nm diode laser.

2.2.2.2 Materials and Methods

Chemicals

ALA powder was dissolved in physiological strength PBS (pH 2.8) and administered intravenously (with a concentration of 25, 50 or 200 mg/ml and a maximum volume of 0.2 ml).

Animal model

Normal, female, Wistar rats (120 - 200 g) were used throughout. The animals were anaesthetised for all parts of the procedure using inhaled halothane and analgesia was administered subcutaneously following surgery (Buprenorphine hydrochloride).

PDT studies

In the first series of experiments, all animals were given 200 mg/kg ALA intravenously, 2 hours prior to surgery. The colon was accessed for PDT via a laparotomy as described in section 2.0.0.2. The pulsed (12 kHz) copper vapour pumped dye laser (tuned to 635 nm) was used to deliver a total energy of 25 J (output power, 100 mW). The fractionation variables studied, were the position of the fractionation interval in the illumination time, the number of fractions (1-10) and the size of the second energy fraction in two fraction studies (5-20 J). The fractionation interval was fixed at 150 seconds throughout. The area of necrosis produced in the colon at three days was determined by measuring the minimum (a) and maximum (b) perpendicular diameters of the lesion macroscopically with a micrometer. These values were then used to calculate the area of necrosis using the formula $\pi ab/4$, as the lesions produced were approximately elliptical. All appropriate drug only, light only and continuous control groups were also conducted.

Subsequent experiments used 25, 50 or 200 mg/kg ALA i.v. with energy doses ranging from 25 - 200 J to determine the effect of the ALA dose and energy dose on the success of the fractionation regime (one interval (150 seconds) placed after either one fifth or one half of the energy dose had been delivered). Groups with these parameters were repeated using 200 mg/kg ALA i.v. but using an energy dose of 100 J delivered by the 628 nm diode laser (instead of 25 J with copper vapour pumped dye laser tuned to 635 nm). In 50 mg/kg ALA i.v. experiments, an energy dose of 50 or 100 J was delivered 75 minutes after ALA administration using the copper vapour pumped dye laser (635 nm). 25 mg/kg ALA i.v. experiments used an energy dose of 100 or 200 J delivered by the 628 nm diode laser, 60 minutes after ALA administration.

The number of animals in each treatment group varied slightly and is, therefore, marked on each figure. Statistical analysis between the means of the different treatment groups in the initial experiments was conducted using a one-way analysis of variance (ANOVA). Unpaired student t-tests were used to statistically analyse the results of subsequent experiments. Error bars on all the figures were determined by the standard error of the mean.

2.2.2.3 Results

Position of a single fractionation interval

All animals in the initial study were sensitised with ALA and received a total of 25 J of light (635 nm) with a single break of 150 seconds during illumination. The position of this break was varied so the initial energy dose varied from 2.5 to 22.5 J. The control groups were those given 25 J in a single fraction, either with or without ALA. The area of necrosis was plotted as a function of the initial energy fraction and is shown in Figure 27. All fractionated groups produced areas of necrosis equal to or larger than that seen with continuous illumination. The largest effect was seen with an initial fraction of 5 J when the area of necrosis was more than three times that of the group with continuous illumination (continuous = 20 mm², fractionated = 76 mm²) (p < 0.002).

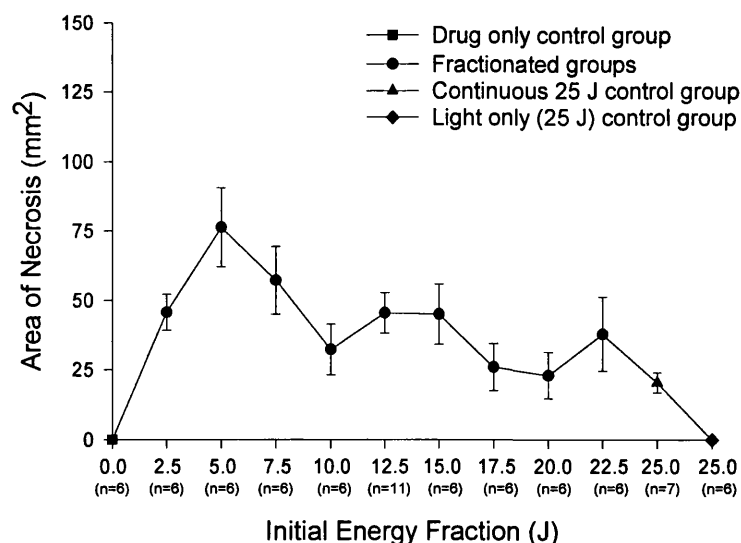


Figure 27 Mean area of necrosis (mm^2) as a function of initial energy fraction (J). 200 mg/kg ALA i.v. was administered 2 hours prior to 25 J of 635 nm light (100 mW) using a copper vapour pumped dye laser. Fractionated groups were interrupted as shown by one interval of 150 seconds. Error bars as determined by the standard error of the mean.

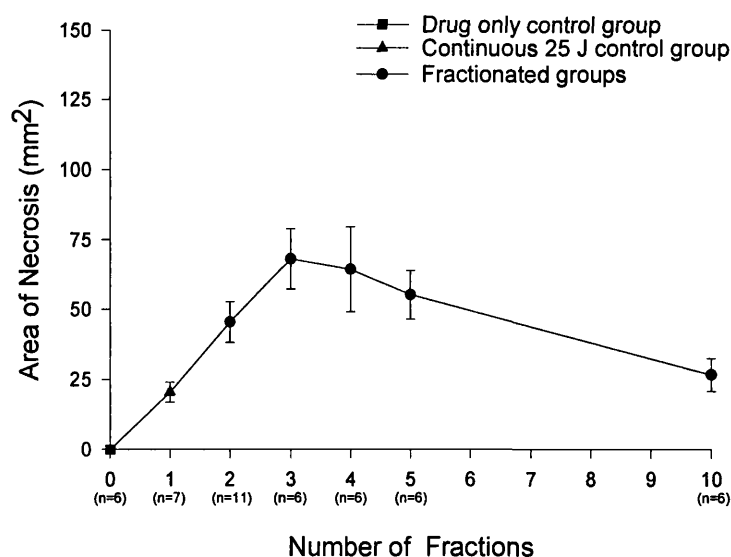


Figure 28 Mean area of necrosis (mm^2) as a function of number of energy fractions. 200 mg/kg ALA i.v. was administered 2 hours prior to 25 J of 635 nm light (100 mW) using a copper vapour pumped dye laser. Fractionated groups were interrupted by the number of intervals shown (150 seconds duration each). Error bars as determined by the standard error of the mean.

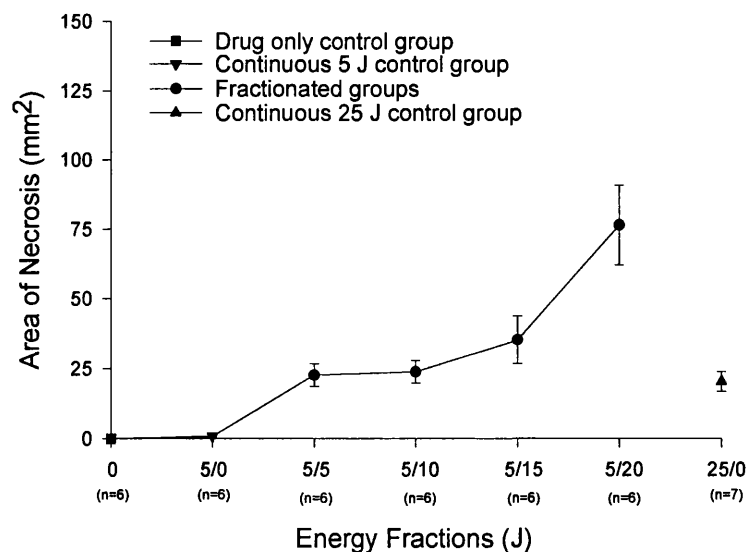


Figure 29 Mean area of necrosis (mm^2) as a function of energy fractions (J). 200 mg/kg ALA i.v. was administered 2 hours prior to 25 J of 635 nm light (100 mW) using a copper vapour pumped dye laser. Fractionated groups were interrupted as shown by one interval of 150 seconds. Error bars as determined by the standard error of the mean.

Number of fractions

Once again, all animals were sensitised with 200 mg/kg ALA i.v. and received a total of 25 J of light (635 nm). The energy dose was divided into 1 - 10 equal fractions with intervals of 150 seconds between each fraction. The area of necrosis is shown as a function of the number of fractions in Figure 28 and was significantly greater than that seen with continuous illumination (20 mm^2) for 2 fractions (45 mm^2) ($p < 0.020$), 3 fractions (68 mm^2) ($p < 0.001$), 4 fractions (64 mm^2) ($p < 0.010$) and 5 fractions (55 mm^2) ($p < 0.002$). Three and 4 fractions produced more necrosis than 2 equal fractions of 12.5 J, but these were no better than the best regime shown in Figure 27 (one break after an initial fraction of 5 J = 76 mm^2).

Second energy fraction

When the most effective initial energy fraction in this model was shown to be 5 J and that multiple fractions did not further enhance the benefit, further experiments were undertaken to study the effect of changing the size of a single second fraction of light. Study animals were sensitised with 200 mg/kg ALA i.v., given an initial energy dose of 5 J and a second energy dose of 5 - 20 J after a dark interval of 150 seconds. The area of necrosis produced is plotted against the energy fractions used in Figure 29. The area of necrosis is less with the smaller second energy fractions, but that produced by the 5/5 J regime (23 mm²) is the same as that using 25 J without fractionation (20 mm²). So the same area of necrosis has been produced with a 60% reduction in the total energy delivered ($p < 0.685$).

Altering ALA and energy doses

Figures 30, 31 and 32 show the effect of altering the ALA and energy doses on the outcome of continuous illumination and fractionation regimes where the illumination had been interrupted with a single 150 second interval either after one fifth (F20/80) or one half (F50/50) of the energy dose had been delivered. All results are shown as area of necrosis (mm²) against total energy delivered (J).

The results using 200 mg/kg ALA i.v. can be seen in Figure 30. Although the results using the different lasers/wavelengths cannot be directly compared, the results follow the same pattern with each energy dose. The fractionated groups produced more necrosis than the groups receiving continuous illumination and the group fractionated after one fifth of the light dose had been delivered (F20/80) was most successful in

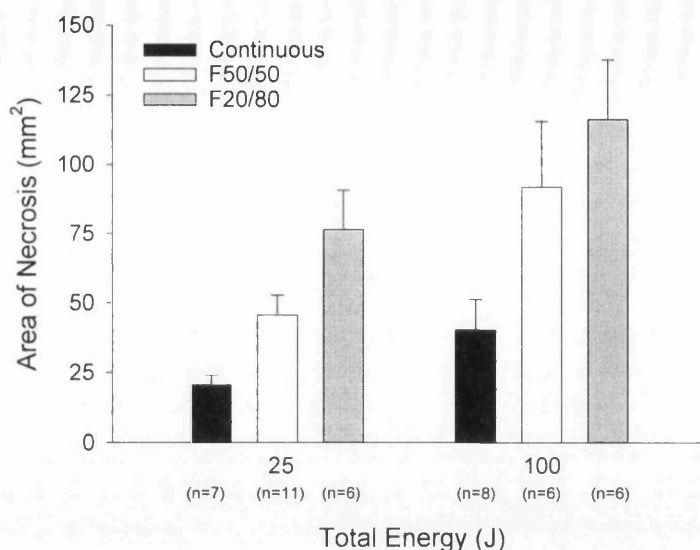


Figure 30 Mean area of necrosis (mm^2) as a function of total energy (J). 200 mg/kg ALA i.v. was administered 2 hours prior to 25 J of 635 nm light (100 mW) using a copper vapour pumped dye laser or 100 J of 628 nm light (100 mW) using a diode laser. Fractionated groups were interrupted as shown by one interval of 150 seconds. Error bars as determined by the standard error of the mean.

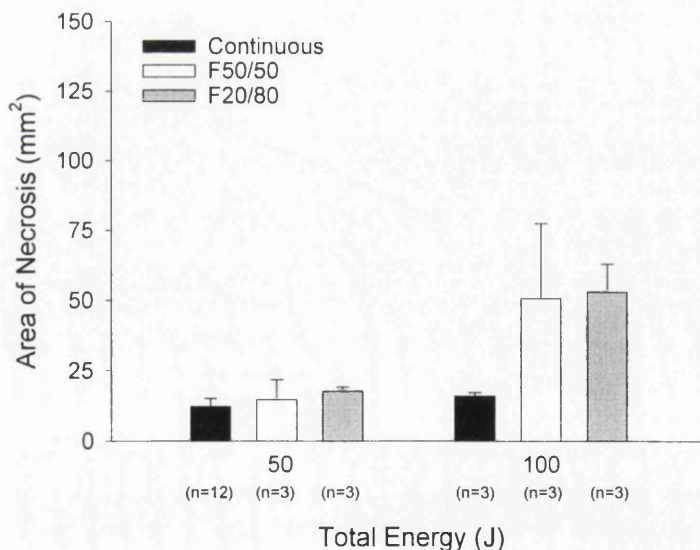


Figure 31 Mean area of necrosis (mm^2) as a function of total energy (J). 50 mg/kg ALA i.v. was administered 75 minutes prior to 50 or 100 J of 635 nm light (100 mW) using a copper vapour pumped dye laser. Fractionated groups were interrupted as shown by one interval of 150 seconds. Error bars as determined by the standard error of the mean.

both cases, producing three times the area of necrosis of their respective continuous groups (25 J continuous = 20 mm² or fractionated = 76 mm² ($p < 0.002$); 100 J continuous = 40 mm² or fractionated = 116 mm² ($p < 0.006$)).

Figure 31 shows the results obtained with 50 mg/kg ALA i.v and 50 or 100 J of 635 nm light. Very little difference was seen between the continuous groups at both of the energy doses (50 J = 12 mm², 100 J = 16 mm²). With fractionation, however, considerably more necrosis was produced with 100 J than with 50 J, although, the difference between the two fractionated regimes at each energy dose was not as great as that seen with 200 mg/kg ALA i.v. At this drug dose, using an energy dose of 100 J, it was also possible to produce with a fractionated regime (F20/80) three times the

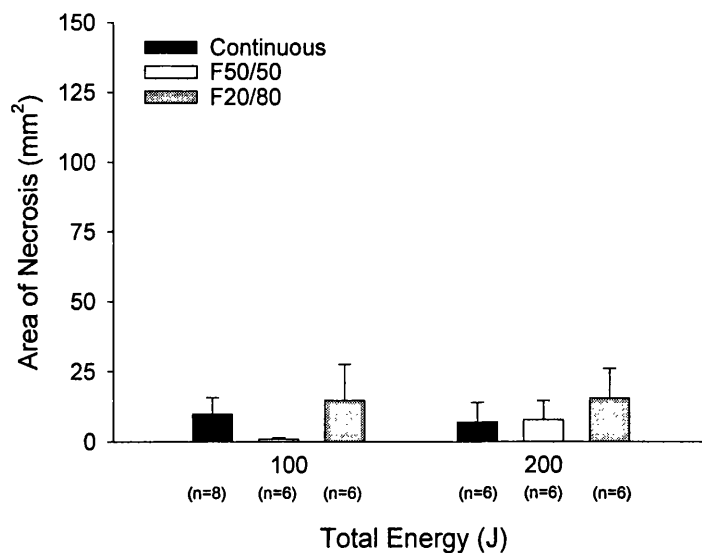


Figure 32 Mean area of necrosis (mm²) as a function of total energy (J). 25 mg/kg ALA i.v. was administered 60 minutes prior to 100 or 200 J of 628 nm light (100 mW) using a diode laser. Fractionated groups were interrupted as shown by one interval of 150 seconds. Error bars as determined by the standard error of the mean.

area of necrosis produced by the same parameters with continuous illumination (continuous = 16 mm², fractionated 20/80 = 53 mm²) ($p < 0.021$). This is the same degree of potentiation found between the continuous and fractionated (20/80) groups when using 200 mg/kg ALA i.v. and 25 or 100 J.

The results using 25 mg/kg ALA i.v. are shown in Figure 32. The area of necrosis produced throughout is small. Increasing the light dose from 100 to 200 J has little effect on the outcome of the treatment. Although there does appear to be a slight improvement when using the 20/80 fractionation regime, rather than the continuous illumination (at both energy doses), this difference is not statistically significant (100 J $p < 0.719$, 200 J $p < 0.520$).

2.2.2.4 Discussion

The results of this section indicate that light dose fractionation can significantly improve the effect of ALA induced PDT, if an appropriate regime is used. Selection of such a regime, at the present time however, is difficult, with many experiments being required to investigate each variable individually.

The experiments with 200 mg/kg ALA i.v. and 25 J, support the finding of Messmann *et al*'s previous work (1995) that showed that light dose fractionation can make substantial differences to the outcome of ALA PDT in this model. Furthermore, that a single 150 second interval is equivalent to multiple intervals of the same length and

that this single interval is more effective when placed earlier rather than later in the illumination.

The timing of the fractionation interval appears to be critical. It was not enough to create a dark period of a particular length; it also had to be placed at a specific point in time. When exactly this should be is likely to vary from tissue to tissue but in this model (with 200 mg/kg ALA i.v.) it is after 5 J of the light dose being delivered. The most important factors are likely to be the size of the initial energy fraction and the degree of vasoconstriction this causes. It is unlikely that repeated short light exposures will be beneficial (such as those received in the 10 fraction group) as a first fraction of less than 50 seconds does not appear to be effective.

The 'best regime' will probably be a compromise; an initial fraction long enough to cause some PDT effect but short enough not to cause permanent constriction/collapse of the microvasculature. This would be followed by an interval long enough to allow oxygen to diffuse throughout the treatment area, to restore the biochemical equilibrium (at least partially). An appropriate number of subsequent fractions could then be applied until all the PPIX available within the area had been consumed and the microvasculature had been permanently damaged, so neither more intervals nor more light fractions would be of any benefit. The current results indicate, however, that one appropriately placed fractionation interval appears to be just as effective as several.

These ideas raise the possibility of developing techniques to monitor PDT in real time. If the oxygen tension and the PPIX fluorescence (to measure photobleaching) could be measured in the area being treated during PDT and could be correlated with the

biological effect, not only could the light be fractionated at the most appropriate time (in any tissue or tumour) but the result could be predicted. Another option for monitoring PDT would be to measure the light fluence. The animal model used in this study is very simple, using effectively a point source of light applied to the surface of a thin organ. Correlating the total light fluence at the junction of viable and non viable colon (which depends on the diameter of the zone of necrosis) with the fractionation regime used is complicated, but as the mechanisms involved become better understood, direct fiberoptic measurement of the fluence at strategic points in the target tissue as described previously (Barr *et al*, 1987) might provide valuable information for estimating how far the zone of PDT necrosis will extend.

It is also possible to use light dose fractionation to produce the same effect as continuous irradiation but with a reduced energy dose. With 200 mg/kg ALA i.v. it was found that a fractionated regime of only 10 J (F5/5) could produce the same effect as a continuous 25 J treatment. The 150 second interruption to the energy dose, therefore, reduced the irradiation required by 60%.

Throughout the experiments with the different ALA and energy doses, the fractionation regime where the irradiation period was interrupted (by an interval of 150 seconds) after one fifth of the light dose had been delivered (F20/80) was found to produce more necrosis than the equivalent continuous or alternative fractionation (F50/50) regimes. The fractionation regimes were more effective at increasing the area of necrosis in the normal rat colon at the higher doses of ALA (200 and 50 mg/kg i.v.). There was no significant difference between the continuous and fractionated regimes at 25 mg/kg ALA i.v.

It is difficult to be sure which of the many possible mechanisms of action is most relevant to the results described in this section. It has been shown in this model, however, that a single interruption to light delivery at an appropriate point can dramatically increase the area of necrosis produced (up to a factor of three). Alternatively, the same area of necrosis can be produced with a 60% lower light dose and hence a shorter treatment time. Both of these findings could have significant benefits clinically but it will be necessary to study light dose fractionation further before its mechanism will be fully understood and it can be used to its greatest effect to enhance clinical PDT.

2.2.3 Light Dose Fractionation in a Colonic Tumour Model

2.2.3.1 Introduction

The results of the previous section have demonstrated that light dose fractionation can increase the area of necrosis produced by ALA PDT by up to a factor of three, if an appropriate fractionation regime is applied. All of this work, however, was conducted in a normal rat colon model. This section will, therefore, investigate the effect of applying one of the successful fractionation regimes (from the previous section) on the MC28 colonic rat tumour model.

2.2.3.2 Materials and Methods

Chemicals

ALA powder was dissolved in physiological strength PBS (pH 2.8) and administered intravenously (with a concentration of 200 mg/ml and a maximum volume of 0.2 ml).

Animal model

Female, Hooded Lister rats (120 - 200 g) were used throughout. The animals were anaesthetised for all parts of the procedure using inhaled halothane and analgesia was administered subcutaneously following surgery (Buprenorphine hydrochloride).

Tumour model generation

Tumours were produced by injection of $2-3 \times 10^6$ MC28 cells (total volume of 0.1 ml) into the site of an anastomosis in the colon as previously described in section 2.1.5.2.

Fluorescence studies

Using the same basic method as the fluorescence studies in section 2.1.2.2, 200 mg/kg ALA i.v. was administered under general anaesthetic, 10 days after tumour cell injection. The animals were then recovered and killed 2 hours later, so that frozen colonic tumour sections could be analysed by fluorescence microscopy (as described previously).

PDT studies

In separate animals, 10 days after tumour cell injection, PDT experiments were conducted using the same basic method as described in section 2.0.0.2. All animals received 200 mg/kg ALA i.v. under general anaesthetic, 2 hours prior to surgery. A total energy of 25 J was delivered to the colonic tumour model via a 200 μm plane cleaved optical fibre (output power, 100 mW) positioned so that it just touched the outside of the tumour, using the 628 nm diode laser as the light source. The rest of the abdominal viscera were shielded from forward light scatter by a piece of opaque paper positioned so that it did not touch the colon or affect its light distribution. The period of illumination was either continuous or fractionated with a single 150 second interval after one fifth of the total energy dose had been delivered (F20/80).

All animals were recovered following surgery and killed three days later. The diameters of the width (a), length (b) and depth (c) of necrosis produced in the tumour

were measured using a micrometer and recorded. In all cases the zone of necrosis fell within the limits of the tumour. These measurements were then used to calculate the volume of necrosis produced by each treatment regime (in mm^3) using the formula of an ellipsoid, $\pi abc/6$. Tumour specimens were fixed in formalin, sectioned and stained with haematoxylin and eosin, so that conventional light microscopy could confirm the macroscopic findings.

There were three animals in each of the treatment groups in the fluorescence studies, and four in each of the PDT groups. Statistical analysis between the means of the different treatment groups was conducted using unpaired student t-tests. Error bars on all the figures were determined by the standard error of the mean.

2.2.3.3 Results

Fluorescence studies

The results of the normal and tumour fluorescence studies, using these parameters, can be seen in Figure 33. The fluorescence in the untreated colonic tumour (autofluorescence) is higher than that of the normal mucosa and muscle (mucosa = 10 a.u., muscle = 6 a.u. and tumour = 34 a.u.). These fluorescence results have only been corrected externally (to remove the inherent background of the experimental set-up) rather than with the background fluorescence of the tissue, so that we can see the autofluorescence of each of the tissues. The administration of ALA, increases the fluorescence in all three tissues. The fluorescence in the normal mucosa increases more than that in the colonic tumour model, however, resulting in a similar degree of

PPIX fluorescence being produced in the normal mucosa and colonic tumour model (mucosa = 86 a.u. and tumour = 90 a.u.) ($p < 0.846$).

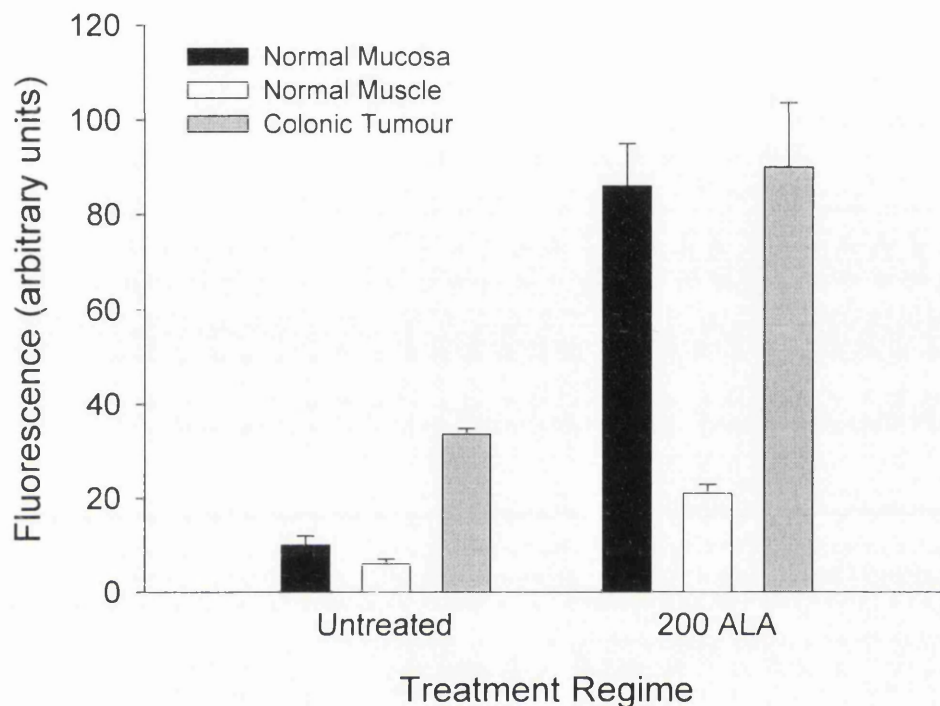


Figure 33 Fluorescence (arbitrary units) of the normal colonic mucosa, normal colonic muscle and colonic tumour model of either blank control tissue or tissue 2 hours after administration of 200 mg/kg ALA i.v. Each bar represents the mean values from three separate animals. Error bars as determined by the standard error of the mean.

PDT studies

The results of the PDT studies can be seen in Figure 34. It shows the volume of necrosis (in mm^3) produced in the colonic tumour model when the irradiation was continuous or fractionated (F20/80). The figure shows, that double the volume of

necrosis was produced when the treatment was fractionated (continuous = 40 mm³, fractionated = 85 mm³) ($p < 0.063$).

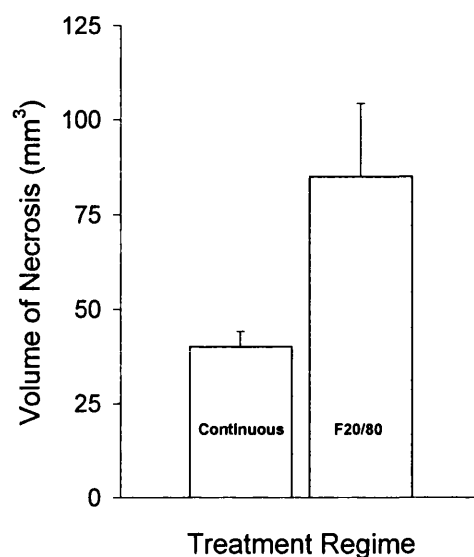


Figure 34 Mean volume of necrosis (mm³) as a function of the PDT treatment regime. 200 mg/kg ALA i.v. was administered 2 hours prior to 25 J of 628 nm light (100 mW) using a diode laser. Each group represents the mean (with the standard error of the mean) from four separate animals.

2.2.3.4 Discussion

The fluorescence studies show that the amount of PPIX fluorescence produced in the MC28 colonic tumour model, following ALA administration, was very similar to that observed in the normal colonic mucosa. This indicated that comparable results should be obtained when using this technique in this tumour model as with the normal mucosa already studied in the previous section, although, in the tumour model, a greater proportion of the fluorescence produced was as a result of autofluorescence. It

can also be concluded from this experiment, that the differences observed in the PDT study were not the result of greater PPIX accumulation in the tumour model (than in normal colonic mucosa), as the PPIX level in each of these tissues (as determined by the fluorescence study) was similar.

The PDT studies investigated whether light dose fractionation could be utilised to produce an enhanced PDT effect in the tumour model and this was found to be the case. The fractionated light regime employed was found to be the best (using these drug and light doses) in the previous normal tissue studies. When the period of irradiation was interrupted for 150 seconds, after only one fifth of the total energy dose had been delivered (F20/80), the volume of necrosis produced by the treatment was double that produced using the same parameters and continuous illumination. This is a substantial improvement in outcome.

These results support the findings of other groups (Hua *et al*, 1995; van der Veen *et al*, 1994) that this technique may be used to enhance the effect of ALA PDT in tumours. Much further work will be needed, however, to determine the appropriate regime(s) required to improve clinical ALA PDT. This will probably involve the development of real time monitoring techniques to ‘tailor-make’ the light fractionation regime for each individual patient/tumour.

2.2.4 Combining the Technique of Light Dose Fractionation with the Administration of an Iron Chelating Agent

2.2.4.1 Introduction

After conducting experiments on the effect of light dose fractionation and the administration of an iron chelating agent on the outcome of ALA PDT separately, it was decided to combine both of the techniques, to see if together, even greater enhancement could be produced.

2.2.4.2 Materials and Methods

Chemicals

ALA powder was dissolved in physiological strength PBS (pH 2.8) and administered intravenously (with a concentration of 200 mg/ml and a maximum volume of 0.2 ml). The iron chelator, CP94, was also prepared in PBS and administered intravenously (with a concentration of 100 mg/ml and a maximum volume of 0.2 ml).

Animal model

Normal, female, Wistar rats (120 - 200 g) were used throughout. The animals were anaesthetised for all parts of the procedure using inhaled halothane and analgesia was administered subcutaneously following surgery (Buprenorphine hydrochloride).

PDT studies

All animals were given 200 mg/kg ALA intravenously, 2 hours prior to surgery either with or without the simultaneous administration of 100 mg/kg CP94 i.v. The colon was accessed for PDT via a laparotomy as described in section 2.0.0.2. The animals either then received continuous or fractionated irradiation using the pulsed (12 kHz) copper vapour pumped dye laser (tuned to 635 nm) to deliver a total energy of 25 J (output power, 100 mW) to all groups (except the F10/90 + ALA + CP94 group which received a total energy dose of 25 J from the 628 nm diode laser). Two fractionation regimes were investigated alongside the continuous irradiation group, both were interrupted by a single 150 second interval either after one tenth (F10/90) or one fifth (F20/80) of the total energy dose had been delivered.

In a subsequent experiment, the same groups were conducted again, but this time with a total energy dose of 100 J being delivered using the diode laser (628 nm).

The area of necrosis produced in the colon at three days was determined by measuring the minimum (a) and maximum (b) perpendicular diameters of the lesion macroscopically with a micrometer. These values were then used to calculate the area of necrosis using the formula $\pi ab/4$, as the lesions produced were approximately elliptical.

The number of animals in each treatment group varied slightly and is, therefore, marked on each figure. Statistical analysis between the means of the different treatment groups was conducted using unpaired student t-tests. Error bars on all the figures were determined by the standard error of the mean.

2.2.4.3 Results

The results of the experiments using an energy dose of 25 J can be seen in Figure 35. This figure shows the area of necrosis (mm^2) produced by each of the three irradiation regimes (continuous, fractionated 10/90 and fractionated 20/80) when ALA was administered either with or without the iron chelating agent, CP94.

With continuous irradiation, the addition of the iron chelator (using these parameters) produces almost three times (ratio = 2.85) the area of necrosis of ALA alone (ALA only = 20 mm^2 , ALA + CP94 = 57 mm^2) ($p < 0.065$). The most successful light dose fractionation regime (F20/80), with ALA alone, produced at least three times (ratio = 3.8) the area of necrosis of continuous irradiation (continuous = 20 mm^2 , fractionated = 76 mm^2) ($p < 0.002$). So, each method of enhancement independently produces (in this situation) approximately three times the area of necrosis of standard, unenhanced ALA PDT. The combination of the two methods, however, failed to improve on this degree of enhancement, when using this energy dose.

Using the higher energy dose of 100 J and the 628 nm diode laser, however, it was possible to improve on the effect of each technique individually, by using them together as a combination. The results of these experiments can be seen in Figure 36.

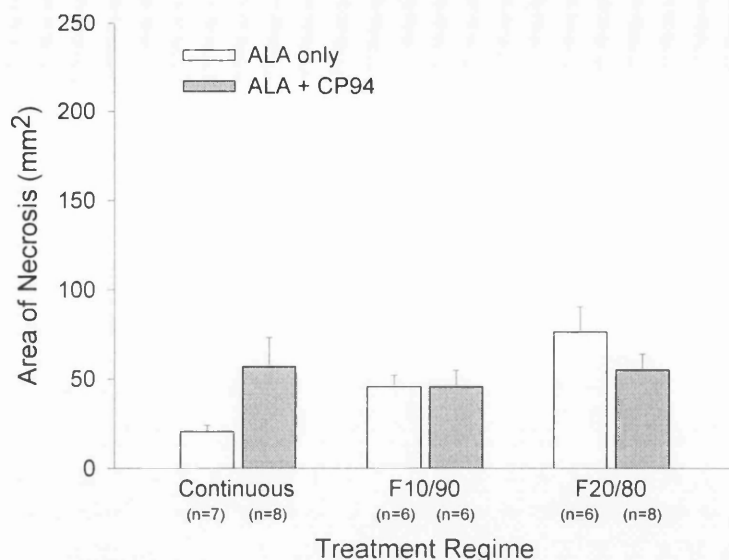


Figure 35 Mean area of necrosis (mm^2) as a function of the treatment regime. 200 mg/kg ALA i.v. was administered 2 hours prior to 25 J of 635 nm light (100 mW) using a copper vapour laser (except ALA + CP94 + F10/90 group which received 25 J 628 nm light (100 mW) using a diode laser). Fractionated groups were interrupted as shown by one interval of 150 seconds. Error bars as determined by the standard error of the mean.

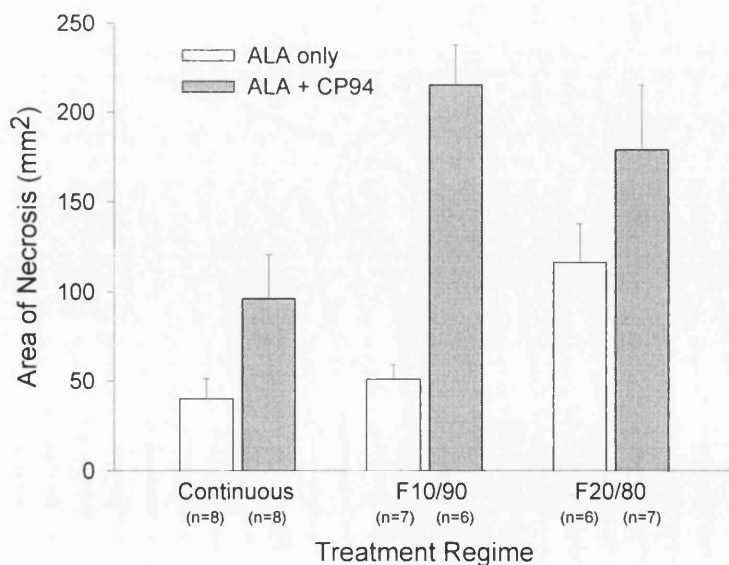


Figure 36 Mean area of necrosis (mm^2) as a function of the treatment regime. 200 mg/kg ALA i.v. was administered 2 hours prior to 100 J of 628 nm light (100 mW) using a diode laser. Fractionated groups were interrupted as shown by one interval of 150 seconds. Error bars as determined by the standard error of the mean.

With continuous irradiation, the addition of the iron chelator produced double (ratio = 2.4) the area of necrosis of ALA alone (ALA only = 40 mm², ALA + CP94 = 96 mm²) ($p < 0.055$). The 20/80 fractionation regime (with ALA alone), however, produced almost three times (ratio = 2.9) the area of necrosis of continuous irradiation (continuous = 40 mm², fractionated = 116 mm²) ($p < 0.006$). So, each method of enhancement independently produced, using this higher energy dose, between two and three times the area of necrosis of a standard ALA PDT treatment without any enhancement.

When CP94 was administered, as well as fractionating the light dose after one fifth of the total energy had been delivered, an additional enhanced effect was produced over and above that of each technique separately (ALA + CP94, continuous = 96 mm²; ALA only, fractionated 20/80 = 116 mm²; ALA + CP94, fractionated 20/80 = 179 mm²). This enhancement was even greater if the fractionation interval was placed even earlier in the irradiation period (F10/90) (ALA + CP94, continuous = 96 mm²; ALA only, fractionated 10/90 = 51 mm²; ALA + CP94, fractionated 10/90 = 215 mm²). This resulted in the area of necrosis of the standard continuous ALA only PDT treatment being increased by a factor of five (ratio = 5.4) when the combination of ALA + CP94 and the 10/90 fractionation regime was applied (ALA only, continuous = 40 mm²; ALA + CP94, fractionated 10/90 = 215 mm²) ($p < 0.000007$) which is a substantial, statistically significant degree of enhancement.

2.2.4.4 Discussion

Each method of enhancement (the addition of the iron chelator, CP94, or light dose fractionation (20/80)) enabled approximately a three fold degree of enhancement of effect over the standard, continuous ALA only PDT treatment, when used independently with a total energy dose of 25 J. Combining the two techniques did not improve the outcome of the treatment at this energy dose. When using a higher energy dose of 100 J, however, although the individual techniques separately could only produce about two to three times the area of necrosis to that of the standard, ALA only continuously irradiated group, when combined together, this enhancement was increased to a factor of five.

This indicates that in the earlier 25 J studies, the size of the energy dose had been limiting the extent of the effect and that 100 J of energy was needed to take full advantage of the potential of the two combined methods of enhancement. As no other energy doses were investigated in this study, future experiments should include an energy dose escalation study to determine the threshold for this effect and if further potentiation can be achieved by applying even more light to the treatment site.

By combining these two very different techniques of enhancement, we are in effect, firstly, increasing the amount of PPIX in the treatment site, through the use of the iron chelating agent, CP94, and secondly, refining the irradiation delivery, through light dose fractionation, to allow the maximal PDT effect possible, to occur. With the increased PPIX level in the treatment site, it wasn't very surprising, that an earlier

fractionation interval would be more beneficial. The increased PPIX level would result in a greater photochemical effect when the irradiation began and thus more rapid oxygen depletion. An even earlier dark interval would, therefore, be required to replenish the oxygen supplies and preserve the microvasculature, improving the overall outcome of the treatment (if this really is the major mechanism of action of light dose fractionation).

This section has, therefore, determined that ALA PDT can be further enhanced by combining the administration of the iron chelator, CP94, with light dose fractionation on irradiation, by a factor even greater than that either of the techniques can achieve independently.

2.2.5 Monitoring Oxygen During Light Dose Fractionation

2.2.5.1 Introduction

Although, the previous sections have demonstrated that light dose fractionation can significantly enhance the effect of ALA PDT both in normal and malignant rat colon, little is known about the mechanism of action of this technique. The next few sections will investigate the three major proposed mechanisms in normal rat colon; i) reoxygenation of the treatment site during the dark period, ii) relocation of the photosensitiser during the dark period and iii) reperfusion injury. This section will determine the effect of both continuous and fractionated ALA PDT on the level of oxygen at the treatment site.

It has been well established that PDT can produce vascular damage (in varying degrees with different photosensitisers) and this results in localised hypoxia (which limits the photodynamic effect) (Leveckis *et al*, 1995 and Roberts *et al*, 1994). Few studies, however, have monitored the tissue level of oxygen at the treatment site in detail throughout PDT treatment, with more emphasis being placed on establishing above threshold light and drug doses. Reed *et al* (1989) used Clark-style and Whalen type oxygen microelectrodes to measure tumour partial pressures before and after PDT with Photofrin II on a rat subcutaneous tumour model. They found that mean tumour pO_2 was significantly reduced one hour after treatment and this reduction persisted at 24 hours. Tromberg *et al* (1990) also found that significant tissue hypoxia can be

produced using Photofrin II PDT on a transplanted rabbit skin carcinoma (using a transcutaneous (non-invasive) Clark-style oxygen electrode to measure pO_2). More recently, Chen *et al* (1996) and Sitnik *et al* (1998) both used pO_2 microelectrode systems to monitor pO_2 in mice tumour models during Photofrin PDT. Chen *et al* found that the pre-PDT oxygenation level of the tumour had a profound effect on its post-PDT oxygenation and that a transient period of reoxygenation occurred following PDT. Sitnik *et al* also showed that a significant and rapid decrease in oxygen occurs shortly after the light dose commences (within one minute). It has, therefore, been shown that PDT using Photofrin and continuous illumination can induce a significant reduction in tumour pO_2 which may have a profound effect on the outcome of the treatment.

The degree of oxygenation in the treatment site and how it is affected by PDT is particularly crucial when investigating the mechanism of light dose fractionation. It has already been shown in normal rat liver (using a non-invasive optical spectroscopic method of monitoring oxygen) that a significant and rapid decrease in oxygen can be induced by ALA PDT (McIlroy *et al*, 1998). The use of this technique to investigate fractionated PDT regimes is limited, however, as it is not possible to sample continuously throughout the treatment, as no measurements can be taken whilst the laser is in operation. In this section an Eppendorf microelectrode (a polarographic measure of pO_2) is used to monitor the oxygen levels in the treatment area continuously before, during and after PDT, both with continuous and fractionated light dose regimes.

2.2.5.2 Materials and Methods

Chemicals

ALA powder was dissolved in physiological strength PBS (pH 2.8) and administered intravenously (with a concentration of 200 mg/ml and a maximum volume of 0.2 ml).

Animal model

Female, Wistar rats (120 - 200 g, University of Leeds, Leeds, UK) were used for all experiments. The animals were sedated for the ALA injections using inhaled halothane. Intraperitoneal injection of Hypnorm (Fentanyl and Fluanisone, Janssen Pharmaceutical Ltd, Oxford, UK) and Diazepam (Phoenix Pharmaceuticals Ltd, Gloucester, UK) was used as anaesthesia for the rest of the procedure, as halothane is known to affect the sensitivity of the Eppendorf system. Analgesia was administered subcutaneously following surgery (Buprenorphine hydrochloride).

PDT studies

ALA was administered at a dose of 200 mg/kg i.v. and with a drug/light interval of 2 hours. PDT of the colon was conducted via laparotomy as described in section 2.0.0.2. The light source was a pulsed (12 kHz) copper vapour pumped dye laser tuned to 635 nm. A total energy of 25 J (100 mW) was delivered to each animal. Continuous illumination was compared with the fractionation regime from the previous sections where the light dose was interrupted after only one fifth of the total energy had been delivered (F20/80) by a single interval of 150 seconds. This fractionation regime produces more than three times the area of necrosis than that

produced with continuous illumination (continuous = 20 mm², fractionated = 76 mm²) ($p < 0.002$). All animals were recovered following surgery and killed three days later, so that the lesion could be measured macroscopically with a micrometer. The minimum (a) and maximum (b) perpendicular diameters of the lesion were recorded and the area (which was approximately elliptical) calculated using the formula $\pi ab/4$. Representative specimens were fixed in formalin, sectioned and stained with haematoxylin and eosin, so that conventional light microscopy could confirm the macroscopic findings. Laser only, drug only and complete blank (surgery only) control groups of animals were also included. There was a minimum of three animals in each group.

Measurement of pO_2

Colonic pO_2 was measured every 5 seconds, before, during and after PDT using the polarographic Eppendorf pO_2 histogram system (Eppendorf-Netheler-Hinz GmbH, Hamburg, Germany). Before and after each treatment the instrument was calibrated in 0.9% saline bubbled alternatively with air and nitrogen. The temperature of the colon during this procedure was assumed to be 31°C (as previously measured by Barr *et al*, 1987) and was used to calibrate the data. The 300 μ m diameter polarographic needle probe was carefully inserted into the colonic wall (from the serosal side of the colon) and withdrawn slightly prior to measurements commencing, using the system's automated mechanism. It was not possible to accurately ascertain in which layer of the colon wall the tip of the probe was located whilst measurements were being conducted. The Eppendorf's automated probe is normally used in solid tissues to make a series of measurements, advancing and then retracting the probe a little each time to minimise the disruption to the local environment by this invasive technique.

However, due to the thinness of the colon wall, this was not possible in this model. The microelectrode was positioned at varying distances along the colon wall (relative to the irradiation fibre) in separate experiments using different animals (one site per animal).

2.2.5.3 Results

Control subjects

The blank control group of animals received neither ALA nor light. Surgery alone was performed and the partial pressure of oxygen in the colon was measured using the Eppendorf microelectrode. No significant increase or decrease of oxygen was observed in any of the animals in this group throughout the duration of the experiment. The tissue oxygen pressure (mmHg) of the normal rat colon of three separate animals is plotted as a function of time (seconds) in Figure 37a. The pO_2 of the untreated colon was relatively stable and no significant consumption of oxygen by the microelectrode was detected in these studies. The drug only control group (also three animals) received ALA and two hours later underwent surgery and oxygen monitoring but without laser irradiation (Figure 37b). Once again, the oxygen level remained stable throughout the experiment. No necrosis was observed at three days, in either the blank control or drug only control groups.

The tissue oxygen pressure of the continuous laser control groups can be seen in Figures 37c & d. These animals received 25 J of light without ALA administration.

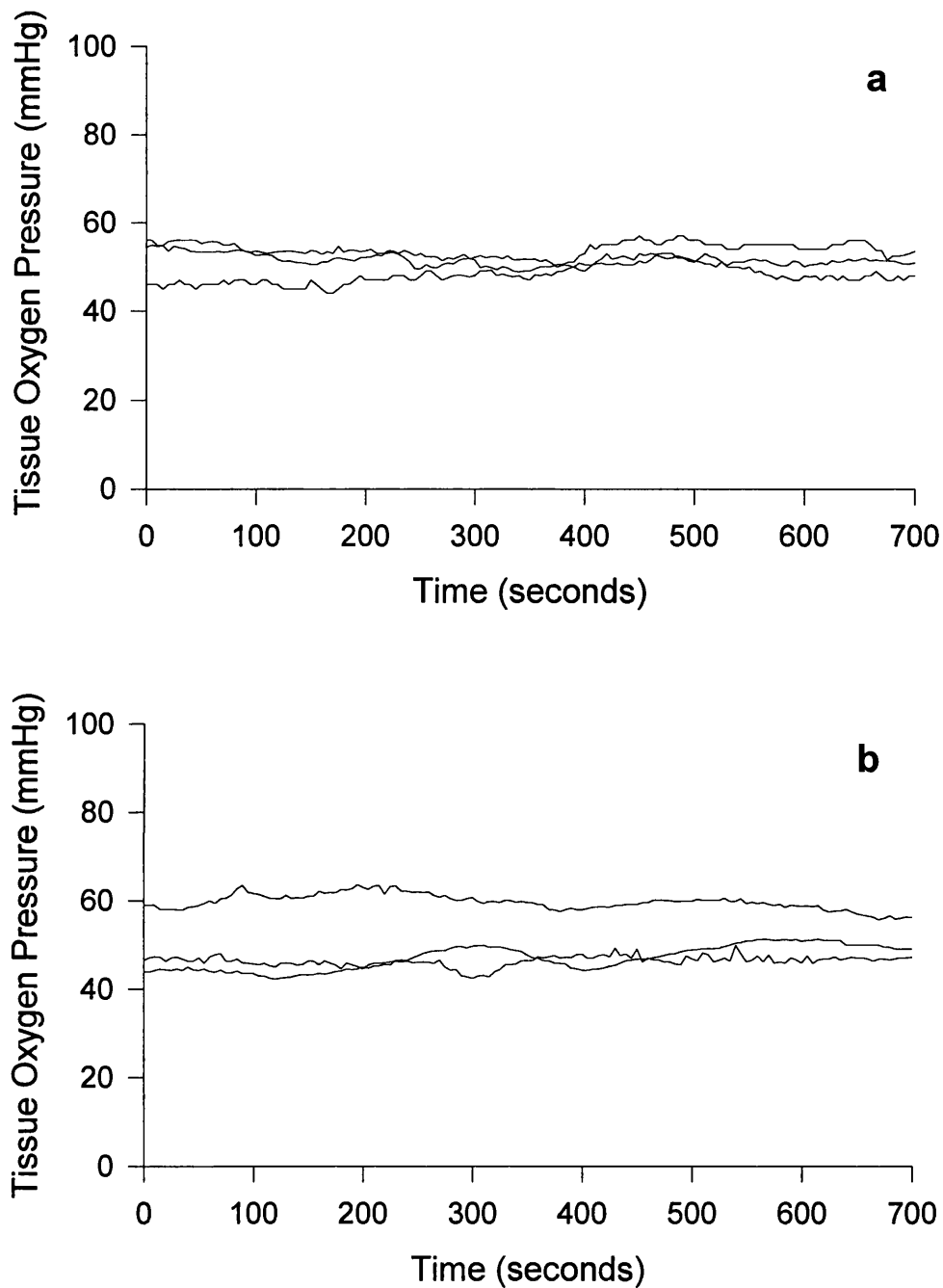


Figure 37 The tissue oxygen pressure (mmHg) of the normal rat colon plotted as a function of time (seconds) for groups of three animals receiving a) neither ALA or light (surgery only blank controls) and b) 200 mg/kg ALA i.v. 2 hours prior to surgery with no light administration (drug only controls).

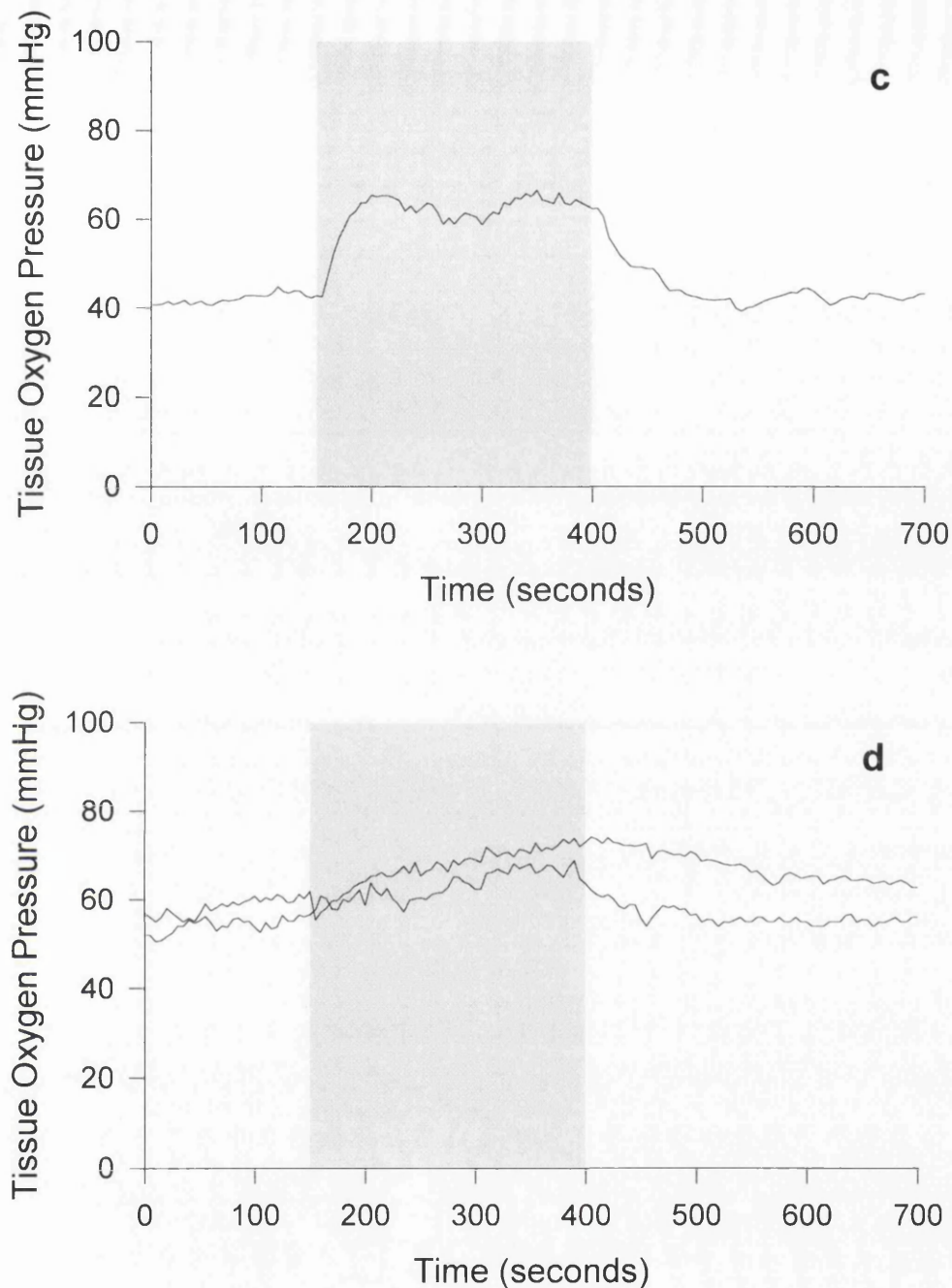


Figure 37 The tissue oxygen pressure (mmHg) of the normal rat colon plotted as a function of time (seconds) for three animals receiving 25 J of continuous light administration (635 nm, 100mW, copper vapour laser) without any ALA (light only controls) and the oxygen measured 1 mm from the irradiation fibre (c) or 3 mm (d). The period of illumination is denoted by the shaded area.

The oxygen level was measured before, during and after light irradiation at 1 mm. (Figure 37c) along the colon wall from the irradiation fibre and at 3 mm (Figure 37d). The period of illumination is denoted by the shaded area. Close to the irradiation fibre (1 mm away) the pO_2 increased sharply as soon as the irradiation started until it reached a plateau. Once the irradiation had finished the pO_2 level returned more slowly to the pre-laser 'baseline' level. Further away from the irradiation fibre (3 mm) the effect was less pronounced with only a slight increase being observed whilst the laser was switched on. Presumably these increases are the result of vasodilatation of the microcirculation and increased blood flow triggered by the heat of the irradiation. However, although the light fluence rate where the fibre touches the colon is high (320 W/cm²) no thermal effect was observed macroscopically in either of the light only control groups at three days.

Continuous illumination

Figures 38a & b show the partial pressure of oxygen (mmHg) as a function of time (seconds) for animals receiving 200 mg/kg ALA i.v. two hours prior to continuous illumination with a total energy dose of 25 J. The partial pressure of oxygen was either measured 1 mm away from the irradiation fibre (Figure 38a) or 3 mm away (Figure 38b). The results from three animals in each group are presented. It can be seen that close to the irradiation fibre (1 mm) the pO_2 of the colon started to drop shortly after the start of the irradiation period, rapidly falling to zero. Further away from the irradiation fibre (3 mm away) no such dramatic effect was observed and profiles more similar to the control groups were observed. The area of necrosis produced by the continuous PDT group in this series of experiments was 27 mm² (average diameter = 6 mm). This is not significantly different from the results of the

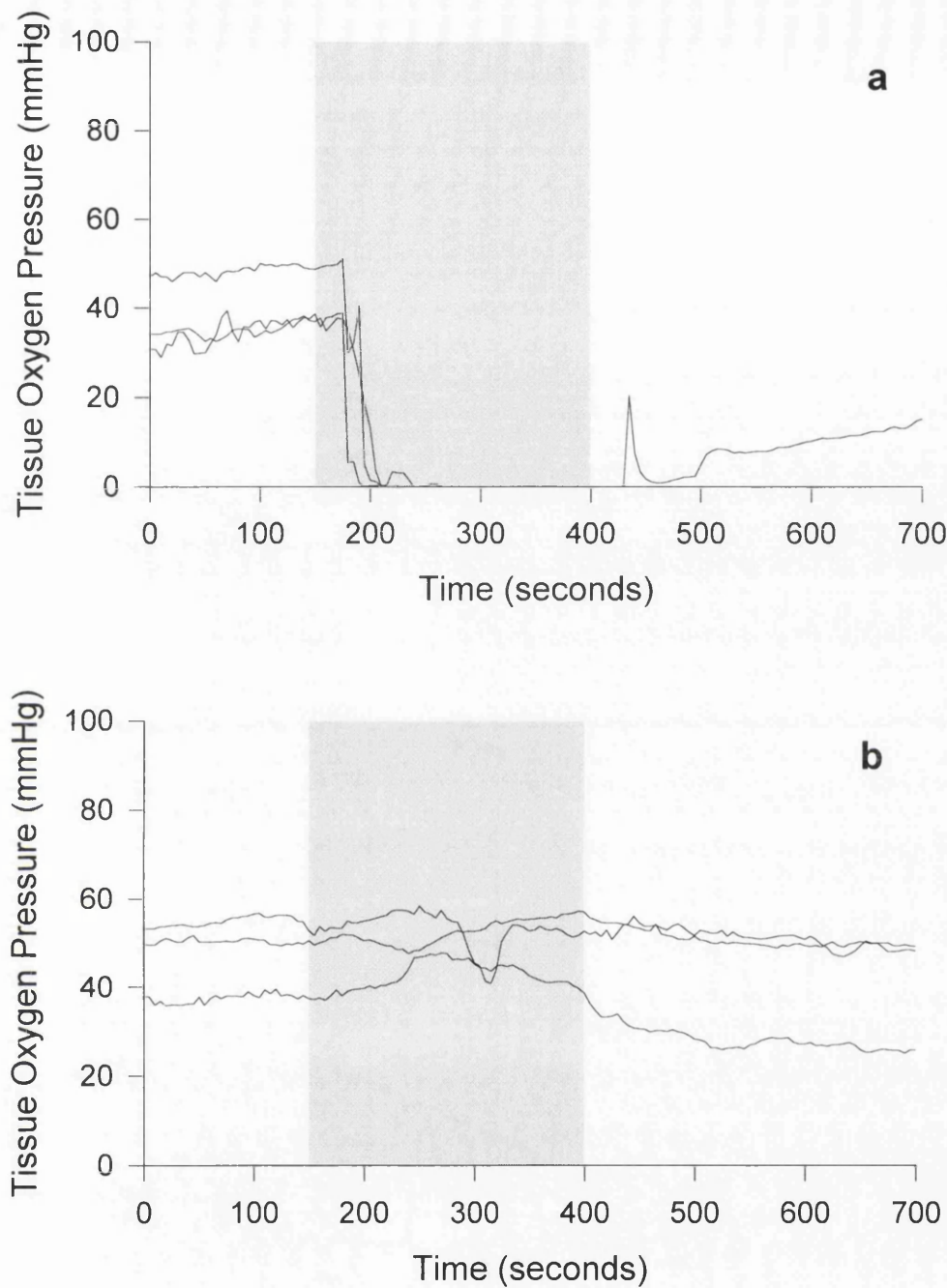


Figure 38 The tissue oxygen pressure (mmHg) of the normal rat colon plotted as a function of time (seconds) for groups of three animals receiving 200 mg/kg ALA i.v. two hours prior to continuous illumination with a total energy dose of 25 J (635 nm, 100 mW, copper vapour laser) with the oxygen measured at 1 mm (a) or 3 mm (b) away from the irradiation fibre. The period of illumination is denoted by the shaded area.

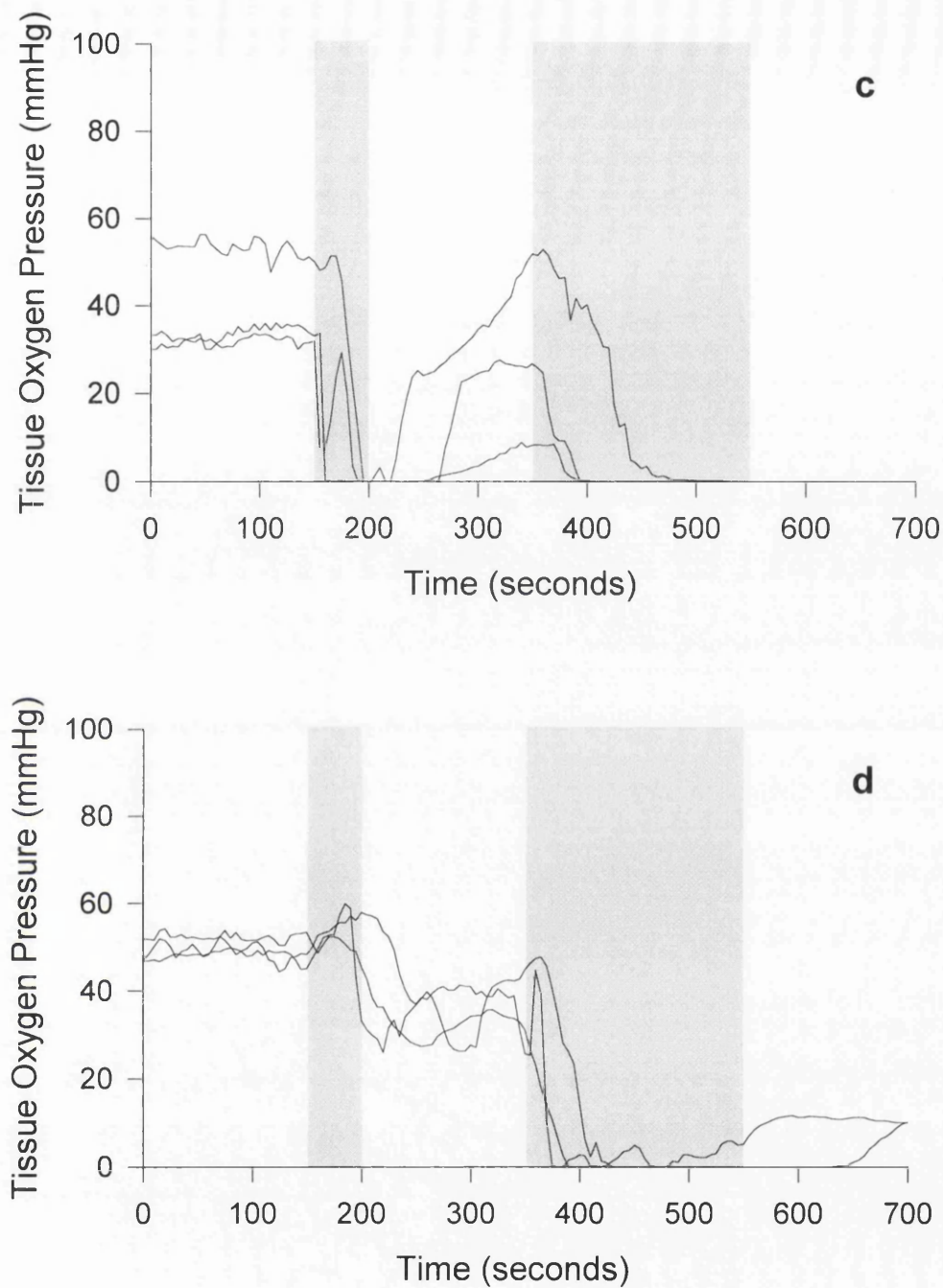


Figure 38 The tissue oxygen pressure (mmHg) of the normal rat colon plotted as a function of time (seconds) for groups of three animals receiving 200 mg/kg ALA i.v. two hours prior to fractionated illumination (50 seconds illumination (5 J), an interval of 150 seconds and then 200 seconds more illumination (20 J)) with a total energy dose of 25 J (635 nm, 100 mW, copper vapour laser) with the oxygen measured at 1 mm (c) or 3 mm (d) away from the irradiation fibre. The periods of illumination are denoted by the shaded areas.

previous sections using the same parameters. The first monitoring point was close to the irradiation fibre (1 mm) and well within this area of necrosis and the second point (3 mm away) was close to the edge of this zone of necrosis.

Fractionated illumination

Figures 38c & d show the partial pressure of oxygen (mmHg) as a function of time (seconds) for animals receiving 200 mg/kg ALA i.v. two hours prior to fractionated irradiation. These animals received the same total energy dose as the continuously irradiated animals (25 J) but fractionated by a 150 second interval after the first 5 J had been delivered. Once again the pO_2 of the colon was measured before, during and after irradiation both close to the irradiation fibre (1 mm) (Figure 38c) and further along the colon wall (3 mm) (Figure 38d). The periods of illumination are denoted by the shaded areas. The results from three animals in each group are presented. Close to the irradiation fibre the pO_2 of the colon fell to zero within the first fraction of light (5 J delivered over 50 seconds) in a similar manner to the continuous group (monitored at the same point). During the dark interval however, the pO_2 rose again although not as high as the 'baseline' pre-illumination levels. When illumination restarted at the end of the interval, the pO_2 fell back to zero. Further away from the irradiation fibre (3 mm), there was a much smaller fall in pO_2 after the first fraction of light and the fall in pO_2 to zero was delayed until after the second fraction of light had commenced. The pO_2 rose again post-PDT, although never regained the pre-treatment level during the period of observation. The area of necrosis produced by the fractionated PDT groups was 77 mm² (average diameter = 10 mm). This is not significantly different from the results of the previous sections using the same parameters and is approximately three times the area of necrosis produced by the same

parameters using continuous irradiation. The greater area of necrosis produced in the fractionated PDT groups results in the second monitoring point (3 mm away from the irradiation fibre) falling well within the area of necrosis.

2.2.5.4 Discussion

Many groups have found that light dose fractionation can produce beneficial results with a range of photosensitisers (Pe *et al*, 1994 (Haematoporphyrin Derivative); Anholt & Moan, 1991 (Sulphonated Aluminium Pthalocyanine); Muller *et al*, 1998 (meta-tetrahydroxyphenylchlorin) and van der Veen *et al*, 1994 (ALA induced PPIX)) although the effect has been seen to be greatest with ALA. It is possible in the normal rat colon to increase the area of necrosis produced by ALA PDT by a factor of three by simply interrupting the light dose for 150 seconds, after only one fifth of the total energy dose had been delivered. The mechanism which enables such a short interruption in the light dose to produce such a large increase of effect is not yet clearly understood. Several hypotheses have been proposed, including relocalisation of the photosensitiser, reoxygenation of the treatment site during the dark interval and reperfusion injury. This section uses an Eppendorf pO_2 microelectrode to look at the oxygenation of the treatment site during PDT.

In the measurements taken just 1 mm from the irradiation fibre, a rapid decline in pO_2 was observed soon after irradiation commenced in both the continuous and fractionated groups. In the fractionated group, a small but definite recovery in pO_2 was observed during the dark interval. This recovery was reversed when the second

fraction of irradiation commenced. This short period of reoxygenation during the dark interval was the only difference observed in the measurements taken 1 mm from the irradiation fibre when comparing fractionated and continuous light regimes.

This rapid fall in pO_2 close to the irradiation fibre is most likely due to the photochemical consumption of molecular oxygen outstripping the oxygen supply provided by the microcirculation, which is itself impaired by PDT (Leveckis *et al*, 1995 and Roberts *et al*, 1994). These results are consistent with the findings of other groups who have monitored oxygen during Photofrin PDT, particularly Sitnik *et al* (1998) who observed a significant and rapid decline in oxygen shortly after commencing irradiation using a similar microelectrode system in a RIF tumour model.

The small rise in oxygen level observed during the dark interval was anticipated. By turning the light off, the photochemical consumption of molecular oxygen (to produce singlet oxygen) is temporarily paused and as long as the microcirculation remains viable the tissue should reperfuse (which appears to be the case with these particular fractionation parameters). When the light is restarted the photochemical oxygen consumption should restart and the pO_2 falls once more.

Differences in pO_2 monitored 3 mm away from the irradiation fibre were also observed between the two different PDT regimes. The monitoring position was chosen carefully so that it would fall on the edge of the zone of necrosis produced by the continuous regime. In the continuous treatment the pO_2 at this point was not affected significantly. With the fractionated regime, however, the pO_2 did decline to zero but this fall was delayed until after the second fraction of light had commenced.

Further, the pO_2 recovered a little at the end of treatment (in some of the animals) and stayed above zero until sampling finished. These differences are important as the monitoring point was on the edge of the zone of necrosis in the continuous group and well within the area of necrosis in the fractionated group. It appears that in this model, necrosis occurred at all sites where a fall in pO_2 was documented during treatment (1 mm from irradiation fibre with both treatment regimes and 3 mm with fractionation). At the edge of the zone that was necrotic after treatment (3 mm, continuous), no change in pO_2 level was seen. This result could be of importance for real time monitoring of PDT in clinical practice as it suggests that a documented fall in pO_2 at the time of treatment may be a useful indicator of later necrosis at that site. If such a change could be demonstrated at a series of strategically located sites around a tumour, where it meets adjacent normal tissue, it could be a way of judging whether sufficient light has been delivered at the time of treatment. However, many further studies will be required to establish whether our conclusion reached from experiments on normal rat colon will be valid when treating human tumours.

The fractionation parameters used in this study were found to be optimal in the previous sections simply by trial and error. The position of the dark interval was found to be critical. If more than half the light dose was delivered before the interval, the fractionated regime was not significantly better than the same dose delivered in a single fraction. This may be due to the microcirculation not remaining viable past this point in the treatment (although, we have not studied the viability of the microcirculation directly in this model). The length of the dark interval in this model has also been investigated (Messmann *et al*, 1995) and longer intervals have not been found to be beneficial, indicating that 150 seconds is long enough for the tissue to

reperfuse (in this situation). This is consistent with Foster *et al*'s calculations (1991) which predicted that effective reoxygenation can take place in a hypoxic tissue in a period of about 45 seconds (depending on the degree of hypoxia caused by the previous light fraction and the maintenance of a viable microcirculation).

Multiple intervals were also not found to be any better than this optimal two fraction regime in the earlier experiments. This may be the result of irreversible damage occurring to the microcirculation when the second energy fraction commences, resulting in subsequent intervals having little or no additional effect. The oxygen present when the irradiation restarts allows a greater PDT effect to occur when the light dose is fractionated, although, it is unlikely that this is the sole factor which accounts for the difference in outcome between these two regimes.

The results of this section, therefore, show that there is significant consumption of pO_2 during ALA PDT in the normal rat colon and that there are marked differences in the pattern of pO_2 levels during PDT when comparing continuous and fractionated light regimes. With further investigation it may be possible to use the real-time monitoring of oxygen in patients to exploit these differences to monitor and improve the effectiveness of clinical PDT.

2.2.6 PPIX Relocalisation During Light Dose Fractionation

2.2.6.1 Introduction

Both Anholt and Moan (1991) and van der Veen *et al* (1994) using AlS₄Pc and ALA induced PPIX photosensitisation respectively, have observed reappearance of the photosensitiser following photobleaching, when fractionating the light dose. Anholt and Moan switched the light on and off repeatedly for periods of 15 seconds and postulated that their success could be explained by relocalisation of the photosensitiser during the dark periods. Van der Veen *et al*, however, detected partial recovery of the photobleaching of PPIX fluorescence observed after the first light fraction. This was attributed to new PPIX being produced during the long, 75 minute fractionation interval.

To determine whether PPIX relocalisation/new production of PPIX is occurring during the relatively short, 150 second intervals employed in this study and if this factor can account for the success obtained with light dose fractionation, PPIX fluorescence was monitored during continuous and fractionated PDT regimes.

2.2.6.2 Materials and Methods

Chemicals

ALA powder was dissolved in physiological strength PBS (pH 2.8) and administered intravenously (with a concentration of 25 mg/ml and a maximum volume of 0.2 ml).

Animal model

Normal, female, Wistar rats (120 - 200 g) were used throughout. The animals were anaesthetised for all parts of the procedure using inhaled halothane and analgesia was administered subcutaneously following surgery (Buprenorphine hydrochloride).

Fluorescence studies

All animals were given 200 mg/kg ALA intravenously, 2 hours prior to surgery. The colon was accessed for PDT via a laparotomy as described in section 2.0.0.2. The pulsed (12 kHz) copper vapour pumped dye laser (tuned to 635 nm) was used to deliver a total energy of 25 J (output power, 100 mW). The light dose was either continuous or fractionated either by one interval after one fifth of the light dose had been delivered or into five equal fractions (by four dark periods). The fractionation interval was fixed at 150 seconds throughout.

Fluorescence studies were undertaken to look at the levels of PPIX and photoproducts before and after PDT and in the dark intervals between fractions. Fluorescence emission spectra were recorded using a spectrograph (Multispec 1/8 m focal length, Oriel Instruments, USA) coupled to a slow-scan cooled CCD camera (600 x 400

pixels, Wright Instruments Ltd, UK). The technique was that used by Dietel *et al* (1997) with a few modifications. Fluorescence was excited using a 0.5 mW helium-neon laser at 543 nm and emission spectra were recorded over the range 600 - 750 nm with 1 nm resolution. A long-pass Schott filter (RG590) was used to suppress scattered excitation light. The spectrograph grating was blazed at 650 nm so the detection efficiency of the system was relatively uniform over this range and the spectra presented are, therefore, uncorrected.

A fibre-optic bundle consisting of a 200 μm core fibre surrounded by six collection fibres (also with 200 μm cores) was used to excite and collect fluorescence. The tip of the fibre bundle was placed on the tissue surface 3 mm away from the 200 μm PDT irradiation fibre which was also positioned on the tissue surface. This configuration was selected so that the edge of the anticipated zone of necrosis could be probed. Spectra were recorded before and after the light dose and during the fractionation interval so that there was no interference from fluorescence excited by the PDT laser. A two second integration time was used to record the spectra and sequential measurements during periods without red light illumination found no evidence of photobleaching effects (diminution of the porphyrin spectra or appearance of photoproduct emission). The intensity of fluorescence from control animals that had not received ALA was negligible ($< 5\%$ of the initial PPIX peak at 636 nm seen in ALA treated animals). All the spectra presented have been normalised.

2.2.6.3 Results

Fluorescence maxima were detected at 636 \pm 2 nm in each case and the spectral profiles recorded conform to the standard PPIX emission spectra described by Dietel *et al* (1997) and Sailer *et al* (1997). A previous HPLC analysis of colon samples after intravenous administration of ALA to Wistar rats (Loh *et al*, 1993) has shown that PPIX is the predominant porphyrin present (> 95 %) and it is, therefore, concluded that the fluorescence measured in the present study is produced predominantly by PPIX.

Continuous PDT

Figure 39 shows the fluorescence emission spectra recorded before and after 25 J of continuous PDT. Substantial photobleaching occurred during treatment and photoproduct emission near 675 nm is evident between the two porphyrin emission peaks. At the end of treatment the fluorescence intensity had declined to about 20 % of its pre-treatment value.

Fractionated PDT

Figure 40 shows the fluorescence emission spectra recorded at different points throughout a fractionated PDT regime where the light dose was interrupted by a single 150 second interval, after one fifth of the energy dose had been delivered (F20/80). A significant level of photobleaching occurred during the short, first energy fraction (5 J). A small recovery in the fluorescence intensity then took place over the period of the 150 second dark interval, followed by considerable photobleaching during the

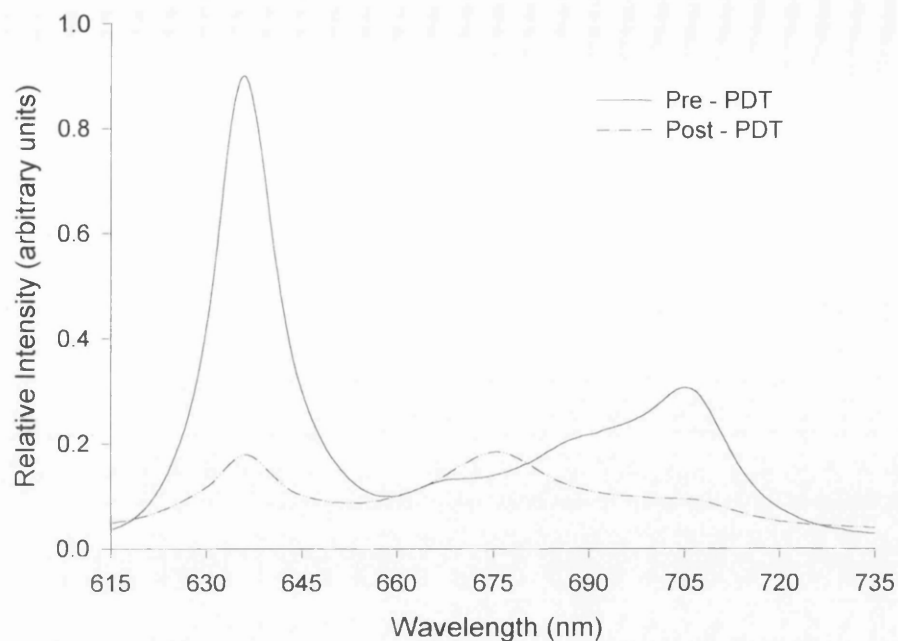


Figure 39 Fluorescence spectra recorded using 543 nm excitation light during a PDT treatment using 200 mg/kg ALA i.v. 25 J of continuous 635 nm light was delivered.

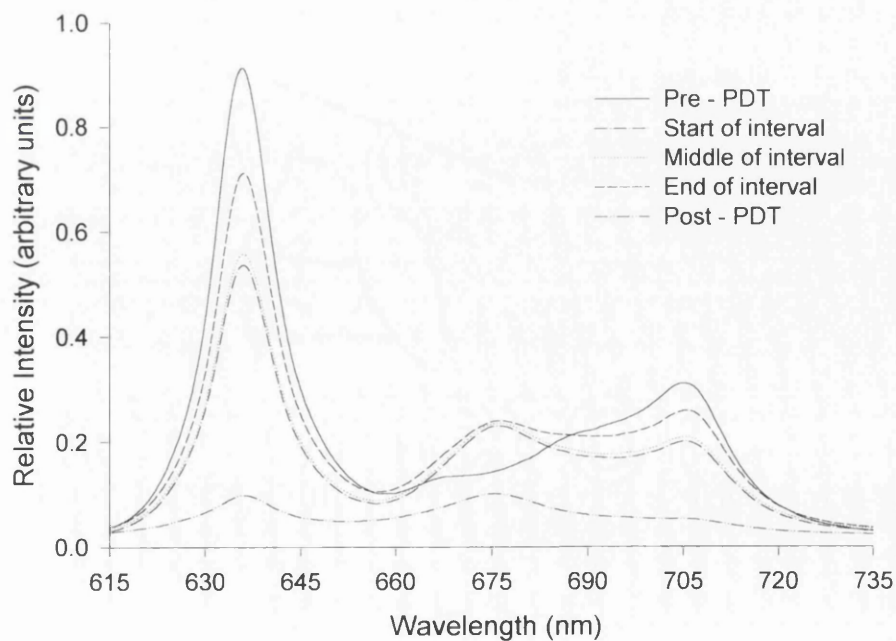


Figure 40 Fluorescence spectra recorded using 543 nm excitation light during a PDT treatment using 200 mg/kg ALA i.v. 25 J of 635 nm light was delivered fractionated into two parts (5/20 J) by a 150 second interval.

second energy fraction (20 J). Once again, photoproduct emission near 675 nm was evident. At the end of treatment the fluorescence intensity had declined to about 10 % of its pre-treatment value in a similar manner to the continuous treatment.

Figure 41 shows the fluorescence emission spectra recorded at different points throughout a fractionated PDT regime where the energy dose was split into five equal fractions by four, 150 second intervals. Spectra were recorded before and after the treatment, as well as at the beginning, middle and end of each interval. During the first (5 J) energy fraction, photobleaching occurred as before. This was partially reversed during the first dark interval. Subsequent energy fractions produced further photobleaching but the partial recovery in PPIX fluorescence during the intervals diminished each time until there was little or no recovery during the final interval. Photoproduct emission near 675 nm was evident and the fluorescence intensity declined to about 25 % of its pre-treatment value by the end of the treatment.

The fluorescence spectra were not corrected to account for any PDT induced changes in tissue optics, but this is almost certainly unnecessary as the recovery in intensity of the 636 and 710 nm peaks (corresponding to PPIX) are comparable, whereas the photoproduct peak at 675 nm (which includes an underlying PPIX contribution) increases only slightly. Any change in tissue optics would cause all peaks to change in a similar manner.

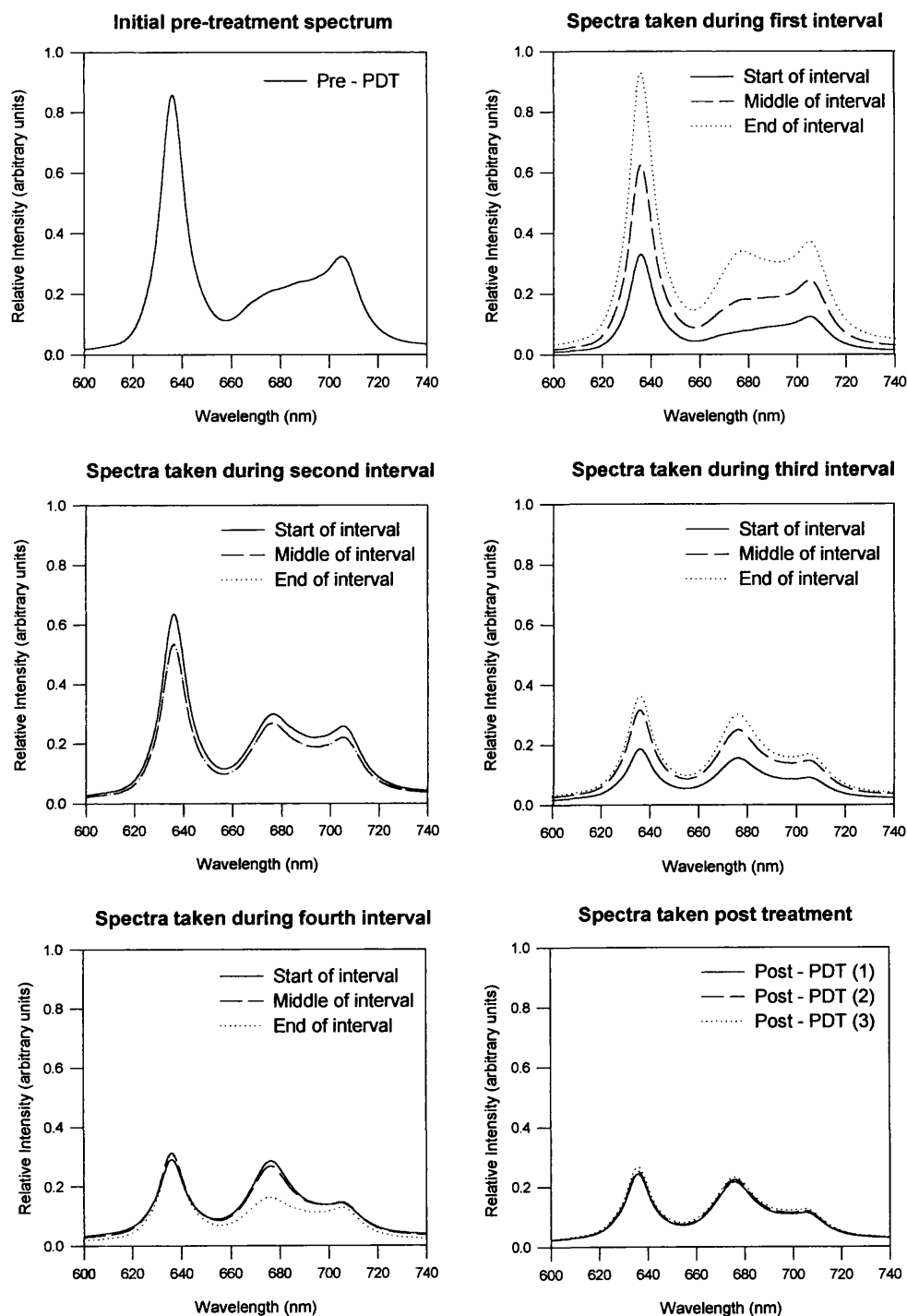


Figure 41 Fluorescence spectra recorded using 543 nm excitation light during a PDT treatment using 200 mg/kg ALA i.v. 25 J of 635 nm light was delivered fractionated into five equal fractions by four 150 second intervals.

2.2.6.4 Discussion

It appears that the recovery of tissue levels of PPIX, during the short dark interval employed in this study, could contribute to the enhanced effect of light fractionation on ALA PDT, observed in this model.

The fluorescence results with the continuous PDT treatment show that PPIX fluorescence photobleaching (recorded 3 mm from the PDT irradiation fibre) is nearly complete by the end of treatment (after 25 J) indicating that the rate of photochemical oxygen consumption declines substantially during treatment. The production of a photoproduct at about 675 nm was also detected.

With the 5/20 J fractionation regime, a partial recovery in fluorescence was seen during the dark interval of 150 seconds. This is probably due to PPIX relocalisation as it is unlikely that substantial PPIX synthesis could occur during this short period of time (light on for 50 seconds, off for 150 seconds and on again for 200 seconds). The relocalisation could be the result of local diffusion or reperfusion of plasma-bound PPIX, as suggested by Dietel *et al* (1997). They observed a doubling in PPIX fluorescence within three minutes of PDT treatment, when blood-flow restricting clamps were removed from a murine tumour. The relocalisation of the PPIX during the fractionation interval, as detected in this study, makes more PPIX available to cause photochemical damage when the illumination recommences, thus producing more necrosis. It is unlikely, however, that this sole difference could account for the large difference in outcome obtained by fractionating the light dose.

In the previous sections, multiple intervals were not found to be more beneficial than the best two fraction regime (F20/80). The current results indicate that although substantial PPIX relocalisation occurs during the first interval, the effect during subsequent intervals (when multiple intervals are employed) becomes increasingly diminished. This could explain, at least partially, why multiple intervals are not more beneficial than one appropriately placed interval. If the PPIX is in fact relocalising from the plasma during the dark interval, fractionating the illumination would only remain beneficial whilst the microvasculature remained viable.

It is difficult to determine to what degree PPIX relocalisation or reoxygenation (during the fractionation interval) accounts for the success of a particular light dose fractionation regime, particularly as the two factors are interrelated (the photobleaching of PPIX to form the 675 nm photoproduct is oxygen dependent). It has been determined, however, (in separate experiments) that there is an increase in both PPIX and oxygen levels in the treatment site, when the light dose is fractionated. It may be possible in the future, to use this fact to improve clinical ALA PDT, through the real-time monitoring of PPIX fluorescence and oxygen levels, if alterations in these variables can be conclusively correlated with the overall biological effect of the treatment.

2.2.7 The Effect of Reperfusion Injury During Light Dose Fractionation

2.2.7.1 Introduction

An alternative mechanism to explain the enhanced outcome of light dose fractionation is through the effect of reperfusion injury.

Reperfusion injury can occur as tissues are reperfused after a transient period of ischaemia. This happens as the enzyme, xanthine oxidase, becomes activated in a poorly oxygenated environment. Concomitantly, ATP is broken down, producing the purine substrates necessary for this enzyme to produce superoxide when oxygen is reintroduced (McCord, 1987). If reversible vasoconstriction is in fact occurring during the first fraction of a fractionated PDT treatment, this would result in such an oxygen and thus energy compromised environment, making it conceivable that free radical damage could occur in this manner when the tissue is reperfused during the dark interval.

This section will investigate the contribution of reperfusion injury to the damage produced by continuous and fractionated light regimes, through the use of free radical scavengers and enzyme inhibitors (to prevent the damage produced by reperfusion injury from occurring).

McCord's proposed mechanism for the generation of superoxide and secondary species of active oxygen after ischaemia and reperfusion (as adapted from McCord, 1985) can be seen in Figure 42. Although, this process is not completely understood and several mechanisms of injury may be in operation, this is currently the best description available. Figure 43 summarises some of the reactions possible following reperfusion injury.

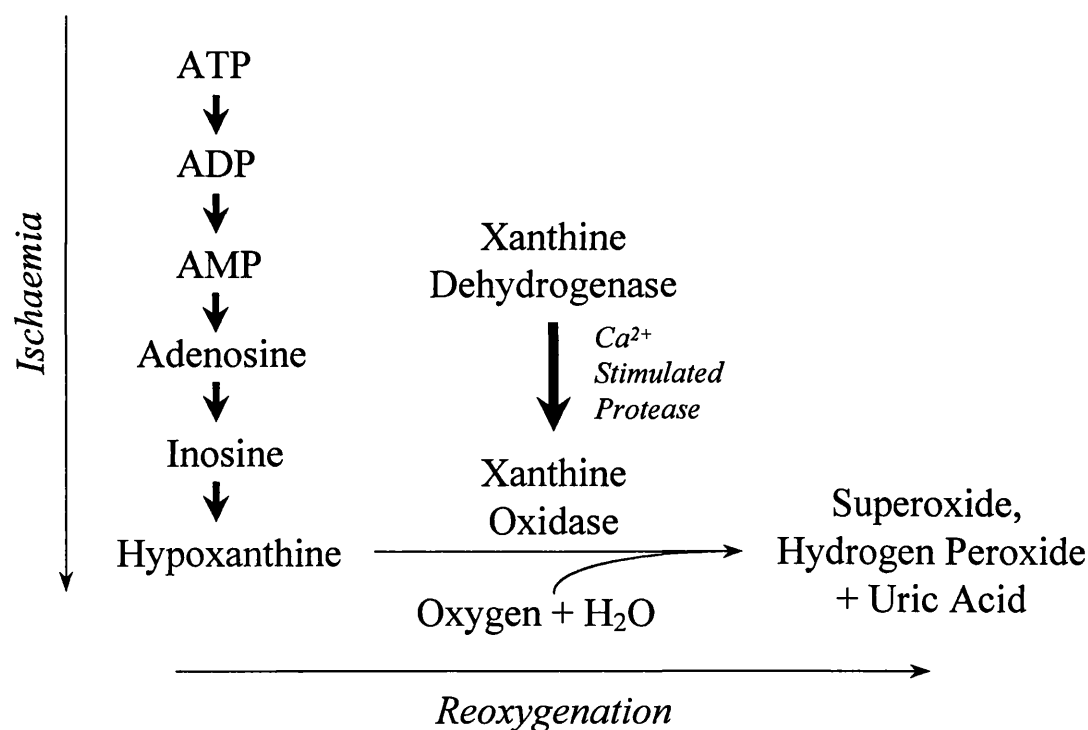


Figure 42 Proposed mechanism for the ischaemia induced production of reactive oxygen species as adapted from McCord (1985).

Reduced blood flow limits oxygen supply and, therefore, ATP production. As the cell's energy level drops, it can no longer maintain the ion gradients across its

membranes. This results in an increase of calcium ions in the cytosol (as the energy starved cell is unable to keep the calcium ions pumped out). This activates a protease which converts the innocuous enzyme, xanthine dehydrogenase into xanthine oxidase. At the same time, the energy depleted cell breaks down ATP forming the purine substrates, hypoxanthine and xanthine. When the tissue is reperfed, the enzyme xanthine oxidase uses these purine substrates along with the new supply of oxygen to produce the oxygen radical, superoxide (McCord, 1987).

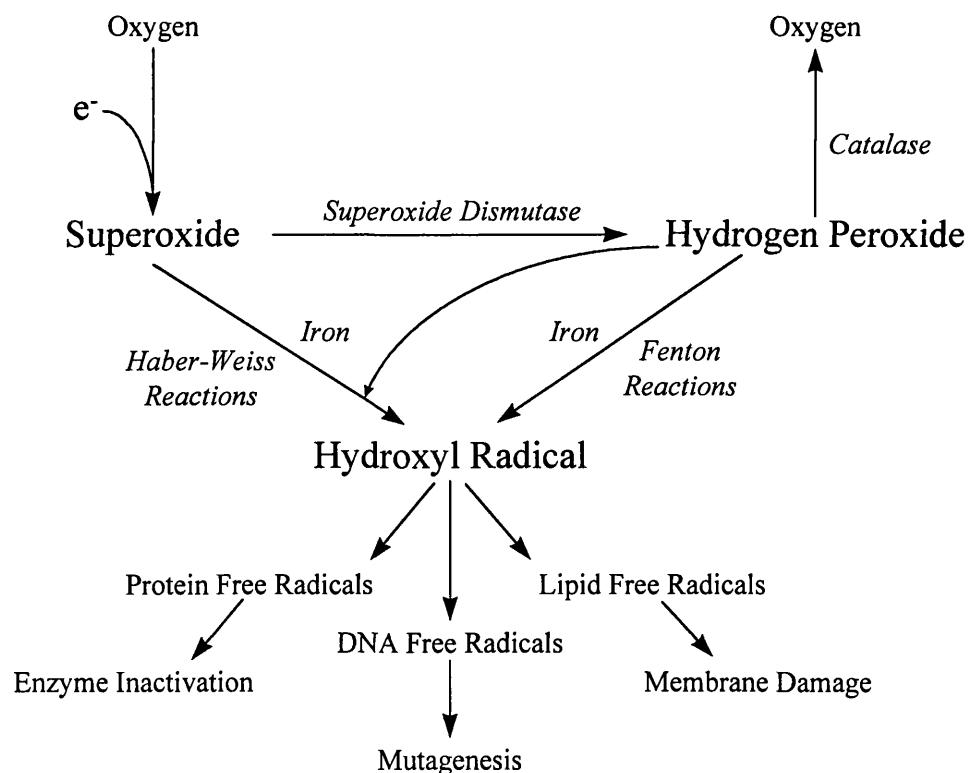


Figure 43 Summary of some of the reactions possible following reperfusion injury (Hammond *et al*, 1985).

Superoxide is produced in most, if not all aerobic cells and the enzyme superoxide dismutase (SOD) is present intracellularly to remove it. Dismutation of superoxide produces hydrogen peroxide and the enzymes catalase and glutathione peroxidase exist to remove this compound. Together, these enzymes protect cells against the reduced oxygen intermediates produced during normal aerobic metabolism. When superoxide and hydrogen peroxide production is excessive, however, such as following reperfusion injury, the protective enzymes are unable to cope, thus resulting in cell damage. Some of this damage may be mediated by the transition metal, iron, which can convert superoxide and hydrogen peroxide into aggressive oxidants such as the hydroxyl radical (by Haber-Weiss and Fenton-type reactions), which can then damage DNA, proteins and lipids, resulting in cell death. It is also possible that hydroxyl radicals can be produced (in a reaction independent of metal ions) from peroxynitrite (which itself can damage the cell membrane). Peroxynitrite can be produced from superoxide and nitric oxide (which can also be toxic to cells) both of which can be increased when ischaemic tissues are reperfused (Gutteridge and Halliwell, 1990). The ultimate destructive effect of these reactive species is amplified many times by the cascade of free radical production they generate.

If SOD and catalase are present together in large quantities, pre-ischaemia or at the start of reperfusion (through exogenous administration), they can produce significant protection against reperfusion injury (Gross *et al*, 1986; Jolly *et al*, 1984; Mittal *et al*, 1988). It is also possible to use allopurinol, a potent and highly specific inhibitor of the conversion of xanthine dehydrogenase to xanthine oxidase, to prevent reperfusion injury (Crowell *et al*, 1969; Paller *et al*, 1984). It was, therefore, decided to study the effect of the combination of the scavenging enzymes, SOD and catalase or the enzyme

inhibitor, allopurinol, on the damage produced by continuous or fractionated ALA PDT, to determine whether some of the damage was free radical mediated and if this destruction was mediated by the reperfusion injury enzyme, xanthine oxidase.

2.2.7.2 Materials and Methods

Chemicals

ALA powder was dissolved in physiological strength PBS (pH 2.8) and administered intravenously (with a concentration of 200 mg/ml and a maximum volume of 0.2 ml). Superoxide dismutase (SOD) and catalase (Sigma-Aldrich Co. Ltd., Poole, UK) were also dissolved in PBS as a combination and were administered intravenously (at a concentration of 23.3 and 10 KU/ml respectively, maximum volume 0.2 ml) either up to five minutes prior to illumination or immediately afterwards. Allopurinol (Sigma-Aldrich Co. Ltd., Poole, UK) was also dissolved in PBS and administered intravenously (at a concentration of 50 mg/ml and a maximum volume of 0.2 ml) either 15 minutes prior to illumination or immediately afterwards.

Animal model

Normal, female, Wistar rats (120 - 200 g) were used throughout. The animals were anaesthetised for all parts of the procedure using inhaled halothane and analgesia was administered subcutaneously following surgery (Buprenorphine hydrochloride).

PDT studies

All animals were given 200 mg/kg ALA intravenously, 2 hours prior to surgery. The colon was accessed for PDT via a laparotomy as described in section 2.0.0.2. The 628 nm diode laser was used to deliver a total energy of 25 J (output power, 100 mW). This light dose was either continuous or fractionated after one fifth of the energy dose had been delivered by a single interval of 150 seconds. Groups of three animals either receiving continuous or fractionated PDT were either administered with the combination of 10 mg/kg SOD i.v. and 7.5 mg/kg catalase i.v. or 50 mg/kg allopurinol i.v., either prior to PDT or immediately after illumination. Uninhibited continuous and fractionated PDT groups were also conducted as controls. The area of necrosis produced at three days was determined using the image analysis system.

The dosage and administration time of the inhibitory compounds were carefully chosen to mimic those of previous studies where these compounds had been successfully used to prevent reperfusion injury (Crowell *et al*, 1969; Gross *et al*, 1986; Jolly *et al*, 1984; Mittal *et al*, 1988; Paller *et al*, 1984). It should also be noted that due to the short half-life of SOD in blood (6 minutes), the combination of SOD and catalase was administered as close to the beginning of the irradiation period as possible, so it would still be around in significant amounts by the end of the treatment (Gross *et al*, 1986).

2.2.7.3 Results

The area of necrosis (mm^2) produced by each of the treatment regimes when the inhibitory compounds were administered prior to the light irradiation can be seen in Figure 44. The administration of the combination of SOD and catalase (CAT) prior to irradiation prevented damage (as detected macroscopically) being produced by either the continuous or fractionated regimes. The same was true of the pre-administration

	Treatment Regime					
	Uninhibited		SOD + CAT (pre-PDT)		Allopurinol (pre-PDT)	
	C	F20/80 (150)	C	F20/80 (150)	C	F20/80 (150)
Area of Necrosis (mm^2)	13	45	0	0	0	0
n =	8	3	3	3	3	3

Figure 44 Mean area of necrosis (mm^2) as a function of treatment regime. 200 mg/kg ALA i.v. was administered 2 hours prior to 25 J of 628 nm light (100 mW) using a diode laser. The energy dose was either continuous or fractionated. Fractionated groups were interrupted by one interval of 150 seconds after one fifth of the light dose had been delivered (F20/80). The SOD + CAT or Allopurinol were administered intravenously prior to illumination.

of allopurinol, no macroscopic damage being produced by either the continuous or fractionated PDT. Only uninhibited control groups produced any damage, with the fractionated group producing approximately three times the area of necrosis of that of continuous ALA PDT.

The area of necrosis (mm^2) produced by each of the treatment regimes when the inhibitory compounds were administered immediately after the light irradiation can be seen in Figure 45. The administration of the combination of SOD and catalase (CAT) after irradiation resulted in only a little necrosis being produced by either the continuous or fractionated regimes. Both sets of parameters produced similar amounts

	Treatment Regime					
	Uninhibited		SOD + CAT (post-PDT)		Allopurinol (post-PDT)	
	C	F20/80 (150)	C	F20/80 (150)	C	F20/80 (150)
Area of Necrosis (mm^2)	13	45	3	4	2	6
n =	8	3	3	3	3	3

Figure 45 Mean area of necrosis (mm^2) as a function of treatment regime. 200 mg/kg ALA i.v. was administered 2 hours prior to 25 J of 628 nm light (100 mW) using a diode laser. The energy dose was either continuous or fractionated. Fractionated groups were interrupted by one interval of 150 seconds after one fifth of the light dose had been delivered (F20/80). The SOD + CAT or Allopurinol were administered intravenously immediately after illumination.

of damage and much lower than that of either of the control groups. Similar results were also obtained when allopurinol was administered immediately after the illumination period, with little damage being produced by either regime.

2.2.7.4 Discussion

It has been shown that the administration of the combination of the scavenging enzymes, SOD and catalase, or the xanthine oxidase inhibitor, allopurinol, prior to illumination, can prevent ALA PDT from producing macroscopic damage in the normal rat colon at three days, whether the light dose is fractionated or continuous. These compounds, therefore, protect the tissue against the PDT damage.

The combination of SOD and catalase is not a specific inhibitor of reperfusion injury, the action of these enzymes is to remove the harmful superoxide and hydrogen peroxide from the cell (thus preventing hydroxyl radical formation) no matter how these oxygen free radicals and reduced oxygen intermediates are formed. These reactive oxygen species are known to be produced during reperfusion injury.

This series of experiments alone, however, tells us little about the involvement of reperfusion injury in ALA PDT damage, as it is conceivable that cellular damage via singlet oxygen production would trigger a similar cascade of oxygen free radicals and reduced oxygen intermediates, particularly as the mitochondrion is reported to be a major site of ALA PDT induced damage (Peng^a *et al*, 1997) and this would uncouple the electron transport chain 'leaking' further electrons to oxygen to form these reactive

oxygen species. The disruption of cellular membranes is also reported and once lysis of cellular compartments has been induced, the resultant free radical cascade would be cataclysmic for the cell.

The experiments with allopurinol are different, however. Allopurinol is known to be a specific inhibitor of the conversion of xanthine dehydrogenase into xanthine oxidase, which results in allopurinol being a specific inhibitor of reperfusion injury (if the proposed mechanism is correct). The pre-administration of this compound would, therefore, not have any effect on the production of reactive oxygen species or free radicals by any mechanism, other than reperfusion injury. As the presence of this compound by itself, prior to light irradiation, prevented the necrosis normally produced by ALA PDT, it can, therefore, be concluded that reperfusion injury must be playing some role in producing the necrosis in this model.

It is known that if a tissue is ischaemic, even for a very short period of time, it is possible for xanthine dehydrogenase to be converted into xanthine oxidase. In normal rat ileum, nearly complete conversion of this enzyme can occur within 10 seconds of non-perfusion (Roy and McCord, 1983) and so, even if the treatment site in the current study was ischaemic for only a very short period of time, reperfusion injury could still have taken place.

The light regime used had little bearing on the results, similar results being obtained with both continuous and fractionated light regimes. It is known from the results of section 2.2.5 that the oxygen level in certain parts of the treatment site can fall to zero during both continuous and fractionated regimes and monitoring points where this

occurs were found to be within the zone of necrosis produced at three days. Monitoring points where this oxygen consumption was not seen, fell outside the subsequent zone of necrosis.

In the continuous group, monitored at 1 mm away from the irradiation fibre, this significant fall in oxygen was partially reversed in one animal after the light irradiation had finished. The same occurred in two animals after receiving a fractionated light regime and being monitored at 3 mm away from the irradiation fibre. The reintroduction of oxygen to the tissue after such a temporary period of ischaemia is known to cause reperfusion injury and it is, therefore, possible that this might be occurring in this model. If it had been possible to follow each animal in the oxygen study for a longer period of time after the light irradiation had finished, it may have been possible to detect reoxygenation in more of the animals.

This reoxygenation, which occurred after the irradiation period had finished, may also explain the results obtained when the inhibitory compounds were administered immediately after light irradiation (partial but incomplete inhibition). It is known from other reperfusion studies that these compounds will only completely prevent reperfusion injury, if they are present either before the ischaemic period or before reoxygenation commences. If reoxygenation had already commenced in some animals by the time the compound was injected and circulated to the colon, the protective effect of the compound would have been reduced.

It, therefore, appears that the increased area of necrosis produced by the fractionation regime may be the result of reperfusion injury following the temporary ischaemia

produced at distances further away from the irradiation fibre than possible with continuous illumination. This effect may be further enhanced by relocalisation of the photosensitiser during the interval.

As iron also appears to play a role in reperfusion injury by catalysing superoxide and hydrogen peroxide into the highly reactive and, therefore, highly destructive hydroxyl radical (by Haber-Weiss and Fenton type reactions) and it is known that this function can be exacerbated by administering exogenous intracellular iron and inhibited by the administration of an iron chelator (van der Kraaij *et al*, 1988; van der Kraaij *et al*, 1989; Lesnefsky and Ye, 1994; Paller and Hedlund, 1994), future studies of reperfusion injury should also include an investigation of ALA PDT enhanced by an iron chelator, particularly, as ALA is known to induce iron release from iron stores (Oteiza *et al*, 1995).

2.2.8 Discussion

This experimental section has investigated the effectiveness of light dose fractionation as a potential enhancer of ALA PDT and has also started to investigate the mechanism of this technique.

Initial studies determined that light dose fractionation could be used to significantly enhance the effect of ALA induced PDT in normal rat colon, if an appropriate regime was used. The best regime in this model was found to be a single 150 second interval placed early in the illumination period, after only one fifth of the light had been delivered (F20/80). Multiple intervals were not found to be more beneficial than this two fraction regime. Alternatively, light dose fractionation was found to be able to produce the same effect as continuous treatment but with the energy dose being reduced by 60%. Light dose fractionation was more effective at increasing the area of necrosis produced by ALA PDT using the higher ALA doses studied (200 and 50 mg/kg i.v.). No enhancement was observed when using an ALA dose of 25 mg/kg i.v. Studies using the colonic tumour model, also found this best two fraction regime (F20/80) to be more effective than continuous illumination, producing double the volume of necrosis than that produced by continuous treatment.

By combining the technique of light dose fractionation with the administration of the iron chelator, CP94, it was found that an effect much greater than that produced by either method separately could be produced. The combination of these techniques,

basically increased the amount of PPIX in the treatment site (using the administration of an iron chelator) in the first instance and then refined the irradiation delivery (using light dose fractionation) to allow the maximal PDT effect possible to occur.

More detailed studies of the effect of the best two fraction regime (F20/80) on various measurable parameters were then conducted, once again in the normal rat colon, and compared with the results using continuous irradiation. Firstly, the effect of these light regimes on the oxygen level at specific points in the treatment site was determined using a polarographic measure of pO_2 . It was found that there was significant consumption of pO_2 during ALA induced PDT in this model and that there were marked differences in the pattern of pO_2 levels between the continuous and fractionated regimes. Monitoring points where the pO_2 level fell to zero during the treatment, were found to be within the area of necrosis produced by the treatment at three days. Monitoring points where this significant oxygen consumption was not observed, were found to be outside the produced zone of necrosis. With further investigation, this fact may turn out to be a useful indicator of treatment outcome.

A small increase in PPIX fluorescence was also observed during the fractionation interval in subsequent experiments and may contribute to the enhanced effect of this technique in this model. With both continuous and fractionated regimes (monitored at a point 3 mm away from the irradiation fibre) PPIX fluorescence photobleaching was almost complete by the end of the treatment and production of a photoproduct (at about 675 nm) was detected. The probable relocation of the PPIX during the fractionation interval, as detected by this study, would result in greater photochemical damage and thus necrosis being produced when the illumination was recommenced. It

is unlikely that the increase in PPIX fluorescence was due to new PPIX production as the interval was only 150 seconds long. The relocalisation of PPIX through local diffusion or the reperfusion of plasma bound PPIX is, however, feasible.

Reperfusion injury was the final mechanism investigated by this thesis as an explanation of the enhanced effect produced by light dose fractionation. It was found that the inhibition of reperfusion injury either through the enzyme inhibitor, allopurinol, or the reactive oxygen species scavengers, superoxide dismutase and catalase, prior to light irradiation, completely inhibited the macroscopic damage normally produced by the continuous or fractionated ALA PDT regimes. This indicates that reperfusion injury must be playing some role in producing the necrosis normally produced by ALA PDT in this model. Considering these results, with those from the oxygenation studies, it is likely that reperfusion injury is being produced as the tissue reoxygenates following a short period of ischaemia during both regimes. The difference between the two regimes, being that with light dose fractionation it is possible to detect such ischaemia and subsequent reoxygenation at distances further away from the irradiation fibre, than possible with continuous irradiation.

It has, therefore, been shown that the technique of light dose fractionation can be used to substantially enhance ALA PDT in both normal and malignant rat colon, if an appropriate fractionation regime is utilised. These results support the findings of numerous other groups, who have studied this technique in a whole range of different models.

It has not been possible to identify one sole factor responsible for the difference observed between the continuous and fractionated irradiation regimes employed in these studies. The mechanism of action appears to involve several different interrelated factors and is as a result, complex. It does seem, however, that reperfusion injury (a complicated and not yet fully understood process) may be playing an important role in the production of necrosis in this model. Whether this is also true during clinical ALA PDT is yet to be established, however.

The monitoring of pO_2 at the treatment site, currently appears to be a promising method of real-time monitoring of clinical ALA PDT and may give some indication of the success or failure of the treatment (at the time of irradiation) and as such, warrants further detailed study. Real-time monitoring will be essential, if light dose fractionation is to be used successfully, to enhance clinical ALA PDT, as the fractionation regime employed will need to be determined on an individual basis, so the full potential of this technique can be realised.

SECTION III

DISCUSSION

3.1 General Discussion

The enhancement of ALA induced PDT is an up and coming area of research. Considerable work has been conducted in this field over the last few years and much is currently in progress. A whole range of different approaches are being employed to try to improve the effect of this treatment, two of which have been studied in this thesis.

The administration of the hydroxypyridinone iron chelator, CP94, in combination with ALA, was found to be of significant benefit when conducting PDT (with the compounds being administered intravenously, topically or as an instillation) in several animal models. This makes it potentially possible to apply this technique of enhancement to many clinical applications of ALA PDT.

The addition of CP94 produced greater PPIX fluorescence in all the models studied (rat colon, rat colonic tumour model, rat skin and rabbit uterus), than the administration of ALA alone. By chelating free iron in the system, CP94, therefore, increased the temporary accumulation of PPIX by reducing its conversion into haem (through the addition of iron by the enzyme ferrochelatase). The PDT studies established that this increase in PPIX accumulation could be utilised to substantially enhance the effect of ALA induced PDT in all of the animal models studied.

In the normal rat colon it was found that the same amount of ^{mucosal fluorescence} ~~necrosis~~ could be achieved through the intravenous administration of 100 mg/kg CP94 and 25 mg/kg ALA i.v., as produced by 50 mg/kg ALA i.v. alone. It was also determined that the same combination of ALA and CP94 produced six times the area of necrosis than that produced by the same dose of ALA alone (25 mg/kg ALA). This is a significant degree of enhancement which, if it could be reproduced clinically, could substantially improve ALA PDT treatment. Further experiments are necessary, however, to investigate the effect of the oral administration of this iron chelator, as this is the most usual route of systemic ALA administration.

It was also noted, in the normal colon fluorescence and PDT studies, that as the dose of ALA was increased, the degree of potentiation obtained with the addition of CP94, reduced. This has been observed before with other iron chelators (Berg *et al*, 1996) and is probably the result of the saturation of the enzyme pathway with the higher doses of ALA alone. This factor indicates that the administration of CP94 may be particularly advantageous during clinical ALA PDT, where only relatively low doses of ALA are administered, thus enabling full potentiation to occur.

In normal rat skin, the administration of CP94 with ALA in a topical cream, produced a small increase in PPIX fluorescence (29% increase), which substantially improved the PDT effect on irradiation. Future work to determine the depth of the PDT effect is necessary, however, as this is a crucial factor in the successful treatment of thicker cutaneous lesions.

In the rabbit uterus, the administration of CP94 in combination with ALA as an uterine instillation both increased endometrial PPIX fluorescence (66% increase) and improved the selectivity of PPIX fluorescence between the endometrial and myometrial layers. This resulted in more extensive endometrial ablation in the ALA + CP94 group than in the ALA only group. It must still be determined, however, whether this damage is extensive enough to ablate all endometrial glands clinically, and if this ablation can be prolonged for a substantial period of time in order to avoid continual retreatment.

Although no other types of iron chelators have been investigated by this thesis, it has been previously established that the hydroxypyridinones are more effective intracellular iron chelators and are more easily administered than other commonly available iron chelators, such as desferrioxamine (Brittenham, 1992). It is, therefore, expected that these compounds should be more effective when applied in this manner to enhance clinical ALA PDT.

As the hydroxypyridinone compounds have already been administered to humans (as a treatment for iron overload), they are known to be relatively safe and free from side effects, especially when given as a single dose, rather than on a daily basis over a prolonged period of time. No adverse effects are, therefore, expected from these compounds when administered in combination with ALA PDT. It is possible, nevertheless, that by temporarily increasing the accumulation of PPIX, these compounds may exacerbate the already established side effects of ALA PDT, particularly through increasing cutaneous photosensitivity. These compounds, however, like ALA, PPIX and the other haem biosynthesis pathway intermediates, are

rapidly cleared from the human body, so these effects should not be greatly worsened and should be more than compensated by the improved outcome of the treatment.

The results of this thesis indicate that the administration of the iron chelator CP94, is a promising technique of ALA PDT enhancement. Carefully designed clinical trials will be necessary, however, to determine whether the same degree of enhancement can be reproduced in the clinical setting as has been observed in these *in vivo* studies. As a technique, it should be relatively simple to apply clinically, simply involving the addition of the iron chelator to the ALA preparation prior to administration. The only modification that may be required is the optimisation of the drug/light interval to achieve the best results possible.

Light dose fractionation was also found to significantly enhance the effect of ALA PDT and although this technique has been shown to be of benefit previously (Messmann *et al*, 1995; van der Veen *et al*, 1994; Hua *et al*, 1995) little is known about its mechanism of action.

Light dose fractionation is a simple idea but there are numerous treatment parameters to be studied individually which makes optimisation difficult. Initial studies, in normal rat colon, found that a single 150 second interval was equivalent to multiple intervals of the same length and that this single interval was more effective when placed earlier rather than later in the illumination period. The timing of the dark interval and the size of the initial energy fraction appear to be the critical factors in the success of the fractionation regime and will probably need to be determined on an individual treatment basis to obtain the greatest effect possible.

The most advantageous fractionation regimes could be used to increase the area of necrosis by up to three times when using 200 or 50 mg/kg ALA i.v., unfortunately, no such enhancement was observed (using the parameters of this study) when using the more clinically relevant ALA dose of 25 mg/kg i.v. It was also possible, however, to use a fractionation regime to reduce the amount of light required (by 60%) to produce the same amount of damage as continuous illumination (when using 200 mg/kg ALA i.v.).

Investigations were also conducted to determine the reasons for these effects. The oxygen level at different locations in the treatment site was found to be significantly affected by different irradiation regimes. A rapid fall in pO_2 was observed close to the irradiation fibre soon after illumination commenced and was probably caused by the photochemical consumption of oxygen outstripping the supply. Without a sufficient supply of oxygen, the photochemical reactions necessary to cause PDT damage would cease, limiting the effect of the treatment. During the dark interval of the fractionated treatment, however, a small recovery of oxygen was observed, which was reversed when the illumination restarted. This would have enabled further PDT damage to occur, especially as the fluorescence study observed a slightly increased level of PPIX present in the tissue by the end of the fractionation interval.

The administration of the combination of the scavenging enzymes, SOD and catalase, or the xanthine oxidase inhibitor allopurinol, prior to illumination, prevented continuous or fractionated ALA PDT regimes from producing necrotic lesions in the normal rat colon. This indicated that the damage normally produced by these

treatments in this model, must involve free radicals produced through reperfusion injury.

Reperfusion injury can occur when a tissue is reperfused after a temporary period of ischaemia. It was noted during the oxygen monitoring experiments that monitoring points where the oxygen level fell to zero during treatment, were within the area of necrosis at three days. Monitoring points where this oxygen depletion was not observed, fell outside the zone of necrosis. Therefore, it may be that light dose fractionation actually produces larger areas of necrosis in this model (than continuous illumination) as it is able to cause oxygen depletion at distances further away from the treatment fibre. If this tissue is then reperfused following irradiation, the reperfusion injury that would follow would create a larger area of necrosis.

The viability of the microvasculature during these experiments was not investigated in this study. Further work should, therefore, include such a measure to obtain a more complete picture of the complex mechanisms at work during both continuous and fractionated ALA PDT.

To get the full benefit of this technique clinically, it will be necessary to conduct real-time monitoring as ALA PDT is in progress, so that the fractionation regime can be determined and applied on an individual basis. The results of this thesis suggest that a measure of pO_2 may be a useful parameter to study for this purpose, as it may give an indication of treatment outcome at the time of illumination, as well as a guide to the appropriate placement of the fractionation interval. Further detailed study of these

points will, however, be necessary before this technique of enhancement will be able to realise its full potential clinically.

The effect of both light dose fractionation and the iron chelator, CP94, were also investigated (separately), in preliminary studies conducted in a colonic tumour model. This work found that both the techniques were able to enhance ALA PDT in a tumour model. This was particularly important to establish with the iron chelator as it had not been previously investigated in an *in vivo* tumour model and the success of this method of enhancement is highly dependent on the biochemical abilities of the tumour to be treated. In the MC28 tumour model studied in this thesis, the administration of 100 mg/kg CP94 i.v. in combination with 50 mg/kg ALA i.v. was able to produce over seven times the volume of necrosis as 50 mg/kg ALA i.v. alone, which is a highly significant degree of enhancement.

The two techniques were also investigated as a combination, to see if even greater enhancement could be achieved when using them together. When using 200 mg/kg ALA i.v. and 100 J of 628 nm continuous irradiation, it was found that the addition of the iron chelator doubled the area of necrosis produced. Fractionating the light dose (F20/80) without the administration of the iron chelator was found to increase the damage produced via the treatment by a factor of three. It was possible, however, through the administration of CP94 and the fractionation of the light dose (F10/90), to produce five times more damage than that produced by the standard, unenhanced treatment. The combination of these two methods of ALA PDT enhancement can, therefore, produce even greater enhancement of ALA PDT than either technique independently.

Although, the application of these techniques of ALA PDT enhancement may potentially seem troublesome, the lack of substantial cutaneous photosensitivity makes ALA induced PPIX a very attractive photosensitising agent for a whole range of medical applications, if it can only be made more effective. If the improved effects observed in this thesis can be reproduced in the clinic, however, the outcome will make the effort worthwhile. The effective clinical application of light dose fractionation will be more demanding than the administration of an iron chelating agent, but comfort should be taken from the fact that radiotherapists routinely use fractionation techniques to improve the effect of radiotherapy, without too much difficulty.

3.2 Conclusions

ALA PDT is a promising method, ideal for the treatment of superficial cancers and precancers in the linings of hollow organs and on the skin. The much reduced skin photosensitivity and good healing without scarring following treatment makes this technique worth pursuance, even if it only currently produces a limited clinical effect. This thesis has investigated two different methods of ALA PDT enhancement and found that the administration of the iron chelator CP94, and the technique of light dose fractionation can each be used successfully to significantly enhance ALA induced PDT.

More specifically, 635 nm has been shown to be a more effective excitation wavelength of ALA induced PPIX photosensitisation *in vivo* than 628 nm. Also, the more lipophilic hydroxypyridinone iron chelator CP94, when administered in combination with ALA, was found to produce greater mucosal PPIX fluorescence in normal rat colon than CP20 (the other hydroxypyridinone iron chelator investigated by this thesis) and significantly more than that produced by ALA administered alone. Spectrofluorimetry confirmed that the fluorescence produced could be attributed to PPIX and no other fluorescent porphyrin. PDT studies determined that this increase in PPIX fluorescence could be utilised, on irradiation, to substantially enhance the effect of ALA PDT.

The PDT effect was found to be greatest when CP94 was administered at the same time as the ALA and the compounds could be prepared as a mixed solution with no detrimental effect. It was also noted that as the ALA dose was increased, the beneficial effect of adding the iron chelator was reduced and that the greatest enhancement occurred when using the lowest dose of ALA studied (25 mg/kg i.v.).

CP94 was also found to produce the same positive effects, i.e. increased PPIX fluorescence and PDT effect, in a colonic tumour model, normal rat skin and normal rabbit uterus, whether using an intravenous injection, topical cream or an instillation to administer the compounds. It can, therefore, be concluded that CP94 can be used effectively *in vivo* to significantly enhance ALA PDT using an number of routes of administration.

A single light fractionation interval of 150 seconds, placed after only one fifth of the energy dose had been delivered (F20/80) was found to be the most effective light fractionation regime of all those investigated in this thesis and significantly increased the effect of ALA PDT in the normal and malignant rat colon. The success of this regime was highly dependent on the size of the initial energy fraction and thus the position of the fractionation interval. Multiple intervals were not found to be significantly better than this best two fractionation regime.

It was also noted that light dose fractionation could be used to produce the same PDT effect as continuous irradiation but with a much reduced light dose. No significant enhancement could be achieved through fractionating ALA PDT using the lowest ALA dose studied (25 mg/kg i.v.) but it was found that light dose fractionation could

be used successfully in this model to significantly enhance ALA PDT when using higher ALA doses (50 and 200 mg/kg i.v.).

The greatest enhancement of ALA PDT observed in thesis was achieved through the combination of both these techniques of enhancement. This produced an effect greater than either the administration of CP94 in combination with ALA or light dose fractionation could produce independently.

Investigations of the mechanism of light dose fractionation found that significant consumption of oxygen occurred during ALA PDT in normal rat colon and marked differences in the pattern of pO_2 levels were observed when comparing continuous and fractionated light regimes. It was also determined that a small increase in PPIX fluorescence could occur during the fractionation interval of 150 seconds and that the inhibition of reperfusion injury, through the administration of SOD and catalase or allopurinol (a xanthine oxidase inhibitor) prior to illumination, was found to protect the normal rat colon against PDT damage.

This thesis has, therefore, shown that the administration of the iron chelator, CP94, or the technique of light dose fractionation, when applied appropriately, can be used to significantly enhance ALA PDT *in vivo*. The task for the future will be determining whether this is possible clinically. There is now strong evidence, however, that through the appropriate application of these techniques of enhancement, the current clinical effect of ALA PDT could be substantially improved, without increased light or drug doses being required. This would enable ALA induced PDT to become a more effective medical treatment.

REFERENCES

- Abeyasinghe RD, Roberts PJ, Cooper CE, MacLean KH, Hider RC and Porter JB. (1996). The environment of the lipoxygenase iron binding site explored with novel hydroxypyridinone iron chelators. *J. Biolog. Chem.*, **271**, 7965-7972.
- Al-Refaie FN, Wonke B, Hoffbrand AV, Wickens DG, Nortey P and Kontoghiorghes GJ. (1992). Efficacy and possible adverse effects of the oral iron chelator 1,2-dimethyl-3-hydroxypyridin-4-one (L₁) in Thalassemia Major. *Blood*, **3**, 593-599.
- Anholt H and Moan J. (1991). Fractionated treatment of CaD2 tumours in mice sensitised with aluminium phthalocyanine tetrasulfonate. *Cancer Letters*, **61**, 263-267.
- Barr H, Tralau CJ, MacRobert AJ, Krasner N, Boulos PB, Clark CJ and Bown SG. (1987). Photodynamic therapy in the normal rat colon with phthalocyanine sensitisation. *Br. J. Cancer*, **56**, 111-118.
- Barr H, MacRobert AJ, Tralau CJ, Boulos PB and Bown SG. (1990). The significance of the nature of the photosensitiser for photodynamic therapy: quantitative and biological studies in the colon. *Br. J. Cancer*, **62**, 730-735.
- Barr H, Shepherd NA, Dix A, Roberts DJH, Tan WC and Krasner N. (1996). Eradication of high-grade dysplasia in columnar-lined (Barrett's) oesophagus by photodynamic therapy with endogenously generated protoporphyrin IX. *Lancet*, **348**, 584-585.
- Battle AMC. (1993). Porphyrins, porphyrias, cancer and photodynamic therapy - a model for carcinogenesis. *J. Photochem. Photobiol. B: Biol.*, **20**, 5-22.
- Baumgartner R and Stepp H. (1998). Photodynamic diagnosis using 5-aminolevulinic acid (5-ALA) for minimally-invasive treatment of cancer. *Min. Invas. Ther. & Allied Technol.*, **7/6**, 495-501.
- Bech O, Phillips D, Moan J and MacRobert AJ. (1997). A hydroxypyridinone (CP94) enhances protoporphyrin IX formation in 5-aminolaevulinic acid treated cells. *J. Photochem. Photobiol. B: Biol.*, **41**, 136-144.
- Bedwell J, MacRobert AJ, Phillips D and Bown SG. (1992). Fluorescence distribution and photodynamic effect of ALA-induced PPIX in the DMH rat colonic tumour model. *Br. J. Cancer*, **65**, 818-824.

- Berg K, Anholt H, Bech O and Moan J. (1996). The influence of iron chelators on the accumulation of protoporphyrin IX in 5-aminolaevulinic acid-treated cells. *Br. J. Cancer*, **74**, 688-697.
- Bonnett R. (1995). Photosensitisers of the porphyrin and phthalocyanine series for photodynamic therapy. *Chemical Society Reviews*, **24**, 19-33.
- Bourletias L, Lenz P and Margonari J. (1994). Characteristics of PDT performed very shortly after sensitizer injection. *Journal de Physique IV*, **4**, C4-241 - C4-244.
- Bremner JCM, Adams GE, Pearson JK, Sansom JM, Stratford IJ, Bedwell J, Bown SG, MacRobert AJ and Philips D. (1992). Increasing the effect of photodynamic therapy on the RIF-1 murine sarcoma, using the bioreductive drugs RSU1069 and RB6145. *Br. J. Cancer*, **66**, 1070-1076.
- Brittenham GM. (1992). Development of iron-chelating agents for clinical use. *Blood*, **80**, 569-574.
- Carruth JAS. (1998). Clinical applications of photodynamic therapy. *IJCP*, **52**, 39-42.
- Casas A, Fukuda H and Batlle AMC. (In Press). Tissue distribution and kinetics of endogenous porphyrins synthesized after topical application of ALA in different vehicles.
- Chang SC, MacRobert AJ, Porter JB and Bown SG. (1997). The efficacy of an iron chelator (CP94) in increasing cellular protoporphyrin IX following intravesical 5-aminolaevulinic acid administration: an *in vivo* study. *J. Photochem. Photobiol. B: Biol.*, **38**, 114-122.
- Chen Q, Chen H and Hetzel FW. (1996). Tumor oxygenation changes post-photodynamic therapy. *Photochemistry and Photobiology*, **63**, 128-131.
- Cooper CE, Lynagh GR, Hoyes KP, Hider RC, Cammack R and Porter JB. (1996). The relationship of intracellular iron chelation to the inhibition and regeneration of human ribonucleotide reductase. *J. Biolog. Chem.*, **271**, 20291-20299.
- Cox TC, Bawden MJ, Martin A and May BK. (1991). Human erythroid 5-aminolaevulinate synthase: promoter analysis and identification of an iron-responsive element in the mRNA. *EMBO Journal*, **10**, 1891-1902.

- Crowell JW, Jones CE and Smith EE. (1969). Effect of allopurinol on hemorrhagic shock. *American Journal of Physiology*, **216**, 744-748.
- De Jode ML, McGilligan JA, Dilkes MG, Cameron I, Grahm MF and Williams NS. (1996). An *in vivo* comparison of the photodynamic action of a new diode laser and a copper vapour dye laser at 652 nm. *Lasers in Medical Science*, **11**, 117-121.
- Dietel W, Fritsch C, Pottier RH and Wendenburg R. (1997). 5-Aminolaevulinic-acid-induced formation of different porphyrins and their photomodifications. *Lasers in Medical Science*, **12**, 226-236.
- Dougherty TJ, Gomer CJ, Henderson BW, Jori G, Kessel D, Korbely M, Moan J and Peng Q. (1998). Photodynamic therapy. *Journal of the National Cancer Institute*, **90**, 889-905.
- Elfsson B, Wallin I, Eksborg S, Rudaeus K, Ros AM and Ehrsson H. (1998). Stability of 5-aminolevulinic acid in aqueous solution. *European Journal of Pharmaceutical Sciences*, **7**, 87-91.
- Fan KFM, Hopper C, Speight PM, Buonaccorsi G, MacRobert AJ and Bown SG. (1996). Photodynamic therapy using 5-aminolevulinic acid for premalignant and malignant lesions of the oral cavity. *Cancer*, **78**, 1374-1383.
- Fehr MK, Wyss P, Tromberg BJ, Krasieva T, DiSaia PJ, Lin F and Tadir Y. (1996). Selective photosensitizer localization in the human endometrium after intrauterine application of 5-aminolevulinic acid. *Am. J. Obstet. Gynecol.*, **175**, 1253-1259.
- Fijan S, Honigsmann H and Ortel B. (1995). Photodynamic therapy of epithelial skin tumours using delta-aminolaevulinic acid and desferrioxamine. *British Journal of Dermatology*, **133**, 282-288.
- Foster TH, Murant RS, Bryant RG, Knox RS, Gibson SL and Hilf R. (1991). Oxygen consumption and diffusion effects in photodynamic therapy. *Radiation Research*, **126**, 296-303.
- Gannon MJ, Johnson N, Roberts DJH, Holroyd JA, Vernon DI, Brown SB and Lilford RJ. (1995). Photosensitization of the endometrium with topical 5-aminolevulinic acid. *Am. J. Obstet. Gynecol.*, **173**, 1826-1828.

- Gannon MJ, Stringer M and Brown SB. (1998). A phase I clinical trial of endometrial ablation by ALA-PDT. Conference Presentation; 7th Biennial Congress, International Photodynamic Association, Nantes, France. Abstract n° RC29.
- Goff BA, Bachor R, Kollias N and Hassan T. (1992). Effects of photodynamic therapy with topical application of 5-aminolevulinic acid on normal skin of hairless guinea pigs. *J. Photochem. Photobiol. B: Biol.*, **15**, 239-251.
- Gossner L, Stolte M, Sroka R, Rick K, May A, Hahn EG and Ell C. (1998). Photodynamic ablation of high-grade dysplasia and early cancer in Barrett's oesophagus by means of 5-aminolaevulinic acid. *Gastroenterology*, **114**, 448-455.
- Gross GJ, Farber NE, Hardman HF and Warltier DC. (1986). Beneficial actions of superoxide dismutase and catalase in stunned myocardium of dogs. *American Physiological Society*, H372-H377.
- Gutteridge JMC and Halliwell B. (1990). Reoxygenation injury and antioxidant protection: A tale of two paradoxes. *Archives of Biochemistry and Biophysics*, **283**, 223-226.
- Halling BP, Yuhas DA, Fingar VF and Winkelmann JW. (1994). Protoporphyrinogen oxidase inhibitors for tumour therapy. *American Chemical Society Symposium Series*, **559**, 280-290.
- Hammond B, Kontos HA and Hess ML. (1985). Oxygen radicals in the adult respiratory distress syndrome, in myocardial ischemia and reperfusion injury, and in cerebral vascular damage. *Can. J. Physiol. Pharmacol.*, **63**, 173-187.
- Hanania J and Malik Z. (1992). The effect of EDTA and serum on endogenous porphyrin accumulation and photodynamic sensitisation of human K562 leukemic cells. *Cancer Letters*, **65**, 127-131.
- Henderson BW and Dougherty TJ. (1992). How does photodynamic therapy work? *Photochemistry and Photobiology*, **55**, 145-157.
- Hershko C, Link G, Pinson A, Peter HH, Dobbin P and Hider RC. (1991). Iron mobilization from myocardial cells by 3-hydroxypyridin-4-one chelators: Studies in rat heart cells in culture. *Blood*, **77**, 2049-2053.

- Hoyes KP and Porter JB. (1993). Subcellular distribution of desferrioxamine and hydroxypyridin-4-one chelators in K562 cells affects chelation of intracellular iron pools. *Br. J. Haematol.*, **85**, 393-400.
- Hua Z, Gibson SL, Foster TH and Hilf R. (1995). Effectiveness of δ -aminolevulinic acid-induced protoporphyrin as a photosensitiser for photodynamic therapy *in vivo*. *Cancer Research*, **55**, 1723-1731.
- Jolly SR, Kane WJ, Bailie MB, Abrams GD and Lucchesi BR. (1984). Canine myocardial reperfusion injury. *Circulation Research*, **54**, 277-284.
- Jordan PM. (1991). Biosynthesis of tetrapyrroles. In: Neuberger A and van Deenen LLM (Eds). *New Comprehensive Biochemistry*. Vol 19. pp. 1-100. Elsevier Science: New York.
- Kennedy JC, Pottier RH and Pross DC. (1990). Photodynamic therapy with endogenous protoporphyrin IX: Basic principles and present clinical experience. *J. Photochem. Photobiol. B: Biol.*, **6**, 143-148.
- Kennedy JC and Pottier RH. (1992). Endogenous protoporphyrin IX, a clinical useful photosensitiser for photodynamic therapy. *J. Photochem. Photobiol. B: Biol.*, **14**, 275-292.
- Kennedy JC, Marcus SL and Pottier RH. (1996). Photodynamic therapy and photodiagnosis using endogenous photosensitisation induced by 5-aminolaevulinic acid: Mechanisms and clinical results. *J. Clin. Laser Med. & Surg.*, **14**, 289-304.
- Lawrance RJ, Cooper AJ, Loizidou M, Alexander P and Taylor I. (1990). Blood transfusion and recurrence of colorectal cancer: the role of platelet derived growth factors. *Br. J. Surg.*, **77**, 1106-1109.
- Lesnefsky EJ and Ye J. (1994). Exogenous intracellular, but not extracellular, iron augments myocardial reperfusion injury. *American Physiological Society*, H384-H392.
- Leveckis J, Brown NJ and Reed MWR. (1995). The effect of aminolaevulinic acid-induced, protoporphyrin IX-mediated photodynamic therapy on the cremaster muscle microcirculation *in vivo*. *Br. J. Cancer*, **72**, 1113-1119.
- Levy JG. (1994). Photosensitisers in photodynamic therapy. *Seminars in Oncology*, **21**, 4-10.

- Li G, Szewczuk MR, Pottier RH and Kennedy JC. (1999). Effect of mammalian cell differentiation on response to exogenous 5-aminolevulinic acid. *Photochemistry and Photobiology*, **69**, 231-235.
- Loh CS, Vernon D, MacRobert AJ, Bedwell J, Bown SG and Brown SB. (1993). Endogenous porphyrin distribution induced by 5-aminolaevulinic acid in the tissue layers of the gastrointestinal tract. *J. Photochem. Photobiol. B: Biol.*, **20**, 47-54.
- Malik Z and Lugaci H. (1987). Destruction of erythroleukaemic cells by photoactivation of endogenous porphyrins. *Br. J. Cancer*, **56**, 589-595.
- Marcus SL, Sobel RS, Golub AL, Carrol RL, Lundahl S and Shulman DG. (1996). Photodynamic therapy and photodiagnosis using endogenous photosensitization induced by 5-aminolevulinic acid: Current clinical and development status. *Journal of Clinical Laser Medicine and Surgery*, **14**, 59-66.
- McCord JM. (1985). Oxygen-derived free radicals in postischemic tissue injury. *New England Journal of Medicine*, **312**, 159-163.
- McCord JM. (1987). Oxygen-derived radicals: a link between reperfusion injury and inflammation. *Federation Proceedings*, **46**, 2402-2405.
- McIlroy BW, Curnow A, Buonaccorsi G, Scott MA, Bown SG and MacRobert AJ. (1998). Spatial measurement of oxygen levels during photodynamic therapy using time-resolved optical spectroscopy. *J. Photochem. Photobiol. B: Biol.*, **43**, 47-55.
- Messmann H, Milkvy P, Buonaccorsi G, Davies CL, MacRobert AJ and Bown SG. (1995). Enhancement of photodynamic therapy with 5-aminolaevulinic acid-induced porphyrin photosensitisation in normal rat colon by threshold and light fractionation studies. *Br. J. Cancer*, **72**, 589-594.
- Mittal VK, Dewan S, Amaria Y, Parikh Y, Toledo-Pereyra LH and Hans SS. (1988). Role of oxygen free radical scavengers in preservation of intestinal villi in the presence of ischemia. *Transplantation Proceedings*, **XX**, 1045-1047.
- Milkvy P, Messmann H, Pauer M, Stewart JCM, Millson CE, MacRobert AJ and Bown SG. (1996). Distribution and photodynamic effects of meso-tetrahydroxyphenylchlorin (mTHPc) in the pancreas and adjacent tissues in the Syrian Golden Hamster. *Br. J. Cancer*, **73**, 1473-1479.

-
- Muller S, Walt H, Dolber-Girdziunaite D, Fiedler D and Haller U. (1998). Enhanced photodynamic effects using fractionated laser light. *J. Photochem. Photobiol. B: Biol.*, **42**, 67-70.
- Murphy P, Alexander P, Senior PV, Fleming J, Kirkham N and Taylor I. (1988). Mechanisms of organ selective tumour growth by bloodborne cancer cells. *Br. J. Cancer*, **57**, 19-31.
- Noodt BB, Berg K, Stokke T, Peng Q and Nesland JM. (1996). Apoptosis and necrosis induced with light and 5-aminolaevulinic acid-derived protoporphyrin IX. *Br. J. Cancer*, **74**, 22-29.
- Orenstein A, Kostenich G, Kopolovic Y, Babushkina T and Malik Z. (1999). Enhancement of ALA-PDT damage by IR-induced hyperthermia on a colon carcinoma model. *Photochemistry and Photobiology*, **69**, 703-707.
- Ortel B, Tanew A and Honigsmann H. (1993). Lethal photosensitization by endogenous porphyrins of PAM cells - modification by desferrioxamine. *J. Photochem. Photobiol. B: Biol.*, **17**, 273-278.
- Oteiza PI, Kleinman CG, Demasi M and Bechara EJH. (1995). 5-Aminolevulinic acid induces iron release from ferritin. *Archives of Biochemistry and Biophysics*, **316**, 607-611.
- Paller MS, Holdal JR and Ferris TF. (1984). Oxygen free radicals in ischemic acute renal failure in the rat. *The American Society for Clinical Investigation*, **74**, 1156-1164.
- Paller MS and Hedlund BE. (1994). Extracellular iron chelators protect kidney cells from hypoxia/reoxygenation. *Free Radical Biology and Medicine*, **17**, 597-603.
- Pe MB, Ikeda H and Inokuchi T. (1994). Tumour destruction and proliferation kinetics following periodic, low power light, haematoporphyrin oligomers mediated photodynamic therapy in the mouse tongue. *Oral Oncol. Eur. J. Cancer*, **30**, 174-178.
- Peng Q, Evensen JF, Rimington C and Moan J. (1987). A comparison of different photosensitizing dyes with respect to uptake by C3H-tumours and tissues in mice. *Cancer Letters*, **36**, 1-10.
-

- Peng^a Q, Berg K, Moan J, Kongshaug M and Nesland JM. (1997). 5-Aminolevulinic acid-based photodynamic therapy: Principles and experimental research. *Photochemistry and Photobiology*, **65**, 235-251.
- Peng^b Q, Warloe T, Berg K, Moan J, Kongshaug M, Giercksky KE and Nesland JM. (1997). 5-Aminolaevulinic-based photodynamic therapy: Clinical research and future challenges. *American Cancer Society*, **79**, 2282-2308.
- Pinion SB, Parkin DE, Abramovich DR, Naji A, Alexander DA, Russell IT and Kitchener HC. (1994). Randomised trial of hysterectomy, endometrial laser ablation, and transcervical endometrial resection for dysfunctional uterine bleeding. *BMJ*, **309**, 979-983.
- Porter JB, Abeysinghe RD, Hoyes KP, Barra C, Huehns ER, Brooks PN, Blackwell MP, Araneta M, Brittenham G, Singh S, Bobbin P and Hider RC. (1993). Contrasting interspecies efficacy and toxicology of 1,2-diethyl-3-hydroxypyridin-4-one, CP94, relates to differing metabolism of the iron chelating site. *Br. J. Haematol.*, **85**, 159-168.
- Rang HP and Dale MM. (1991). Pharmacology. 2nd Edition. pp.557-562. Churchill Livingstone: Hong Kong.
- Reed MW, Mullins AP, Anderson GL, Miller FN and Wieman TJ. (1989). The effect of photodynamic therapy on tumor oxygenation. *Surgery*, **106**, 94-99.
- Regula J, MacRobert AJ, Gorchein A, Buonaccorsi GA, Thorpe SM, Spencer GM, Hatfield AWR and Bown SG. (1995). Photosensitisation and photodynamic therapy of oesophageal, duodenal and colorectal tumours using 5-aminolaevulinic acid induced protoporphyrin IX. *Gut*, **36**, 67-75.
- Richardson D, Ponka P and Baker E. (1994). The effect of the iron (III) chelator, desferrioxamine, on iron and transferrin uptake by the human malignant melanoma cell. *Cancer Research*, **54**, 685-689.
- Roberts DJH, Cairnduff F, Driver I, Dixon B and Brown SB. (1994). Tumour vascular shutdown following photodynamic therapy based on polyhaematoporphyrin or 5-aminolaevulinic acid. *International Journal of Oncology*, **5**, 763-768.
- Roberts DJH and Cairnduff F. (1995). Photodynamic therapy of primary skin cancer: a review. *Br. J. of Plastic Surgery*, **48**, 360-370.

Robinson DJ, de Bruijn HS, van der Veen N, Stringer MR, Brown SB and Star WM. (1998). Fluorescence photobleaching of ALA-induced protoporphyrin IX during photodynamic therapy of normal hairless mouse skin: The effect of light dose and irradiance and the resulting biological effect. *Photochemistry and Photobiology*, **67**, 140-149.

Robinson DJ, de Bruijn HS, van der Veen N, Stringer MR, Brown SB and Star WM. (1999). Protoporphyrin IX fluorescence photobleaching during ALA-mediated photodynamic therapy of UVB-induced tumours in hairless mouse skin. *Photochemistry and Photobiology*, **69**, 61-70.

Roy RS and McCord JM. (1983). Superoxide and ischemia: conversion of xanthine dehydrogenase to xanthine oxidase. In: Greenwald R and Cohen G (Eds). *Oxyl radicals and their scavenger systems*. Vol. 2. Cellular and molecular aspects. pp. 145-153. Elsevier Science: New York.

Sailer R, Strauss WSL, Konig K, Ruck A and Steiner R. (1997). Correlation between porphyrin biosynthesis and photodynamic inactivation of *Pseudomonas aeruginosa* after incubation with 5-aminolaevulinic acid. *J. Photochem. Photobiol. B: Biol.*, **39**, 236-242.

Sitnik TM, Hampton JA and Henderson BW. (1998). Reduction of tumour oxygenation during and after photodynamic therapy *in vivo*: effects of fluence rate. *Br. J. Cancer*, **77**, 1386-1394.

Skipper D, Jeffrey MJ, Cooper AJ, Taylor I and Alexander P. (1988). Preferential growth of bloodborne cancer cells in colonic anastomoses. *Br. J. Cancer*, **57**, 564-568.

Smetana Z, Malik Z, Orenstein A, Mendelson E and Ben-Hur E. (1997). Treatment of viral infections with 5-aminolaevulinic acid and light. *Lasers in Surgery and Medicine*, **2**, 351-358.

Stewart F, Baas P and Star W. (1998). What does photodynamic therapy have to offer radiation oncologists (or their cancer patients)? *Radiotherapy and Oncology*, **48**, 233-248.

Stringer M, Collins P, Robinson D, Stables G and Sheehan-Dare R. (1996). The accumulation of protoporphyrin IX in plaque psoriasis after topical application of 5-aminolaevulinic acid indicates a potential for superficial photodynamic therapy. *J. Invest. Dermatol.*, **107**, 76-81.

Stryer L. (1988). Biochemistry. 3rd Edition. pp. 594-597. W. H. Freeman and Company: New York.

Szeimies RM, Abels C, Fritsh C, Karrer S, Steinbach P, Baumler W, Goerz G, Goetz AE and Landthaler M. (1995). Wavelength dependency of photodynamic effects after sensitisation with 5-aminolaevulinic acid *in vitro* and *in vivo*. *The Journal of Investigative Dermatology*, **105**, 672-677.

Szeimies RM, Calzavara-Pinton PG, Karrer S, Ortel B and Landthaler M. (1996). Topical photodynamic therapy in dermatology. *J. Photochem. Photobiol. B: Biol.*, **36**, 213-219.

Tadir Y, Hornung R, Pham TH and Tromberg BJ. (1999). Intrauterine light probe for photodynamic ablation therapy. *Obstetrics and Gynecology*, **93**, 299-303.

Tromberg BJ, Orenstein A, Kimel S, Barker SJ, Hyatt J, Nelson JS and Berns MW. (1990). *In vivo* tumour oxygen tension measurements for the evaluation of the efficiency of photodynamic therapy. *Photochemistry and Photobiology*, **52**, 375-385.

Vander AJ, Sherman JH and Luciano DS. (1990). Human physiology: The mechanisms of body function. 5th Edition. pp. 351-355. McGraw Hill Publishing Co: New York.

Van der Kraaij AMM, Mostert LJ, van Eijk HG and Koster JF. (1988). Iron-load increases the susceptibility of rat hearts to oxygen reperfusion damage. *Circulation*, **78**, 442-449.

Van der Kraaij AMM, van Eijk HG and Koster JF. (1989). Prevention of post-ischemic cardiac injury by the orally active iron chelator 1,2-dimethyl-3-hydroxy-4-pyridinone (L1) and the antioxidant (+)-cyanidanol-3. *Circulation*, **80**, 158-164.

van der Veen N, van Leengoed HLLM and Star WM. (1994). *In vivo* fluorescence kinetics and photodynamic therapy using 5-aminolaevulinic acid-induced porphyrin: increased damage after multiple irradiations. *Br. J. Cancer*, **70**, 867-872.

van Geel IPJ, Oppelaar H, Marijnissen JPA and Stewart FA. (1996). Influence of fractionation and fluence rate in photodynamic therapy with Photofrin or mTHPc. *Radiation Research*, **145**, 602-609.

Wyld L, Smith O, Lawry J, Reed MWR and Brown NJ. (1998). Cell cycle phase influences tumour cell sensitivity to aminolaevulinic acid-induced photodynamic therapy *in vitro*. *Br. J. Cancer*, **78**, 50-55.

Wyss P, Steiner R, Liaw LH, Wyss MT, Ghazarians A, Berns MW, Tromberg BJ and Tadir Y. (1996). Regeneration processes in rabbit endometrium: a photodynamic model. *Human Reproduction*, **11**, 1992-1997.

Yang JZ, van Vugt DA, Kennedy JC and Reid RL. (1993). Intrauterine 5-aminolevulinic acid induces selective fluorescence and photodynamic ablation of the rat endometrium. *Photochemistry and Photobiology*. **57**, 803-807.

APPENDIX I

CONFERENCE PRESENTATIONS

British Medical Laser Association Annual Spring Meeting.

Swallow Hotel, Liverpool (13 - 14 May 1999).

- Enhancement of ALA induced PDT (as a method of endometrial ablation) using iron chelating agents.
- Oral presentation.
- Conference Presentation Award.

7th Biennial Meeting of the International Photodynamic Association.

Nantes, France (7 - 9 July 1998).

- Enhancement of ALA induced PDT using iron chelating agents.
- Oral presentation.
- Scientific Communication Prize.

ALA PDT Workshop.

Weetwood Hall Hotel, Leeds (24 - 26 April 1998).

- Enhancement of ALA PDT using iron chelating agents.
- Poster + short oral presentation.

BiOS 1998.

San Jose, California, USA (24 - 30 January 1998).

- Enhancement of ALA induced PDT using light dose fractionation and iron chelating agents.
- Oral presentation + proceedings manuscript.

7th Congress of the European Society for Photobiology.

Stresa, Italy (8 - 13 September 1997).

- An investigation of the effects of iron chelating agents on ALA PDT.
- Oral presentation.

BIOS Europe 1997.

Hotel Londra, San Remo, Italy (4 - 8 September 1997).

- A systematic comparison of light fractionation regimes for the enhancement of PDT using ALA.
- Oral presentation.

The Rank Prize Fund Mini-Symposium on Photodynamic Therapy.

Wordsworth Hotel, Grasmere, Cumbria (13 - 16 May 1996).

- Enhancement of ALA PDT in colon, by fractionation of the light dose.
- Oral presentation.

6th Biennial Meeting of the International Photodynamic Association.

Hilton on the Park Hotel, Melbourne, Australia (10 - 14 March 1996).

- Enhancement of ALA PDT in colon, by fractionation of the light dose.
- Oral presentation.
- Student Investigator Award.

ALA PDT Workshop.

Weetwood Hall Hotel, Leeds (29 - 31 August 1995).

- Enhancement of ALA PDT in colon, by fractionation of the light dose.
- Poster + short oral presentation.

APPENDIX II

PUBLICATIONS

Published papers:-

Curnow A, McIlroy BW, Postle-Hacon MJ, MacRobert AJ and Bown SG. (1999). Light dose fractionation to enhance photodynamic therapy using 5-aminolaevulinic acid in the normal rat colon. *Photochemistry and Photobiology*, **69**, 71-76.

Curnow A, McIlroy BW, Postle-Hacon MJ, Porter JB, MacRobert AJ and Bown SG. (1998). Enhancement of 5-aminolaevulinic acid induced photodynamic therapy using iron chelating agents. *British Journal of Cancer*, **78**, 1278 - 1282.

Curnow A, Postle-Hacon MJ, MacRobert AJ and Bown SG. (1998). Enhancement of 5-aminolaevulinic acid induced photodynamic therapy using light dose fractionation and iron chelating agents. *SPIE Conference Proceedings; Optical methods for tumour treatment and detections; Mechanisms and techniques in photodynamic therapy VII*, **3247**, 118 - 127.

McIlroy BW, **Curnow A**, Buonaccorsi G, Scott MA, Bown SG and MacRobert AJ. (1998). Spatial measurements of oxygen levels during photodynamic therapy using time-resolved optical spectroscopy. *Journal of Photochemistry and Photobiology: B*, **43**, 47 - 55.

Papers currently submitted for publication:-

Curnow A, Haller JC, Brown SB and Bown SG. Oxygen monitoring during 5-aminolaevulinic acid induced photodynamic therapy in normal rat colon - A comparison of continuous and fractionated light regimes. *International Journal of Cancer*.

Curnow A, Postle-Hacon MJ, Porter JB, MacRobert AJ and Bown SG. Enhancement of 5-aminolaevulinic acid induced photodynamic therapy in normal rat skin using an hydroxypyridinone iron chelating agent. *Journal of Investigative Dermatology*.